LMU LUDWIG-MAXIMILIANS-UNIVERSITÄT MÜNCHEN

Gc9 is involved in the efficient ring assembly of the chloroplast F_OF_1 ATP synthase in Arabidopsis

Dissertation

zur Erlangung des Doktorgrades der Fakultät für Biologie

der Ludwig-Maximilians-Universität München

Vorgelegt von

Jafar Angouri Razeghi

München

September 2013

1. Gutachter: Prof. Dr. Dario Leister

2. Gutachter: Prof. Dr. Jörg Nickelsen

Tag der Einreichung: 30.07.2013

Tag der mündlichen Prüfung: 05.09.2013

Summary

Photosynthetic light reactions take place in the thylakoid membranes of cyanobacteria, algae and plants. Photosynthetic electron transport is coupled to proton pumping from the stroma into the thylakoid lumen. The resulting proton gradient drives ATP production by the ATP synthase complex. The free energy released from the ATP hydrolysis is used for numerous cellular enzymatic reactions. The ATP synthase is composed of chloroplast- and nucleus-encoded subunits which are coordinately assembled by the assistance of additional auxiliary and regulatory factors to form a functional complex. By comparative genomic analyses, a set of proteins was previously identified in photosynthetic organisms (green algae, flowering and nonflowering plants) which is not found in non-photosynthetic organisms. Those proteins are called GreenCut proteins and are associated with chloroplast function. Remarkably, around 50 % of them have not been functionally characterized yet.

Here, we show that Gc9, one of the unknown GreenCut proteins is located in the thylakoid membrane. Sequence alignments of Gc9 revealed that the C-terminal, transmembrane domain of Gc9 shares some similarity to the Atp1/UncI proteins which are encoded in the ATP synthase operons of bacteria and cyanobacteria. Arabidopsis Gc9 knock-out mutant lines (*gc9-1*) display a reduction in growth relative to wild type plants. In addition, increased non-photochemical quenching, elevated ΔpH-dependent quenching and an activated xanthophyll cycle could be observed in the mutant lines which are caused by a drastically lowered ATP synthase content in *gc9-1* by 70-90 % compared to wild type plants. Gc9 neither forms a stable complex with the ATP synthase nor is it an ATP synthase subunit. Furthermore, no drastic transcriptional or translational defect related to ATP synthase subunit expression could be detected in *gc9-1*, whereas BN-PAGE analyses of ATP synthase complex intermediates indicated a significant accumulation of AtpH monomers in *gc9-1*. Split-Ubiquitin assays confirmed that Gc9 interacts with AtpH, the ring-forming subunit of the membrane-integral CF_O part of the ATP synthase. Taken together, Gc9 is involved in the efficient AtpH ring assembly in chloroplasts of *Arabidopsis thaliana*. Thus, lack of Gc9 has more severe effects on ATP synthase assembly than its counterpart UncI in bacteria.

Zusammenfassung

Die Photosynthese findet in den Thylakoidmembranen von Cyanobakterien, Algen und Pflanzen statt. Durch absorbierte Lichtenergie wird im Innenraum der Thylakoidmembran (Lumen) Wasser gespalten, wobei Sauerstoff, Protonen und Elektronen mobilisiert werden. Elektronen werden über membranständige Photosynthesekomplexe transportiert und auf Reduktionsäquivalente im Stroma übertragen, die essentiell für die enzymatische Fixierung von Kohlenstoff sind. Zusätzlich ist der Elektronentransport an den Protoneneinstrom in das Lumen gekoppelt, was zu einem Membranpotential zwischen Lumen und Stroma führt. Beim Rücktransport von Protonen in das Stroma wird ATP durch den ATP-Synthase-Komplex generiert, was für zahlreiche, zelluläre enzymatische Reaktionen benötigt wird. In Algen und Pflanzen setzt sich die ATP Synthase aus chloroplastenkodierten und kernkodierten Untereinheiten zusammen. Bei deren Integration zu einem funktionellen Komplex in die Thylakoidmembran werden zusätzliche Hilfsproteine und regulatorische Faktoren benötigt. In einer vorrausgehenden Studie wurden durch vergleichende Genomanalysen Proteine identifiziert, die nur in photosynthetischen, eukaryotischen Organismen (Grünalgen und blühenden und nicht blühenden Pflanzen) vorkommen. Diese Proteine übernehmen hauptsächlich Funktionen im Chloroplasten und werden als *GreenCut* Proteine bezeichnet. Bemerkenswert ist, dass rund 50 % von ihnen noch nicht funktionell charakterisiert sind.

Im Rahmen dieser Arbeit wurde gezeigt, dass Gc9 (At2g31040), eines der unbekannten *Greencut* Proteine, essentiell für eine effiziente Photosynthese ist. Anhand von Sequenzvergleichsstudien konnte gezeigt werden, dass die C-terminale Transmembrandomäne von Gc9 moderate Ähnlichkeiten zu den Atp1/UncI Proteinen aufweist, welche in den ATP-Synthase-Operons von Bakterien und Cyanobakterien codiert sind. Die Gc9 *knock-out* Linien bei *Arabidopsis thaliana* (*gc9-1*) zeichnen sich durch ein verringertes Wachstum im Vergleich zu den Wildtyppflanzen aus. Zusätzlich konnte in den Linien eine erhöhte Wärmeabgabe, eine Protonenanreicherung im Lumen und ein aktivierter Xanthophyll-Zyklus ermittelt werden. Diese Phänomene lassen sich durch einen stark gesenkten ATP-Synthase-Gehalt in *gc9-1* um 70-90 % gegenüber dem Wildtyp erklären. Gc9 ist weder eine Untereinheit noch bildet es einen stabilen Komplex mit der ATP-Synthase. Transkription oder Translation von ATP-Synthase-Untereinheiten in *gc9-1* sind ebenfalls nur gering beeinträchtigt. Jedoch konnte über Assemblierungsstudien des ATP-Synthase-Komplexes eine Anreicherung von AtpH-Monomeren in *gc9-1* nach gewiesen werden. Split-Ubiquitin-Analysen bestätigten, dass Gc9 mit AtpH, der ringbildenden Untereinheit des CF_O Teils der ATP-Synthase, interagiert. Zusammengefasst konnte gezeigt werden, dass Gc9 für eine effiziente AtpH Ringassemblierung erforderlich ist und dass das Fehlen von Gc9 zu einer stärkeren Beeinträchtigung der ATP Synthase-Assemblierung im Vergleich zum bakteriellen Gegenstück Atp1/UncI führt.

Index

Summary i
Zusammenfassung ii
Index iii
List of figures vi
List of tables vii
Abbreviations viii
1 Introduction 1
1.1 Photosynthesis 1
1.2 ATP synthase structure 2
1.2.1 General aspects of ATP synthase 2
1.2.2 CF_1 portion 4
1.2.3 CF_O portion 4
1.3 ATP synthase function 5
1.4 ATP synthase regulation 6
1.5 Assembly of photosynthetic protein complexes 7
1.5.1 A dual genetic origin of photosynthetic proteins 7
1.5.2 ATP synthase assembly factors 10
1.6 Photoprotection 11
1.6.1 Heat dissipation of excess light energy as a photoprotective mechanism 11
1.6.2 Xanthophylls and photoprotection 12
1.7 GreenCut proteins 13
1.8 Aim of this thesis 14
2 Materials and Methods 15
2.1 Plant material 15
2.1.1 *Arabidopsis thaliana* mutant lines 15
2.1.2 Complementation of *gc9-1* mutant lines 15
2.2 Plant growth conditions 16
2.3 Bioinformatic sources 17

2.4 Genomic DNA extraction and recovery of the T-DNA flanking sequences 17
2.5 RNA extraction 18
2.6 Northern analysis 18
2.7 cDNA synthesis and RT-PCR analysis 19
2.8 Real time PCR analyses 19
2.9 Leaf pigment analysis 20
2.10 Chlorophyll a fluorescence measurement (PAM) 20
2.11 Generation of a Gc9 antibody and determination of the molar ratio of Gc9 to AtpC1 21
2.12 Protoplasts isolation and GFP signal detection 22
2.13 Intact chloroplast and envelope isolation from Arabidopsis leaves 23
2.14 Thylakoid isolation from Arabidopsis leaves 24
2.15 Blue Native analysis and second dimension gel 24
2.16 Complex isolation using sucrose density gradient centrifugation 25
2.17 Salt washing 25
2.18 Western blot analysis 26
2.19 Association of mRNAs with polysomes 26
2.20 *In vivo* translation assay 27
2.21 Split-Ubiquitin assay 27
2.22 Primers list 28
3 Results 29
3.1 GreenCut protein 9 (Gc9) is found in all photosynthetic eukaryotes 29
3.2. Gc9 knock-out plants grow slower than wild type plants 33
3.3 *Gc9::EGFP* overexpressors show the same growth phenotype as the wild type 36
3.4 Subcellular and suborganellar localization of Gc9 38
3.5 Photosynthesis is altered in *gc9-1* 39
3.6 Photosynthetic complexes are altered in *gc9-1* 45
3.7 Gc9 is not a subunit of the ATP synthase complex 47
3.8 Gc9 does not form a stable complex with the ATP synthase 48
3.9 The transcript abundances of chloroplast-encoded ATP synthase subunits are slightly altered in *gc9-1* 49
3.10 *atpH*-transcript-polysome loading and chloroplast protein synthesis are affected in *gc9-1* .. 51
3.11 AtpH monomer is enriched in the *gc9-1* mutant 53

3.12 Gc9 interacts with the AtpH subunit 55

4 Discussion 56

4.1 Photosynthetic electron transport rates are only moderately affected in *gc9-1* 56

4.2 Conserved secondary structure in Gc9 57

4.3 Upregulation of *atpH* transcripts can be a compensatory mechanism in response to an altered F_O assembly 58

4.4 Gc9 involvement in the AtpH co-translational membrane integration 59

4.5 Gc9 acts as an AtpH ring assembler in chloroplasts 59

4.6 Current model of the F_OF_1 ATP synthase assembly 61

5 References 64

Acknowledgements 82

***Curriculum vitae* 83**

Ehrenwörtliche Versicherung 85

List of figures

Figure 1.1 Assembly of photosynthetic protein complexes in the thylakoid membrane 9
Figure 3.1 Overview of *Gc9* mRNA expression in different tissues of *A.thaliana* 31
Figure 3.2 Characterization and protein sequence alignment of Gc9 33
Figure 3.3 T-DNA insertion mutant lines and growth phenotype of *gc9-1* and *gc9-2* 34
Figure 3.4 *Gc9* transcription and protein abundance in the two mutant lines 36
Figure 3.5 Complementation analyses by introducing a *Gc9::EGFP* overexpressor construct into *gc9-1* 37
Figure 3.6 Subcellular and suborganellar localization of Gc9 39
Figure 3.7 Leaves of 6 weeks-old wild type and *gc9-1* plants grown in the climate chamber under short day conditions 40
Figure 3.8 Chlorophyll *a* fluorescence induction kinetics of wild type and *gc9-1* plants 44
Figure 3.9 Imaging-PAM analyses of wild type, mutant (*gc9-1* and *gc9-2*) and two complemented plants 44
Figure 3.10 Photosynthetic complex abundance in wild type, *gc9-1* and *gc9-2* 46
Figure 3.11 Gc9 quantification analyses and abundance in different photosynthetic mutant lines 48
Figure 3.12 Comigration analysis of Gc9 with the ATP synthase complex 49
Figure 3.13 RNA gel blot analyses 50
Figure 3.14 Effect of Gc9 disruption on the translation of ATP synthase subunits 52
Figure 3.15 Blue Native analyses of wild type and *gc9-1* thylakoid membranes 54
Figure 3.16 Split-ubiquitin assays to test for transient interactions of Gc9 with photosynthetic complexes 55
Figure 4.1 Sequence alignment of the Gc9 transmembrane domain with Atp1 from various cyanobacteria 58
Figure 4.2 Current model of the F_OF_1 ATP synthase assembly 63

List of tables

Table 1.1 Subunit compositions of chloroplastic, mitochondrial (*S. cerevisiae*) and bacterial (*E. coli*) ATP synthase..... 3

Table 2.1 Primers used in Materials and methods. 28

Table 3.1 *Gc9* Coregulation with photosynthetic genes..... 30

Table 3.2 Leaf pigment analyses..... 41

Table 3.3 Photosynthetic parameters of wild type and *gc9-1* leaves were measured with the Dual-PAM system under moderate light intensities (100 µE m^{-2} s^{-1})..... 43

Abbreviations

°C	Degree Celsius
ADP	Adenosine diphosphate
ATP	Adenosine triphosphate
Ax	Antraxanthin
BN	Blue native
bp	Basepair
Car	Carotenoide
cDNA	Complementary deoxyribonucleic acid
CDS	Coding sequence
CF_1	Chloroplast coupling factor 1
CF_O	Chloroplast coupling factor O
Chl	Chlorophyll
CO_2	Carbon dioxide
Col-0	*Arabidopsis thaliana* background Columbia-0
Cub	C-terminus of Ubiquitin
Cyt b_6f	Cytochrome b_6f
DNA	Deoxyribonucleic acid
dNTP	Deoxyribonucleotide
DTT	Dithiothreitol
EDTA	Ethylene diamin tetraacetic acid
ETR	Electron transport rate
g	Gram
g	Force of gravity
GFP	Green fluorescent protein
GI	Gene Identification
h	Hour
HEPES	4-(2-hydroxyethyl)-1-piperazineethanesulfonic acid
H_2O_2	Hydrogen peroxide
HPLC	High performance liquid chromatography
IPTG	Isopropyl β-D-1-thiogalactopyranoside
kDa	Kilo Dalton
LEF	Linear electron flow
LHC	Light harvesting complex
Lut	Lutein
Lx	lutein epoxide
M	Mole(s) per litre
min	Minute
MOPS	3-(N-morpholino) propanesulfonic acid
mRNA	Messenger RNA
NADPH	Nicotinamide adenine dinucleotide phosphate
NPQ	Non-photochemical quenching
Nub	N-terminus of Ubiquitin
OE	Overexpressor
OEC	Oxygen evolving complex
PAGE	Polyacrylamide gel electrophoresis
PAM	Pulse amplitude modulation

PCR	Polymerase chain reaction
PFD	Photon flux density
Pi	Inorganic phosphate
PMSF	Phenylmethanesulfonylfluoride
PSI	Photosystem I
PSII	Photosystem II
PVDF	Polyvinylidene difluoride
qE	Energy- or pH-dependent quenching
qI	Photoinhibitory quenching
qT	State transition quenching
RNA	Ribonucleic acid
ROS	Reactive oxygen species
rRNA	Ribosomal RNA
RT-PCR	Reverse transcriptase-polymerase chain reaction
s	Second
S	Sedimentation coefficient
SDS	Sodium dodecyl sulphate
SPP	Stromal processing peptidase
T-DNA	Transfer- DNA
TIC	Translocon at the inner envelope membrane of Chloroplasts
TOC	Translocon at the outer envelope membrane of Chloroplasts
Tris	Tris(hydroxymethyl)-aminomethane
UTR	Untranslated region
VAZ	Xanthophyll cycle pigments
v/v	Volume per volume
Vx	Violaxanthin
WT	Wild type
w/v	Weight per volume
Zx	Zeaxanthin
β-DM	ß-dodecylmaltoside
µ	Micro
Φ	Effective quantum yield

1 Introduction

1.1 Photosynthesis

Photosynthesis is a photophysical and biochemical process in which light energy is converted into chemical energy and organic compounds. Cyanobacteria, algae and plants use H_2O as an electron donor and release oxygen during photosynthesis.

Oxygenic photosynthesis takes place in thylakoid membranes (Menke, 1962) which are located in the cytosol of prokaryotes (cyanobacteria) and in chlorophyll-containing organelles, the chloroplast, of algae and plants. The major photosynthetic complexes are multimeric proteins which are encoded by chloroplastic and nuclear genes (Sharma et al., 2007; Barkan, 2011 and Maier et al., 2008). Those protein complexes are light harvesting complex II and I (LHCII and LHCI), Photosystem II (PSII), Cytochrome b_6f complex (Cyt b_6f), Photosystem I (PSI) and the chloroplast ATP synthase (CF_1F_O-ATP synthase) (Nelson and Ben-Shem, 2004). Thylakoid membranes of land plants are organized in two parts, the grana stacks and the stroma lamellae which connect different grana stacks. PSII-LHCII complexes are mainly found in grana stacks, whereas PSI-LHCI and ATP synthase complexes are located in the stroma lamellae and in the edges of grana membranes. The Cyt b_6f complex is distributed throughout all the domains of the thylakoid membranes (Albertsson, 2001; Staehelin, 2003; Dekker and Boekema, 2005; Jansson et al., 1997; Vallon et al., 1991).

Light harvesting proteins (LHCI and LHCII) are attached non-covalently to PSII and PSI and absorb light energy which is transferred to the reaction centre of the two photosystems. Absorbed light energy drives electron transfer from H_2O to the final electron acceptor ($NADP^+$) through PSII, Cyt b_6f and PSI during linear electron flow (LEF). The linear electron transport is coupled to the generation of a proton gradient by oxidation of plastoquinone in the Q_0-center of the Cyt b_6f complex (Cramer et al., 2006). In addition, the oxygen evolving complex (OEC) of PSII releases protons by water oxidation. It was shown that during photophosphorylation, the proton concentration (pH) in the thylakoid lumen is about 6.0-6.2 and in the stroma 7.8-8.0, respectively. The difference in pH generates a transmembrane electrochemical proton gradient $\Delta\tilde{\mu}_{H^+}$ (or the so-called proton-motive force). In mitochondria, chloroplasts and in bacterial cells,

the proton-motive force is 11.6-19.3 kJ/mol, which is equivalent to 160-220 mV (Tikhonov, 2012). The major fraction of this energy is used for ADP to ATP conversion (Evron et al., 2000) by the ATP synthase complex. For each mol of NADPH generated by oxygenic photosynthesis, about 1.5 molecules of ATP are produced simultaneously. Generated ATP and $NADPH/H^+$ are used mostly for CO_2 and nitrate assimilation to synthesise carbohydrates and amino acids, but also for the biosynthesis of other organic substances such as nucleotides, lipids, vitamins, plant hormones and secondary metabolites.

1.2 ATP synthase structure

1.2.1 General aspects of ATP synthase

Mitochondria and chloroplast are known as the power sources in living cells. They generate biochemical energy by the ATP synthase complex. The free energy released from the ATP hydrolysis drives numerous cellular enzymatic reactions e.g., biosynthesis, mechanical motility, transport through membranes, regulatory networks and nerve conduction (von Ballmoos et al., 2009). The structure, composition and basic organisation of the ATP synthase is conserved among eubacteria, mitochondria and plastids (Strotmann et al., 1998; Groth and Pohl 2001).

The core subunit composition of the chloroplastic ATP synthase is like in mitochondria and bacteria but the mitochondrial ATP synthase contains 7–9 additional subunits, which are involved in oligomerization of the enzyme and also take over regulatory functions. ATP synthases share high amino acid sequence similarities within structural and functional regions (Walker et al., 1985), which suggests a common ancestry and a common core structure for all ATP synthases. It is also accepted that all ATP synthases undergo the same catalytic mechanism for ATP production or hydrolysis and the basic molecular mechanisms are essentially the same. The chloroplast ATP synthase belongs to the F_1F_O-type ATP synthase family, which is composed of two functionally and structurally different parts: 1) CF_O (chloroplast coupling factor O), a hydrophobic, membrane-embedded protein complex which is responsible for proton transport and 2) CF_1 (chloroplast coupling factor 1) which is a globular water-soluble protein complex and contains the nucleotide-binding site (s) for reversible ATP synthesis (Boekema et

al., 1988). Structure and function of CF_1 have been extensively studied by various biochemical and biophysical techniques, whereas CF_O is less characterised than CF_1 due to its high hydrophobicity (Seelert and Dencher, 2011).

CF_O is composed of four different polypeptides (AtpF/b/I, AtpG/b'/II, AtpH/c/III, AtpI/a/IV) with molecular weights of 19, 16.5, 8 and 25 kDa, respectively (Pick and Racker, 1979; Fromme et al., 1987a) and the subunit stoichiometry is I/II/III/IV=1/1/9-12/1 (Fromme et al., 1987b).

The CF_1 part has five different subunits (AtpA/α, AtpB/β, AtpC/γ, AtpD/δ and AtpE/ε) with molecular weights of 55.5, 53.8, 35.9, 20.5 and 14.7 kDa, respectively. The subunit stoichiometry is α/β/γ/ δ/ ε = 3/3/1/1/1 (Süß and Schmidt, 1982; Moroney et al., 1983).

The annotation varies among chloroplastic, mitochondrial and bacterial ATP synthase subunits. In addition, the mitochondrial ATP synthase contains subunits which are neither present in chloroplasts nor in bacteria (Table 1.1). To avoid confusion, subunits will be annotated according to the first column (Chloroplast) in table 1.1 throughout the dissertation. The two portions of the chloroplast ATP synthase are physically connected by two stalks: 1) a central stalk which is built up by the AtpC and AtpE subunits and 2) a peripheral stalk harbouring the AtpD, AtpF and AtpG subunits.

Table 1.1 Subunit compositions of chloroplastic, mitochondrial (*S. cerevisiae*) and bacterial (*E. coli*) ATP synthase

	Chloroplast	**Mitochondria (*S. cerevisiae*)**	**Bacteria (*E. coli*)**
F_1	AtpA	α	α
	AtpB	β	β
	AtpC	γ	γ
	AtpD	δ	ε
	AtpE	ε	-
	-	OSC	δ
F_O	AtpF	6	a
	AtpG	8	-
	AtpH	9	c
	AtpI	4	b
	-	d	-
	-	h	-
	-	f	-
	-	e	-
	-	g	-
	-	i	-
	-	k	-

1.2.2 CF_1 portion

In the CF_1 portion, three AtpA and three AtpB subunits are arranged in a hexamer with alternating AtpA and AtpB subunits, whereas AtpC, AtpD and AtpE subunits are present in single copies. Each AtpA and AtpB subunits harbour a single nucleotide site. The catalytic sites are located on the AtpB subunits, whereas regulatory sites are placed on AtpA subunits (Richter et al., 2000). The central cavity of the hexamer is partially filled by subunit AtpC, which was shown by direct labelling of –SH groups engineered in the AtpC subunit of the *Escherichia coli* enzyme (Groth and Strotmann, 1999). The AtpC subunit forms a coiled-coil structure which is bound to the three AtpA/B pairs and plays a regulatory role in the catalytic activity of the ATP synthase. It was assumed that AtpD and AtpE subunits are involved in the functional connection between CF_1 and CF_O (Patrie and McCarty, 1984). The AtpE subunit functions as a negative regulator of ATP synthase activity and probably links conformational changes between CF_1 and CF_O during proton translocation via incorporation with the AtpC subunit.

1.2.3 CF_O portion

In the CF_O portion, subunit AtpF and AtpG share similar amino acid sequences. They contain a single transmembrane helix in interaction with CF_1. Subunit AtpF is linked to subunit AtpD (Beckers et al., 1992) and subunit AtpG connects CF_O to CF_1.

Subunit AtpH forms a hairpin like structure and consists of two α-helices. Those subunits are also called proteolipids because of their high hydrophobicity in organic solvents (Folch and Less, 1951). The hairpin loop is orientated towards the stroma and its terminal domains are submerged into the thylakoid lumen. The number of subunit AtpH for ring assembly varies from 8 (mitochondria in animals) to 15 (in the cyanobacterium *Spirulina platensis*) in different organisms (Watt et al., 2010; Pogoryelov et al., 2005). In chloroplasts of higher plants 14 copies of subunit AtpH form a channel for proton traslocation through the membrane (Vollmar et al., 2009).

1.3 ATP synthase function

During photophosphorylation, the ATP synthase complex snythesizes ATP from ADP and inorganic phosphate (P_i) by making use of the transmembrane proton gradient. The kinetics of this process can be described by the Michaelis-Menten equation. The binding of the ADP and phosphate to the catalytic site on subunit AtpB occurs in a random fashion (Kothen et al., 1995) but binding of the first substrate increases the affinity of the second substrate which is known as stochastic binding mechanism (Groth and Junge, 1993).

The nucleotide-bound states on AtpB subunit are in different conformational states during catalysis (Boyer, 1993). The binding of both substrates, ADP and Pi, takes place in the loose site (L), whereas the ATP generation and ATP dissociation occur in the tightly (T) and empty (O) sites, respectively. Those three different conformational states appear during one complete rotation of the AtpC subunit in a stepwise 120° motion which can be observed at very low ATP concentration (Yasuda et al., 1998). The stored energy in the transmembrane proton gradient is used for the substrate (ADP, Pi) binding and/or ATP dissociation and/or opening of the catalytic sites situated on the AtpB subunits.

The catalytic sites are located in the CF_1 portion, whereas luminal proton efflux occurs in the membrane embedded CF_O domain, which also contains the motor for the ATP generation. The latter is composed of the AtpH and AtpI, where subunit AtpH assembles into a ring. In chloroplasts of higher plants 14 copies of AtpH are assembled to form a circular structure which serves as a channel for proton translocation through the membrane (Vollmar et al., 2009). Each AtpH subunit mediates one proton translocation per turn of the ATP synthase. Thus, 14 protons are required for a full turn of the ATP synthase and yield three ATP molecules (Seelert et al., 2000).

Subunits AtpH and AtpI of CF_O are directly involved in transmembrane proton transport. The carboxyl group of Glu61 in AtpH subunit acts as an acceptor for protons coming from the acidic side (lumen) through the input channel. Protonated AtpH subunits than rotate along with the AtpH ring and thereby consecutively release their protons on the alkaline side (stroma) through the output channel (Nelson and Cox, 2005).

The salt bridge between the Glu61 residue (in *E. coli*: Asp61) of one of the subunits AtpH and the Arginine 210 (R210) residue of subunit AtpI is dissociated from the proton-accumulated membrane side by protonation and causes a ratchet-type motion of the rotor (Wang and Oster, 1998). The other critical amino acids for proton translocation in AtpI subunit are E219 (Glutamic acid 219) and H245 (Histidine 245) residues, which are required for proton binding and guidance towards the negatively charged membrane side.

The torque of the AtpH ring might be transmitted to the AtpA/B hexamer via the AtpC and AtpE subunits. The rotation of the AtpC subunit (rotor) induces the conformational rearrangements in each of the three catalytic binding sites of the AtpB subunits (Weber and Senior, 2000).

1.4 ATP synthase regulation

The regulation of ATP synthase activity is important to avoid futile ATP hydrolysis under transient light/dark conditions and to induce ATP synthesis only in the presence of an electrochemical proton gradient. Multiple regulatory mechanisms exist for this purpose. Mg-ADP is an inhibitor of the ATP synthase activity which binds tightly to catalytic and regulatory sites on the AtpA/B hexamer in the dark and prevents subsequent ATP hydrolysis (Bar-Zvi and Shavit, 1982; Vasilyeva et al., 1982). This tight binding of ADP may restrict the rotation of the AtpC subunit within the AtpA/B hexamer, thereby proton translocation through CF_O is inhibited (Richter et al., 2000). During thylakoid illumination, proton flow through CF_O decreases the affinity for ADP binding to the regulatory site, thereby inducing ATP synthase activity. The rotation and conformational changes of central α helices is involved in coupling proton translocation to ATP synthesis, regulation of proton flux and ATP synthase activity (Hisabori et al., 1997; Richter et al., 2000; Sunamura et al., 2012).

Several modifications in the AtpC subunit regulate the ATP synthase activity. The redox-dependent regulation is an exclusive feature for chloroplast ATP synthases in which thiol groups are present in the AtpC subunit (Hisabori et al., 2003). In this process, reduced thioredoxin induces the conformational change of a regulatory domain (Cys199-Cys205) on the AtpC subunit which leads to the reduction of the disulfide bond. The energetic threshold of the ATP

synthesis and proton translocation is lowered by the reduction of disulfide bonds which causes enhanced photophosphorylation (Evron and McCarty, 2000). Therefore, the catalytic activity of the ATP synthase enzyme is regulated by proton accumulation and a redox-state dependent process, in which a disulfide bond in the AtpC subunit is reversibly oxidized and reduced (Mills et al., 1995).

The AtpE subunit plays a role in coupling of proton flow to the ATP synthesis. An extended C-terminal helix-turn-helix structure inhibits the ATP synthase activity to prevent ATP consumption (Richter et al., 1984; Yagi et al., 2007). The oxidized, inactive form of the ATP synthase (in the dark) shows neither ATP hydrolysis nor synthesis activity. In the inactive ATP synthase form, subunit AtpE interacts tightly with CF_1 subunits and thereby AtpC and AtpE subunits are inhibited from rotation by the AtpA/B hexamer. In illuminated thylakoids, conformational changes in the AtpC and AtpE subunits induce movements of these subunits that cause disulfide reduction and AtpC (Cys89) modification. The disulfide bond reduction induces an additional conformational change. The binding affinity of subunit AtpE for CF_1 subunits is lowered and then ATP is synthesized at physiological ΔpH values (Soteropoulos et al., 1992).

1.5 Assembly of photosynthetic protein complexes

1.5.1 A dual genetic origin of photosynthetic proteins

Chloroplasts contain about 3000 different proteins, most of them (> 90 %) are encoded in the nucleus and only a few are chloroplast-encoded polypeptides (Figure 1.1). The nuclear-encoded subunits are synthesized as precursor forms on free cytosolic ribosomes (Keegstra and Cline, 1999; Abdallah et al., 2000; Leister, 2003). Those proteins must be directed to the chloroplast, inserted and folded into the correct conformation. The precursor form contains a transit peptide which is an amino-terminus targeting signal. The precursor proteins are transported post translationally into the chloroplast in an energy-dependent process called chloroplast protein import.

The chloroplast protein import is mediated by protein complexes situated in the outer and inner envelope membranes and are called TOC and TIC (Translocon at the Outer/Inner envelope

membrane of Chloroplasts). The TOC complex is composed of Toc159, Toc34 and Toc75 components. The first two (Toc159 and Toc34) mediate transit peptide recognition and Toc75 forms a channel for precursor protein conductance (Soll and Schleiff, 2004; Li and Chiu, 2010). Different chaperones are required for chloroplast protein import at different stages. Cytosolic factors such as Hsp90, Hsp70 and 14-3-3 proteins may guide pre-proteins to reach the TOC complex and to prevent their misfolding, aggregation or degradation (Zhang and Glaser, 2002; Gokirmak et al., 2010; Qbadou et al., 2006). The chaperone Hsp70 mediates precursor protein passage through the intermembrane space and plays a role in the stroma but the information about this chaperone is still inconclusive (Becker et al., 2004). The stromal chaperones, Hsp93 in cooperation with Tic110 and Tic40 and Hsp70 act to maintain translocation competence of the precursor proteins and to drive transport at the expense of ATP hydrolysis (Balsera et al., 2009; Bukau et al., 2006).

When precursor proteins arrive in the stroma, the transit peptide is removed by the stromal processing peptidase (SPP) and chaperones such as Hsp70, Cpn60, cpSRP43 are involved in their folding, assembly and transport to the internal destinations (Cline and Dabney-Smith, 2008; Li and Chiu, 2010 ; Jackson-Constan et al., 2001).

The first step in the assembly of photosynthetic complexes is the insertion of subunits which act as a scaffold for subsequent assembly steps. Those dominant subunits are D2 for PSII, PsaB for PSI and PetB for Cyt b_6f. In the absence of scaffold proteins, translation of the next protein to be inserted into the complex is inhibited. This type of regulation is called “control by epistasy of synthesis (CES)” and was found to be valid for PSII, the Cyt b_6f, and the ATP synthase complex (Rochaix, 2011). Genetic and biochemical studies have shown that both general and complex-specific factors are needed to assemble functional complexes. An example for a general assembly factor is the nuclear-encoded Albino 3 (ALB3) which is required for the integration of the LHC proteins into thylakoid membranes in vascular plants and green algae (Chlamydomonas). This protein shows homology to the mitochondrial Oxa1p and bacterial YidC proteins (Sundberg et al., 1997; Bellafiore et al., 2002). Oxa1 is involved in the assembly of the cytochrome oxidase, ATP synthase and the cytochrome bc1 complex into the inner membrane of yeast mitochondria (Bauer et al., 1994; Bonnefoy et al., 1994; Jia et al., 2007; Altamura et al.,

1996). YidC is involved in the insertion of most inner membrane proteins in *E. coli* (Urbanus et al., 2002). Also a large number of complex-specific assembly factors were identified e.g., Ycf3, Ycf4, and Ycf37 which are PSI-specific assembly factors (Naver et al., 2001; Ozawa et al., 2009; Dühring et al., 2007).

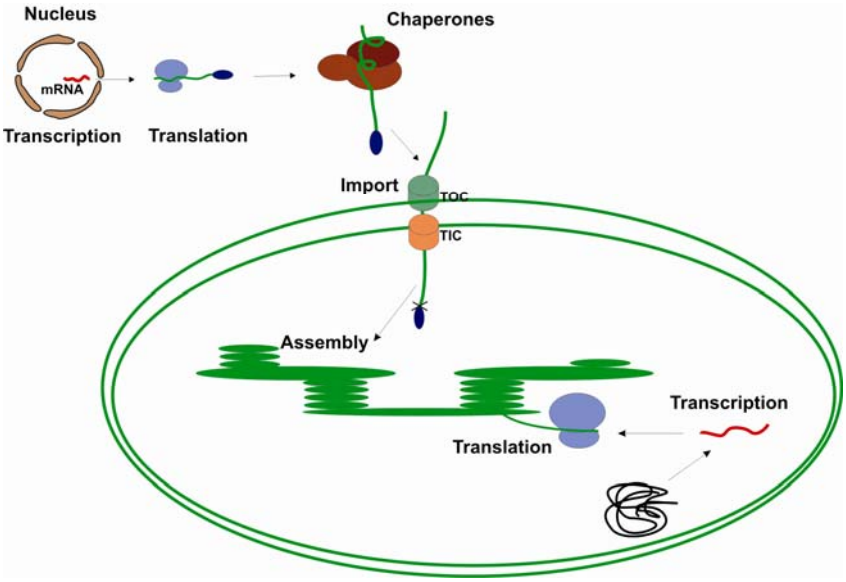

Figure 1.1 Assembly of photosynthetic protein complexes in the thylakoid membrane

Nuclear-encoded subunits are translated on cytoplasmic ribosomes and then transported into the chloroplast. The chloroplast protein import is mediated by the two TOC and TIC protein complexes. Chloroplast-encoded subunits are translated by the chloroplast translation machinery and inserted directly into the thylakoid membrane. In the last step, imported subunits and plastome-derived subunits are assembled into functional complexes in the thylakoid membrane.

1.5.2 ATP synthase assembly factors

The ATP synthase assembly process in chloroplast is less understood than the assembly process in *E. coli* and yeast cells. The biochemical study of ATP synthase biogenesis in yeast cells is not simple, because of the rapid turnover of some F_O and stator subunits in ATP synthase-deficient mutants (Contamine and Picard, 2000). To assemble a functional ATP synthase a series of factors for subunit recognition, for establishing correct interactions and for correct folding are required. In addition, several nuclear-encoded factors which have a function at pre- and post-translational steps of the biogenesis pathway have been characterized (Pícková et al., 2005).

Some substrate-specific proteins were identified in *Saccharomyces cerevisiae* which have a chaperone type function: Atp10p, Atp11p, Atp12p, Atp22p and Fmc1p. Atp10p, Atp11p and Atp12p are general ATP synthase assembly factors which are present in the majority of eukaryotic organisms, whereas Fmc1p and Atp22p are yeasts-specific ATP synthase assembly factors.

Atp11p and Atp12p belong to the families of molecular chaperones *pfam06644* and *pfam07542*, respectively, which are needed for mitochondrial ATP synthase assembly in all eukaryotic cells (Marchler et al., 2003). Atp11p and Atp12p mediate the formation of the mitochondrial F_1 via transient interactions with AtpB and AtpA subunits, respectively. The absence of those factors leads to AtpA/AtpB aggregation into insoluble inclusion bodies in the mitochondrial matrix (Ackerman, 2002). Atp11p/AtpB and Atp12p/AtpA interactions prevent the formation of functional inactive AtpA/AtpA, AtpB/AtpB and AtpA/AtpB complexes. Subsequently, subunit AtpC initiates the release of chaperones from AtpA and AtpB subunits and binds to the mature complex (Ludlam et al., 2009).

Atp10p and Atp22p are required for the formation of the mitochondrial F_O. Atp10p acts in the incorporation of the F_O-AtpF subunit (Ackerman and Tzagoloff, 1990; Helfenbein et al., 2003). The role of Fmc1p is unclear but it seems to be associated with F_1 assembly and is required for correct folding of Atp12p (Lefebvre et al., 2001).

1.6 Photoprotection

1.6.1 Heat dissipation of excess light energy as a photoprotective mechanism

Light is one of the most important environmental factors for photosynthetic organisms. But excess light energy leads to the formation of reactive oxygen species (ROS) (mainly hydrogen peroxide (H_2O_2)) and singlet oxygen ($^1O_2^*$), which cause photo-oxidative damage of the photosynthetic complexes and of other cellular components. Photosynthetic organisms have evolved a series of mechanisms for sensing and responding to excess light energy.

Different classes of photoreceptors, including phototropins, phytochromes, neochromes, rhodopsins and cryptochromes are involved in sensing high light (Li et al., 2009). In addition, excess light energy can be sensed indirectly via metabolic (e.g., accumulation of Chl intermediates) and biochemical signals (e.g., production of ROS and changes in thylakoid lumen pH) which trigger protective responses. These responses include several mechanisms like chloroplast movements, changes in gene expression and non-photochemical quenching.

Heat dissipation of excess light energy (NPQ= non-photochemical quenching) is an important photoprotective mechanism leading to the reduction of ROS generation which is as an indicator for oxidative stress (Jahns and Holzwarth, 2012). At least three different NPQ components exist: 1) qE, energy- or pH-dependent quenching (Krause et al., 1982), 2) qT, state transition quenching (Allen et al., 1981) and 3) qI, photoinhibitory quenching (Krause, 1988). In Arabidopsis, the relative contribution of those components is dependent on the light intensity and light exposure time. Total NPQ at moderate light intensities under short time illumination (10-200 s) can be mainly attributed to pH-dependent quenching (qE). qI is the dominant component at high light intensity and longer light exposure (> 30 min) which leads to degradation of D1 (Nilkens et al., 2010; Lambrev et al., 2010). qT does not contribute significantly to NPQ in higher plants (Nilkens et al., 2010).

The induction of qE occurs in minutes and is independent of gene expression but is dependent on the proton gradient formation across the thylakoid membrane (Briantais et al., 1979), PsbS (Li et al., 2002) and xanthophyll cycle activation (Demmig et al., 1987). The qE component is controlled by the PsbS protein which acts as a pH-sensing protein in vascular plants (Li et al.,

2004). Monomerization of a PsbS dimer and association with the antenna proteins occur at low lumen pH (high light), whereas the PsbS dimer is associated with the PSII reaction center in low light or darkness (Bergantino et al., 2003). The decrease in thylakoid lumen pH generates a signal under excess light absorption. The signal is transferred to PSII antenna proteins, induces their conformational changes or changes in the protein-protein interactions and trigger qE activation. Two quenching sites were identified in higher plants which are active in the regulation of photosynthetic light-harvesting. The PsbS-dependent quenching site (Q1) is located in the LHCII and becomes detached from photosystem II (PSII) and a Zx-dependent quenching site (Q2) which is located in the remaining antenna of PSII (Holzwarth et al., 2009).

1.6.2 Xanthophylls and photoprotection

Xanthophylls are assumed to be photoprotective isoprenoids that play a role either directly or indirectly in non-photochemical quenching processes in the antenna of PSII (Li et al., 2009; Horton et al., 2005).

Two different xanthophyll cycles are known to be important for photoprotection in land plants: 1) violaxanthin (Vx) cycle and 2) lutein epoxide (Lx) cycle. The violaxanthin cycle is present in all land plants in which violaxanthin is reversibly converted to zeaxanthin via antheraxanthin (Jahns et al., 2009). The lutein epoxide cycle is present in some species, in which lutein epoxide is reversibly converted into lutein (Garcia-Plazaola et al., 2007; Esteban et al., 2009). Vx and Lx are epoxidized forms of xanthophylls which are present in low light or darkness, whereas de-epoxidized xanthophylls (Zx, Ax and Lut) are present in excess light energy.

The decrease in luminal proton concentration and saturated electron transport under high light activate the violaxanthin de-epoxidase enzymes via conformational changes (Kalituho et al., 2007). The activated enzymes convert violaxanthin to zeaxanthin causing zeaxanthin accumulation under excess light energy. Zx is involved in the deactivation of excited singlet chlorophylls in the antenna of PSII and also acts as an antioxidant in the lipid phase of the thylakoid membrane under extreme high light stress (Havaux et al., 2007). The exact role of Zx in qE is still not clear but it was shown that qE can be modulated by Zx (Johnson et al., 2008).

The most abundant xanthophyll, lutein, plays a role in photoprotection of PSII by deactivation of triplet chlorophyll in higher plants (Mathis et al., 1979). Lutein is also involved in structural stabilization of antenna proteins and excitation energy transfer to chlorophylls (Siefermann-Harms, 1985).

1.7 GreenCut proteins

Extensive genetic, biochemical and structural analyses have been performed to elucidate the architecture of photosynthesis and to identify the function of photosynthesis-relevant factors (Eberhard et al., 2008; Nelson and Ben-Shem, 2004). But gaps of knowledge especially in biogenesis of photosynthetic complexes and regulation of photosynthesis are still existent. Forward genetic screens of mutants affected in photosynthesis have been employed to identify new factors (Dent et al., 2005). A new approach to identify important proteins involved in photosynthesis is the use of comparative genomic analyses. This type of reverse genetic approach has become more and more popular since the number of sequenced genomes has increased almost exponentially over the last decades making phylogenomic comparison analyses more robust. In 2007, Merchant and co-workers released the ~120-megabase-long nuclear genome of Chlamydomonas in line with extensive comparative phylogenomic analyses. The comparison of the *Chlamydomonas reinhardtii* proteome with the proteome of the higher plant *Arabidopsis thaliana*, the moss *Physcomitrella patens*, the two algae *Ostreococcus tauri, Ostreococcus lucimarinus* and the proteome of human revealed that 349 proteins are conserved in photosynthetic organisms but not in non-photosynthetic organisms. In a second version (GreenCut2), additional sequenced genomes (*Micromonas*, *Selaginella* and soybean) have been included in the phylogenomic comparison resulting in a cross section of 597 proteins which are conserved in plants, moss and green algae but which are absent in non-photosynthetic organisms. GreenCut proteins are likely associated with photosynthesis and chloroplast function. However, 311 proteins of the GreenCut2 proteins (52 %) are not functionally characterized yet. Not all of those proteins play directly a role in photosynthetic processes but can be involved in maintenance of chloroplast structure and function or in plant-specific processes e.g., signalling or regulatory activities. Based on gene ontology and molecular functions of predicted domains,

unknown GreenCut2 proteins have been placed in three different functional groups (Karpowicz et al., 2011): 1) Photosynthesis, Redox and Pigments, 2) Macromolecular Metabolism and Signaling and 3) Uncategorized proteins.

Group 1 contains 62 proteins with confirmed or predicted chloroplast localization. The three proteins with unknown function in this group are CrCGL30 (At1g77090), CrCGL40 (At1g49975) and CrCGL160 (At2g31040).

1.8 Aim of this thesis

The aim of the thesis was to elucidate the function of one of the GreenCut proteins (At2g31040, named Gc9) by in-depth biochemical and genetic characterization. The effect of *Gc9* disruption on photosynthetic function was examined by chlorophyll *a* fluorescence measurements and by leaf pigment analyses. In addition, the effect of the mutationon on the abundance of photosynthetic protein complexes was analyzed. When it became clear that *Gc9* disruption leads to a defect in ATP synthase complex abundance, the potential role of Gc9 in transcription, translation and assembly of ATP synthase subunits was studied. Moreover, interactions of Gc9 with subunits of the membrane-embedded CF_O complex were tested by the split-ubiquitin system. Finally, the entire experimental informations were combined to establish a model for Gc9 protein function in the assembly of the chloroplast ATP synthase complex in *Arabidopsis thaliana*.

2 Materials and Methods

2.1 Plant material

2.1.1 *Arabidopsis thaliana* mutant lines

Two T-DNA insertion Arabidopsis mutant lines for the *Gc9* gene (*At2g31040*) were used in this work. The *gc9-1* line (SALK_057229) was obtained from the SALK collection and contains a ROK2 T-DNA insertion (Alonso et al., 2003), whereas the *gc9-2* line (WiscDsLoxHs024_02B) was obtained from the Wisconsin DsLox T-DNA collection (Woody et al., 2007). Both lines are in *Columbia-0* ecotype background.

2.1.2 Complementation of *gc9-1* mutant lines

The *Gc9* coding sequence (without the stop codon) was amplified using Gateway primers (for primer information see Table 2.1), and the Phusion DNA polymerase (Finnzymes, Finland Vantaa) according to the manufacturers instructions. The amplified region was introduced into the binary Gateway destination vector pB7FWG2.0 (Karimi et al., 2002) under the control of the *Cauliflower Mosaic Virus* 35S promoter using the Gateway LR Clonase enzyme mix (Invitrogen®). In the obtained construct, the *Gc9* coding sequence is fused at the C-terminus with green fluorescent protein (eGFP) from *Aequorea Victoria*. The final construct was introduced into the *Agrobacterium tumefaciens* strain GV3101, which was then used to transform *gc9-1* plants, by floral dip (Clough and Bent, 1998). For this purpose, *gc9-1* plants were grown on soil under greenhouse conditions and then the flowers of 30-day-old Arabidopsis plants were dipped into *A. tumefaciens* suspension containing 5 % (w/v) sucrose and 0.0005 % (v/v) surfactant Silwet L-77, for 1 min. After dipping, plants were covered with plastic bags for two days and transferred to the greenhouse. Seeds were collected 4 weeks after transformation and BASTA (glufosinate ammonium)-resistant T1 plants were selected after BASTA treatment. The insertion of the *Gc9::EGFP* coding region into the *gc9-1* genome was verified by Northern blot analyses and by immunodetection of the EGFP::Gc9 fusion protein. Successful

complementation was confirmed by measurements of leaf area surfaces from 8 to 25 day-old plants grown under short day conditions and by Non-Photochemical Quenching measurements described in the section 10.2.

2.2 Plant growth conditions

Arabidopsis thaliana wild-type and mutant seeds were stratified in Petri dishes on wet Whatman paper and placed for two days at 4 °C to break dormancy. Subsequently, seeds were transferred on potting soil (A210, Stender AG, Schermbeck, Germany) and grown under greenhouse-controlled conditions (PFD: 70-90 µmol m^{-2} s^{-1}, 16/8 h light/dark cycles) or in climate chambers. Different light regimes were used for plant growth when they were grown in climate chambers (short day: 16h/8h dark/light, normal day: 12h/12h dark/light, long day 8h/16h dark/light). Fertilizer (Osmocote Plus: 15 % N, 11 % P_2O_5, 13 % K_2O, 2 % MgO) was added according to the manufacturer's instruction (Scotts Deutschland GmbH, Nordhorn, Germany). For growth curve comparison, leaf area surfaces from 8 to 25 day-old plants were calculated by using the ImageJ software (Abramoff et al., 2004).

MS (Murashige-Skoog, Duchefa Co., The Netherlands) plates supplemented with 1.5 % (w/v) sucrose were used to grow mutants which are not able to survive photoautotrophically (*psad*, *atpd*, *petc* and *hcf136*) and to select resistant plants after transformation. For this purpose, seeds were first treated for 8 min with 70 % ethanol and then 8 min with a solution containing 7.5 % hypochloride and 0.5 % Triton X-100. Sterilized seeds were washed four times with sterile water and plated on sterile MS plates containing 1.5 % (w/v) sucrose and 0.7 % (w/v) agar. Seeds were incubated in the dark at 4 °C for 48 hours and then transferred into the climate chamber (16 h/8 h light dark cycle) at 22 °C.

Transformed plants were grown on MS medium containing kanamycin (25 µg/ml) for 3 weeks under low light. Then, plants were transferred on soil and grown under greenhouse conditions.

2.3 Bioinformatic sources

Protein and gene sequences were obtained from the Arabidopsis Information Resource server (TAIR; http://www.arabidopsis.org) and the National Center for Biotechnology Information server (NCBI; http://www.ncbi.nlm.nih.gov/). The Vector NTI software (Invitrogen®) was used for protein sequence alignments. Transit peptide lengths were predicted using ChloroP 1.1 (http://www.cbs.dtu.dk/services/ChloroP/), and transmembrane helices were predicted by Aramemnon (http://aramemnon.botanik.uni-koeln.de/), MINNOU (http://minnou.cchmc.org) or SCAMPI (http://scampi.cbr.su.se/), respectively. Alignments were formatted using Boxshade 3.21 (http://www.ch.embnet.org/software/BOX_form.html). Gene expression levels of *Gc9* in different tissues of *Arabidopsis thaliana* were examined by the "Bio-Array Resource for Plant Biology" platform (http://bar.utoronto.ca/efp/cgi-bin/efpWeb.cgi). Sequence identifiers for Gc9 homologs in eukaryotic organisms are: *Vitis vinifera* (GI: 225446613), *Oryza sativa* (GI: 125532550), *Zea mays* (GI: 413950882), *Picea sitchensis* (GI: 148907731), *Selaginella moellendorffii* (GI: 302814051), *Physcomitrella patens* (Pp1s184_139V6.4) and *Chlamydomonas reinhardtii* (GI: 159464014). Sequence identifiers for Gc9 homologs in cyanobacteria and *Propionigenium modestum*are: *Synechocystis spec*. (GI: 443313485), *Synechococcus spec*. (GI: 170077363), *Cyanothece spec.* (GI: 220906906), *Anabaena variabilis* (GI: 75908831), *Gloeocapsa spec.* (GI: 434391846), *Calothrix spec*. (GI: 428298284), *Nostoc punctiforme* (GI: 186684951), *Nostoc spec.* (GI: 427707295) and *Propionigenium modestum* (GI: 45648).

2.4 Genomic DNA extraction and recovery of the T-DNA flanking sequences

Genomic DNA was isolated from three-week-old Arabidopsis leaves. Leaves were frozen in liquid nitrogen and then grounded with metal beads. DNA was isolated by using an extraction buffer containing 0.25 M NaCl, 0.2 M Tris-HCl, pH 7.5, 25 mM EDTA and 0.5 % SDS. First, DNA was precipitated using 0.7 % volumes of isopropanol and then centrifuged for 30 min at 4,700 *g*. The pelleted DNA was washed with 70 % ethanol, centrifuged again for 15 min at

16,000 *g* and then resuspended in 100 µl ultrapure water containing 0.02 mg/ml RNAse A (Invitrogen, Karlsruhe, Germany). 1 µl of genomic DNA was used for a 10 µl reaction in PCR analyses. To identify the exact T-DNA insertion site in the genomic DNA insertion- and gene-specific primers were employed in PCR assays (see primers list). The resulting PCR products were gel-purified and then sequenced by means of the sequencing service at the LMU München (http://www.genetik.biologie .uni/münchen.de/sequencing).

2.5 RNA extraction

Total RNA was extracted from powdered leaves (100 mg) using 4 ml of TRIzol reagent (Invitrogen®). Chloroform (200 µl) was then added to the supernatant. After incubation for 15 min at room temperature, the organic and the aqueous phase were separated by centrifugation for 10 min at 12,000 *g* at 4 ^{o}C. RNA in the aqueous phase was precipitated with isopropanol and a high salt solution (0.4 M Na citrate, 1.2 M NaCl) and then washed with 70 % ethanol. Air-dried RNA was resuspended in DEPC water and RNA concentration was measured by UV/visible spectrophotometer (Amersham Bioscience).

2.6 Northern analysis

Northern blot was performed as described in (Sambrook and Russell, 2001). In brief, 5 µg of total RNA was denatured and electrophoretically separated in formaldehyde-containing agarose gels (1.5 %) using a MOPS running buffer (20 mM MOPS, pH 7.0, 5 mM NaAc, 1 mM EDTA). RNA transfer onto nylon membranes (Hybond-N+, Amersham Bioscience) was carried out using SSC buffer (1.5 M Nacl, 0.15 M sodium citrate, pH 7.0). RNA was crosslinked to the membrane by UV radiation (Stratalinker® UV Crosslinker 1800). Methylene blue staining of rRNAs (0.02 % (w/v) methylene blue, 0.3 M sodium acetate, pH 5.5) was performed to control equal loading. Membranes were pre-hybridized at least for 4 hours at 65 °C with pre-warmed hybridization buffer (7 % SDS, 0.25 M Na_2HPO_4, pH 7.0) containing denaturated Herring sperm DNA. To identify *Gc9*- and ATP synthase-specific transcripts, amplified DNA fragments from cDNA were labeled with radioactive [α-P^{32}] dCTP and subsequently used for hybridization at 65 °C

overnight. Hybridized membranes were treated twice with washing buffer (0.1 % SDS, 2x SSPE) at 60 °C (first time for 30 min and second time for 15 min) and then exposed to the Storage Phosphor Screen (Fuji). Signals were detected and quantified by the Typhoon Phosphor Imager (GE Healthcare, Munich, Germany) and the Bioprofile software (Peqlab, Erlangen, Germany), respectively.

2.7 cDNA synthesis and RT-PCR analysis

For cDNA synthesis, 1 µg RNA was mixed with 1 µl oligo (dT) (500 mg/µl) primers, heated for 5 min at 65 °C and incubated for 1 min on ice. Then, 1 µl dNTP (10 mM), 4 µl 5x first strand buffer (Invitrogen), 1 µl DTT (0.1 M), 1 µl H_2O and 1 µl of Superscript III reverse transcriptase (Invitrogen) were added and heated for 60 min at 50 °C and for 15 min at 70 °C. The quality of synthesized cDNA was tested by PCR using a primer combination for Ubiquitin. Synthesized cDNA was diluted 1:10 in DEPC water for RT-PCR and Real time PCR. *Gc9* transcript levels were analyzed in semi-quantitative PCR (RT-PCR) assays using primers for amplicons flanking the T-DNA insertion sites (see primers list). The RT-PCR program includes an initial denaturation step (94 °C for 3 min) followed by 25 cycles of denaturation (94 °C for 15 sec), annealing (55 °C for 45 sec) and extension (72 °C for 90 sec). Electrophoretic analyses of PCR products were performed on 1-2 % (w/v) agarose gels supplemented with 0.5 µg/ml ethidium bromide in TAE buffer (40 mM Tris-acetate, 20 mM Sodium acetate, 2 mM EDTA, pH 8.2).

2.8 Real time PCR analyses

PCR reaction samples for Real-time PCR analyses are composed of iQ™ SYBR Green Supermix (Bio-Rad, California, USA), transcript-specific primers (see primers list) and cDNA as template. A control reaction without template cDNA was included, in order to calculate primer-dimer formation. Ubiquitin was employed as a reference gene. The PCR program consisted of an initial denaturation step (at 95 °C for 5 min) which was followed by 40 cycles of denaturation (95 °C for 20 sec), annealing (57 °C for 20 sec) and extension (72 °C for 20 sec). DNA amplification was monitored by detecting SYBR-Green fluorescence signals at 530 nm at the

end of each extension period. The fluorescence signals was detected by IQ™5 Multicolor Real time PCR Detection system (Bio-Rad) and then gene expression was calculated using the iQ5™ Optical System Software (Bio-Rad).

2.9 Leaf pigment analysis

Leaves from 5-week-old wild type, *gc9-1* and transgenic *oeGc9::EGFP* plants grown under short-day conditions were harvested 4 h after simulated sunrise. The harvested leaves were powdered in liquid nitrogen and incubated with 100 % acetone on ice for 10 min in the dark. Centrifugation at 16,000 *g* for 20 min at 4 °C was performed and supernatants were transferred into new tubes. Pigment compositions in the supernatants were analyzed by reverse-phase HPLC as described in Färber et al. (1997).

2.10 Chlorophyll a fluorescence measurement (PAM)

In vivo chlorophyll *a* fluorescence was measured by using the Dual-PAM (Pulse Amplitude Modulation) 101/103 fluorometer (Walz GmbH, Effeltrich, Germany). Slow induction and dark relaxation kinetics were measured according to Roháček (2010). Single leaves of dark adapted (20 min) plants grown under short day conditions were first exposed shortly (30 sec) to measuring light for minimal chlorophyll fluorescence yield determination (F_0). Then, a saturating light pulse (10,000 µE m^{-2} s^{-1}, 800 ms) was applied for maximal chlorophyll fluorescence yield determination (F_m). The maximal quantum yield (F_v/F_m) - which reflects PSII functionality - was calculated by the formula $F_V/F_m = (F_m - F_0)/F_m$. Actinic red light was applied for 15 min and steady-state fluorescence yields (F_S) were measured. A saturating light pulse (10,000 µE m^{-2} s^{-1}, 800 ms) at the end of the light phase was applied to determine the maximal fluorescence yield in the light (Fm'). After the dark relaxation phase (10 min), F_m'' and F_0'' were measured by applying a saturating light pulse (10,000 µE m^{-2} s^{-1}, 800 ms). Parameters were calculated as follows:

Effective quantum yield of PSII: $\Phi_{II} = (F_m' - F_0')/F_m' = F_v'/F_m'$

Estimation of minimal fluorescence yield in the light: $F_0' = F_0 / (F_v/F_m + F_0/F_m')$

Electron transport rate through PSII: ETR (II) = ΦII * PAR * 0.84 * 0.5

Excitation pressure: 1- qP = 1 - $(F_m' - F_S) / (F_m' - F_0')$

Nonphotochemical Chl fluorescence quenching: NPQ = $(F_m - F_m') / F_m'$

Nonphotochemical quenching of variable Chl fluorescence:

qN = $((F_m - F_0) - (F_m' - F_0')) / (F_m' - F_0') = 1 - F_v'/F_v$

Energy-dependent quenching of Chl fluorescence: qE = $F_m''/F_m' - F_m/F_m''$

Photoinhibitory quenching: $qI = qI^{DAS} + qI^{LAS} = (0.83 - F_v/F_m) + (F_v - F_v'')/F_v$

Additionally, slow induction and dark relaxation assays were performed under increasing actinic light intensities (13, 22, 53, 95, 216, 339 and 531 µmol m^{-2} s^{-1}) in seven successive measurements to determine ETR, NPQ, qE and qI.

The imaging chlorophyll fluorometer (Walz Imaging PAM, Walz GmbH, Effeltrich, Germany) was used to determine chlorophyll *a* fluorescence parameters for whole plants.

First, the dark adapted plants (20 min) were exposed to blue measuring light (1 Hz, intensity 4) and then to a first saturating light pulse (intensity 4). A second saturating light pulse was applied at the end of the actinic light phase (10 min, 100 µE m^{-2} s^{-1}) to calculate Y (NPQ) values as described by Kramer et al. (2004).

2.11 Generation of a Gc9 antibody and determination of the molar ratio of Gc9 to AtpC1

The partial sequence of *Gc9* coding for the N-terminal part of the protein (without the predicted transit peptide and the transmembrane domain) and the sequence of AtpC1 (without the sequence coding for the predicted transit peptide) were cloned into the pET151 Topo vector (Invitrogen) to overexpress Gc9 and AtpC1 with an N-terminal His-Tag in *Escherichia coli* (see primer list). *E. coli* cultures were grown at 37 °C in LB medium (5 g/L yeast extract, 10 g/L tryptone and 10 g/L NaCl) supplemented with 100 µg/ml carbenecillin. Gc9 and AtpC1 synthesis in *E. coli* cells (BL21 strain) was induced by adding IPTG to a final concentration of 1 mM. Cultures were then grown under continuous shaking for 4 hours at 37 °C. After harvesting the cells, the expressed proteins were purified under denaturating conditions using Ni^{2+}-affinity purification by Ni^{2+}-

NTA Agarose (Qiagen, Hilden, Germany). Gc9 protein was bound to Agarose beads by shaking for 1 h at 4 °C. Agarose beads were washed with 100 mM NaH_2PO_4, 10 mM Tris/HCl, 8 M urea, pH 6.3 in a column and were eluted with elution buffers (100 mM NaH_2PO_4, 10 mM Tris/HCl, 8 M urea, pH 5.9 and pH 4.5).
Elution fractions were loaded on Tricin-SDS-PAGE and fractionated proteins were precipitated by the use of a 0.1 M KCl solution. To generate polyclonal antibodies, Gc9 was electroeluted from the gel and injected into rabbits. Antiserum was employed in 1/200 to 1/1,000 dilutions.

The molar ratio of Gc9 to AtpC1 in wild type thylakoid membranes was determined by comparing immunodetected amounts of heterologously expressed and purified proteins to immunodetected proteins of thylakoid samples. For this purpose, the concentration of purified Gc9 and AtpC1 proteins were calculated by comparing quantified band intensities of elution fractions to a BSA standard curve on coomassie-stained Tricin-SDS-PAGE. Then, decreasing amounts of purified Gc9 or AtpC1 protein samples and wild type thylakoid membrane samples corresponding to 5 µg chlorophyll were separated on Tricin-SDS-PAGE. After blotting on PVDF membranes, proteins were immunodetected with antibodies against Gc9 and AtpC1. Quantified signals from wild type thylakoid samples were compared to signals from the loaded Gc9 or AtpC1 gradient.

2.12 Protoplasts isolation and GFP signal detection

Three week old leaves of transgenic Arabidopsis plants carrying the *35S::Gc9::EGFP* construct were cut into small pieces and incubated with enzyme solution (2.6 mg/ml Macerozyme (Duchefa), 10 mg/ml Cellulase (Duchefa), 10 mM MES pH 5.7, 20 mM KCl, 0.5 mM Mannitol, 10 mM $CaCl_2$ and 1 mg/ml BSA) for 4 h in the dark at room temperature to lyse cell walls. The mixture was filtered through a nylon membrane (pore size 72µm) and transferred into glass tubes. After centrifugation for 10 min at 50 *g*, the pellet was quickly resuspended in 8.5 ml MSC solution (10 mM MES, pH 5.7, 20 mM $MgCl_2$ and 120 mg/ml saccharose) and overlaid carefully with 2 ml MMM solution (10 mM MES, pH 5.7, 10 mM $MgCl_2$, 10 mM $MgSO_4$ and 0.5 M Mannitol). After centrifugation (70 *g* for 10 min), the dark green band in the interphase containing the protoplasts were washed once with MMM solution (50 *g* for 10 min) and

resuspended in MMM solution. The GFP signal and chlorophyll fluorescence from stably transformed protoplasts were detected using an Axio Imager fluorescence microscope with an integrated ApoTome (Zeiss, Jena, Germany).

2.13 Intact chloroplast and envelope isolation from Arabidopsis leaves

Leaves from 4-week-old dark adapted plants were harvested (20 g) and homogenized in homogenization buffer (450 mM Sorbitol, 20 mM Tricine-KOH, pH 8.4, 10 mM EDTA, 10 mM $NaHCO_3$, 0.1 % (w/v) BSA) using a waring blender. The homogenate was filtered through two layers of Miracloth (Calbiochem) and centrifuged (Beckman rotor JA-14) at 500 *g* for 6 min at 4 °C to collect chloroplasts. The supernatant was discarded immediately to remove the toxic vacuole extract and the pelleted chloroplasts were resuspended in 800 µl of 0.3 M sorbitol, 20 mM Tricine-KOH, pH 8.4, 2.5 mM EDTA and 5 mM $MgCl_2$. The suspension was added on a two-step Percoll gradient (40-80 % (v/v)) and centrifuged (low acceleration and no brake) at 6,500 *g* (Beckman, swing rotor JS 13.1) for 20 min at 4 °C. Intact chloroplasts were collected from the 40 % to 80 % Percoll interface and ruptured by treatment in lysis buffer (20 mM HEPES/KOH, pH 7.5, 10 mM EDTA) for 30 min on ice. The insoluble fraction (thylakoid and envelope) and the soluble fraction (stroma) were separated by centrifugation at 42,000 *g* for 30 min at 4 °C.

Leaves from 4 week old wild type plants (300 g) were harvested for envelope and thylakoid membranes isolation. Chloroplast isolation was performed as described above. Envelope and thylakoid membranes were separated on a sucrose step gradient (1.2/1.0/0.46 M sucrose) by centrifugation at 58,000 *g* for 2 h. Envelope membranes were collected from the interface between the layers of 0.46 and 1 M sucrose and thylakoid membranes from the pellet, respectively. Each fraction was washed several times and resuspended in 10 mM HEPES, 5 mM $MgCl_2$, pH 7.6. Intact chloroplast, the thylakoid, the envelope and the stroma fraction were separated on 12 % SDS-PAGE for immunoblot analyses.

2.14 Thylakoid isolation from Arabidopsis leaves

Leaves from 6-week-old dark adapted (16 h) plants were harvested and homogenized by blending in T1 buffer (0.4 M Sorbitol, 0.1 M Tricine, pH 7.8) supplemented with fresh protease inhibitors (0.2 mM PMSF, 1 mM benzamidin, 5 mM aminocaproicacid). The suspension was filtered through double-layered Miracloth (Calbiochem®) and centrifuged at 1,500 *g* for 4 min at 4 °C. The pellet was resuspended in T2 buffer (20 mM HEPES/KOH, pH 7.5, 10 mM EDTA) for 10 min on ice to lyse the chloroplasts and then centrifuged at 9,500 *g* for 10 min at 4 °C. The chlorophyll concentration of the samples was measured as described in Porra et al. (1989). Thylakoid membrane were frozen in liquid nitrogen and stored at -80 °C or were directly resuspended in loading buffer (6 M urea, 50 mM Tris-HCl pH 6.8, 100 mM DTT, 2 % (w/v) SDS, 10 % (w/v) glycerol and 0.1 % (w/v) bromophenol blue) for immune titration analysis as described below.

2.15 Blue Native analysis and second dimension gel

Leaves from 6-week-old plants grown under a short day regime were harvested and thylakoids were isolated as described in section 2.14. Thylakoid membrane samples were adjusted according to chlorophyll and washed four times in washing buffer (25 mM BisTris/Hcl, pH 7.0, 20 % glycerol). The samples were resuspended in solubilization buffer (25 mM BisTris, pH 7.0, 20 % glycerol, 1 % β-dodecyl maltoside (β-DM); adjusted to 1 ml/mg chlorophyll) and incubated for 10 min on ice. Non-soluble material was precipitated by centrifugation at 16,000 *g* for 20 min at 4 ^{o}C and supernatants (soluble material) were supplemented with 1/20 volume of BN loading buffer (100 mM BisTris/HCl, pH 7.0, 750 mM ε- aminocaproic acid, 5 % (w/v) Coomassie G-250). The solubilized samples corresponding to 80 µg of chlorophyll were loaded per lane on BN-PAGE (4-12 % gradient) which was prepared as described in Schägger et al. (1994). The gel was run in cathode buffer (50 mM Tricine, 15 mM BisTris, pH 7.0, 0.02 % Coomassie-G-250) and anode buffer (50 mM BisTris, pH 7.0) with a constant voltage of 25 V at 4 ^{o}C overnight. On the following day, the blue cathode buffer was exchanged with coomassie-free cathode buffer and destaining of gels was performed at 250 V until the dye front reached the bottom of the gel length. The stripes of the Blue Native gels were incubated in denaturing buffer (0.5 M Na_2CO_3,

2 % (w/v) SDS, 0.7 % (v/v) β-mercaptoethanol) for 30 min at room temperature. The gel stripes were then loaded on top of a Tricine-SDS-PAGE (10 % gels supplemented with 4 M urea) which were prepared according to Schägger (2006). The gel was run in cathode buffer (0.1 M Tris, 0.1 M Tricine, 0.1 % (w/v) SDS) and anode buffer (1 M Tris/HCl, pH 8.9) overnight at 25 mA. Gels were subsequently subjected to immunoblot analysis with antibodies against ATP synthase subunits as described below.

2.16 Complex isolation using sucrose density gradient centrifugation

Leaves of 6-week-old plants were harvested and homogenized in isolation buffer (25 mM MES, pH 6.5, 330 mM sucrose, 5 mM $MgCl_2$, 1.5 mM NaCl, and 100 mM NaF). The homogenate was filtered through double-layered Miracloth (Calbiochem®) and centrifuged at 4,500 *g* for 5 min at 4 ^{o}C. The collected thylakoids (pellet) were resuspended in EDTA wash buffer (5 mM EDTA, pH 7.8) with a paint brush and centrifuged at 13,000 *g* for 5 min at 4 ^{o}C. The pellet was resuspended in H_2O and solubilized in 1 % (w/v) DM for 10 min on ice. The soluble material was collected by centrifugation at 16,000 *g* for 5 min at 4 ^{o}C (supernatant fraction) and loaded onto the prepared sucrose gradient (0.1 M to 1 M sucrose, 5 mM Tricine/NaOH, pH 8.0, 0.05 % (w/v) DM).

Solubilized protein complexes were fractionated on sucrose gradients by ultracentrifugation at 191,000 *g* for 21 hours at 4 ^{o}C. Fractions (1-19) were collected and separated on Tricine-SDS-PAGE (10 %, 4 M urea). After blotting on PVDF membranes, ATP synthase subunits and Gc9 were immunodetected with specific antibodies.

2.17 Salt washing

Salt wash treatments were performed as described by Karnauchov et al. (1997). Isolated thylakoid membranes were resuspended to a final chlorophyll concentration of 0.5 mg/ml in 50 mM HEPES/KOH, pH 7.5 supplemented either with 2 M NaCl, 0.1 M Na_2CO_3, 2 M NaSCN or 0.1 M NaOH. Suspensions were incubated for 30 min on ice and then solublilized and insoluble proteins were separated by centrifugation at 10,000 *g* for 10 min at 4 ^{o}C. Samples were

fractionated on Tricin-SDS-PAGE (10 %) and subjected to immunoblot analysis using Gc9, Lhcb1 (Agrisera) and PsaD (Agrisera) antibodies.

2.18 Western blot analysis

Solubilized proteins were fractionated by gel electrophoresis and transferred to PVDF membranes (Immobilon®-P, Millipore, Eschborn, Germany) using a semi-dry blotting apparatus (Bio-Rad). A constant current corresponding to 1 mA cm^{-2} in transfer buffers (cathode buffer: 25 mM Tris, 10 % methanol and 40 mM glycine, pH 9.4; anode buffer 1: 0.3 M Tris, pH 10.4 and 10 % methanol; anode buffer 2: 25 mM Tris, pH 10.4 and 10 % methanol) was used. The PVDF membranes were blocked with 3 % BSA or 5 % (w/v) milk in TBST buffer (10 mM Tris, pH 8.0, 150 mM NaCl and 0.1 % Tween- 20) for 1 hour at room temperature. Then, membranes were incubated (4 ^{o}C overnight) with antibodies against subunits of PSI (Agrisera), PSII (Agrisera), Cyt b_6f (Agrisera), ATP synthase subunits (obtained from Jörg Meurer, University of Munich) and Gc9. After incubation with first antibodies, membranes were washed 3 times (10 min each) with TBST buffer at room temperature and incubated with the corresponding secondary antibodies (conjugated with horseradish peroxidase) for 1 hour at room temperature. After washing 5 times (5 min each) with TBST buffer, signals were detected by enhanced chemiluminescence (ECL kit, Amersham Bioscience®) using an ECL reader system (Fusion FX7, PeqLab®, Erlangen, Germany) and quantified by the Bioprofile software (Peqlab, Erlangen, Germany).

2.19 Association of mRNAs with polysomes

Polysome analyses were performed according to Barkan (1988). Around 300 mg of leaves from four week-old plants were powdered in liquid nitrogen and homogenized in polysome extraction buffer (0.2 M Tris-HCl, pH 9.0, 0.2 M KCl, 35 mM $MgCl_2$, 25 mM EGTA, 0.2 M sucrose, 1 % (v/v) Triton X-100, 2 % (v/v) polyoxyethylene-10-tridecyl ether, 0.5 mg/ml heparin, 100 mM 2-mercaptoethanol, 100 µg/ml chloramphenicol and 25 µg/ml cycloheximide). The homogenate was incubated on ice with 0.5 % (w/v) sodium deoxycholate for 10 min for microsomal

membrane solubilization and centrifuged at 16,000 *g* for 15 min at 4 °C. Supernatants were loaded on top of sucrose gradients (15-55 %) and centrifuged (240,000 *g*) for 65 min at 4 °C in an SW60 rotor (Beckman). Ten fractions were collected starting from the top and were supplemented with 5 % SDS and 0.2 M EDTA, pH 8.0. RNA was extracted from these fractions with phenol/chloroform/isoamyl alcohol (25:25:1) and precipitated with 95 % ethanol at room temperature. Resuspended RNA in TE buffer (10 mM Tris-HCl, 1 mM EDTA, pH 8.0) was subjected to gel electrophoresis and RNA gel blot analyses as described above.

2.20 *In vivo* translation assay

For *in vivo* radioactive labeling of thylakoid proteins, leaf discs of plants grown under short day conditions were used (5 discs for each genotype and for each time point). Leaf discs were vacuum-infiltrated with pulse-chase buffer (50 mM Tris, pH 7.5, 150 mM NaCl, 2 mM EDTA, 0.2 % (v/v) Tween 20) containing 20 µg/ml cycloheximide. Samples were incubated in light for 30 min to block cytosolic translation and then one sample (time point 0) was collected. The other samples were transferred in new tubes and were vacuum–infiltrated with pulse-chase buffer (with cycloheximide) containing 1mCi of [^{35}S] Met, in order to radiolabel newly translated chloroplast proteins. The infiltrated leaf discs were transferred in small Petri dishes, incubated in light (100 µE) and samples were collected after 5 and 30 min of incubation (pulse 5 min and pulse 30 min samples). For thylakoid protein preparation, collected samples were washed, grinded in 20 mM HEPES/KOH, pH 7.5, 10 mM EDTA and filtered into a new tube. The soluble fraction was obtained by centrifugation at 16,000 *g* for 10 min at 4 °C. After adjusting samples according to the chlorophyll concentration, *de novo* synthesized proteins were separated on Tricine-SDS-PAGE (8 % acrylamide, 4 M urea) and blotted on PVDF membranes. PVDF membranes were exposed to Storage Phosphor Screen (Fuji) and radioactive labeled proteins were detected with the Typhoon Phosphor Imager (GE Healthcare, Munich, Germany).

2.21 Split-Ubiquitin assay

Transient interaction partners of Gc9 were identified in split ubiquitin assays. Gc9 (without the ChloroP-predicted, 46 aa long transit peptide) was fused to the C-terminal domain of ubiquitin

(Cub) by cloning the respective CDS into the bait vector pAMBV4 (Dual-systems Biotech). Coding sequences of potential interaction partners (AtpH, AtpF, AtpI, AtpA, PsbA, PsbC, PsaA, PsaB, FNR1, Fd and cpSecY) were fused to the mutated N-terminus of ubiquitin (NubG) by cloning the sequences into the multiple cloning site of the prey vector pADSL (Dual-systems Biotech). The vectors pAlg5-NubG (^{NubG}Alg5) and pAlg5-NubI (^{NubI}Alg5) were used as a negative and positive control. The yeast strain was cotransformed with various combination of bait and prey constructs using the Dual-Membrane kit (Dual-systems Biotech). After cotransformation, yeast cells were plated on permissive medium lacking the two amino acids Leu and Trp (-LT). Then the same colonies were grown on selective medium without Leu, Trp and Histidine (-LTH).

2.22 Primers list

Table 2.1 Primers used in Materials and methods. Overhangs which are necessary for cloning are underlined.

Gene	Forward primer	Reverse primer	Appilication
T-DNA/*Gc9* junction in *gc9-1*	AAGTTAAGATTCCATTTTCGCATC	TCCCTAAACATCACATCCTGC	Genotyping primers *gc9-1*
T-DNA/*Gc9* junction in *gc9-2*	GAGTACAATCAATTTTCCTTGTGGACTTG	TGATCCATGTAGATTTCCCGGACATGAAG	Genotyping primers *gc9-2*
Gc9	CTTTAGCAGAGTTATGAGTC	CAATAGCCTTACTCATTTGC	Amplicon 2 for RT-PCR
Gc9	TACCCAATAAGAAACCTGAG	TAAGTCTGTGGAAGTAATGG	Amplicon 1 for RT-PCR
Gc9	GGGGACAAGTTTGTACAAAAAAGCAGGCTCAATGGCGATTCTTAGTTACAT	GGGGACCACTTTGTACAAGAAAGCTGGGTGATCACTGGCCTGTGTGTCTG	*Gc9* cloning into pB7FWG2.0 for complementation studies
AtpC	CACCGCTTCCTCTGTTTCACCACTCCAAGCG	TCAAACCTGTGCATTAGCTCCAGCA	*AtpC* TOPO cloning into pET151 for overexpression in *E. coli*
Gc9	CACCGGAGAGTACGGTGGTCCTCC	TTATACTTCTGGGTCACCACGTG	*Gc9* TOPO cloning into pET151 for overexpression in *E. coli*
AtpA	GACAGACAGACCGGTAAAAC	AAACATCTCCTGACTGGGTC	Northern probe
AtpB	TTAGGTCCTGTCGATACTCG	ACCCAATAAGGCGGATACCT	Northern probe
AtpE	GTGTACTGACTCCGAATCGA	TATTGAGAGCCTCGACTCGT	Northern probe
AtpF	TCGTTTACTTGGGTCACTGG	TTGTTGGAAAACCCGTTCGC	Northern probe
AtpH	GAATCCACTGGTTTCTGCTG	AGCGCTAATGCTACAACCAG	Northern probe
AtpI	TATCCAGTTACCTCAAGGGGAGTTA	TTAATGATGACCTTCCATAGACTCA	Northern probe
Gc9	CACCGGAGAGTACGGTGGTCCTCC	CAATAGCCTTACTCATTTGC	Northern probe
Gc9	ATTAACAAGGCCATTACGGCCATGAAAATCATTCTACCCAATAAGA	AACTGATTGGCCGAGGCGGCCCCATCACTGGCCTGTGTGTCTGGAG	pAMBV4 cloning for split-ubiquitin assays

3 Results

3.1 GreenCut protein 9 (Gc9) is found in all photosynthetic eukaryotes

The use of comparative genomic analysis is an applicable approach to screen for novel proteins involved in photosynthetic function. By this approach proteins were identified which are shared by organisms from the green lineage among the eukaryotic organisms but which are absent in non-photosynthetic eukaryotes (Merchant et al., 2007). These proteins are designated as GreenCut proteins. This cross section contains 597 Chlamydomonas proteins with homologs in higher plants (*Arabidopsis thaliana*), moss (*Physcomitrella patens*) and green algae (*Chlamydomonas reinhardtii, Ostreococcus tauri* and *Ostreococcus lucimarinus*). One of the GreenCut proteins with unknown function is Gc9/Cgl160 (AT2G31040). This protein is encoded by a single nuclear gene which is located on chromosome 2 of *Arabidopsis thaliana*. The genomic sequence of the gene, from the start to the stop codon, is 1919 bp long, whereas the ORF is constituted of nine exons and is 1044 bp long. The 350-aa-long Gc9 protein (38.6 kDa) is predicted to be targeted to the chloroplast by a 46-aa-long transit peptide sequence (ChloroP, Emanuelsson et al., 1999). Gc9 harbors four transmembrane domains (Aramemnon database, Schwacke et al., 2003) and two phosphorylation sites were experimentally identified in the N-terminal domain in a phosphoproteome study (Reiland et al., 2009) (Figure 3.2 A). Transcriptome data (http://atted.jp/data/locus) show that Gc9 is co-regulated with proteins important for photosynthetic functions, such as TAP38 (regulatory protein), NPQ1 (photoprotective protein), PSAE (structural protein) and HCF136 (assembly factor for PSII) (Table 3.1). Moreover, gene expression profile analyses of *Arabidopsis thaliana* (http://bar.utoronto.ca/efp/cgi-bin/efpWeb.cgi) revealed highest expression levels in photosynthetic tissues (Figure 3.1).

Table 3.1 *Gc9* Coregulation with photosynthetic genes

Gene locus, average correlation to query loci (*Gc9*), putative subcellular targeting and function of the respective genes were obtained from the ATTED database (atted.jp). The putative subcellular targets (C: chloroplast localization; M: mitochondrial localization; Y: cytosolic; O: others) are related to TargetP and WoLF PSORT programs which are shown on the ATTED database.

Locus	Ave. cor. to query loci	Target (TargetP, WoLF PSORT)	Function
At4g27800	0.86	M, C	TAP38/thylakoid-associated phosphatase 38
At3g15840	0.83	C, M	PIFI (post-illumination chlorophyll fluorescence increase)
At1g20020	0.85	C, C	FNR2(ferredoxin-NADP(+)-oxidoreductase 2)
At1g08550	0.77	O, Y	NPQ1 (non-photochemical quenching 1)
At1g18730	0.78	C,Y	NDF6 (NDH dependent flow 6)
At2g28800	0.72	C, C	ALB3 (63 kDa inner membrane family protein)
At5g66190	0.76	C, C	FNR1 (ferredoxin-NADP(+)-oxidoreductase 1)
At3g16250	0.76	C, C	NDF4 (NDH-dependent cyclic electron flow 1)
At1g70760	0.75	C, C	NdhL (inorganic carbon transport protein-related)
At4g11960	0.60	C, C	PGRL1B (PGR5-Like B)
At5g23120	0.75	C, C	HCF136 (photosystem II stability/assembly factor)
At2g20260	0.74	C, C	PSAE-2 (photosystem I subunit E-2)
At4g00895	0.67	C, C	ATPase, F1 complex, OSCP/delta subunit protein
At1g15980	0.73	C, C	NDF1 (NDH-dependent cyclic electron flow 1)

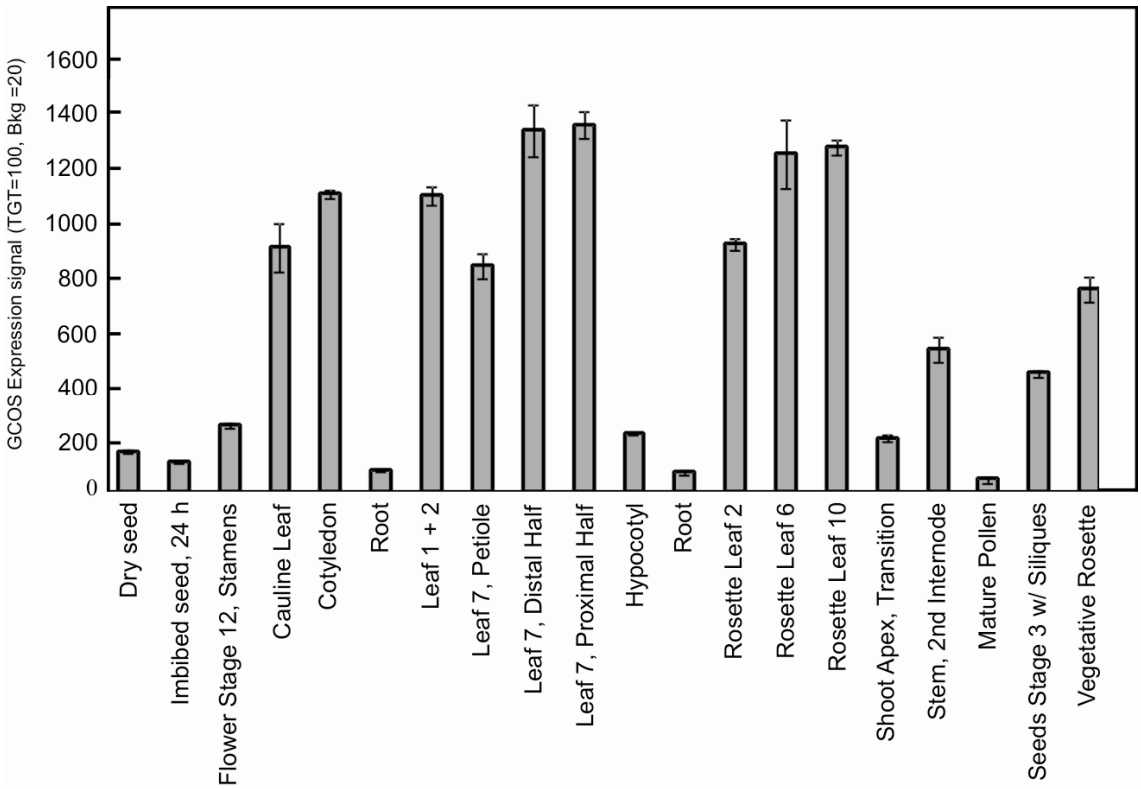

Figure 3.1 Overview of *Gc9* mRNA expression in different tissues of *A. thaliana*

Expression levels ± standard deviation were obtained from the BAR Arabidopsis eFP Browser (http://bar.utoronto.ca/efp/cgi-bin/efpWeb.cgi) for different tissues. Data are normalized by the GCOS method, TGT value of 100. Most tissues were sampled in triplicates.

Protein sequence alignments confirmed that Gc9 is conserved in different species from the green lineage like in higher plants (*Oryza sativa*, *Zea mays*, *Vitis vinifera, Picea sitchensis*) spikemoss (*Selaginella moellendorffii*), moss (*Physcomitrella patens*) and also in eukaryotic green algae (*Chlamydomonas reinhardtii*). The transmembrane domain (84.0/25.7% similarity/identity; 209-350 aa of Gc9) shows higher conservation than the N-terminal domain (59.8/4.3% similarity/identity; 47-208 aa of Gc9) (Figure 3.2 B).

BLAST searches of the Gc9 orthologous using *Chlamydomonas reinhardtii* sequence against the protein domain database CDD (Marchler- Bauer et al., 2011) revealed that the membrane domain shares some sequence similarity with the Atp1/UncI like domain (CDD entry: Pfam03899)

(Figure 3.2 C). Atp1/UncI proteins are encoded in the bacterial F_1F_O ATP synthase operons and are short, hydrophobic proteins. Recent studies showed that UncI plays a chaperone-like role in the c-ring assembly of the ATP synthase in *Propionigenium modestum* (Suzuki et al., 2007; Ozaki et al., 2008).

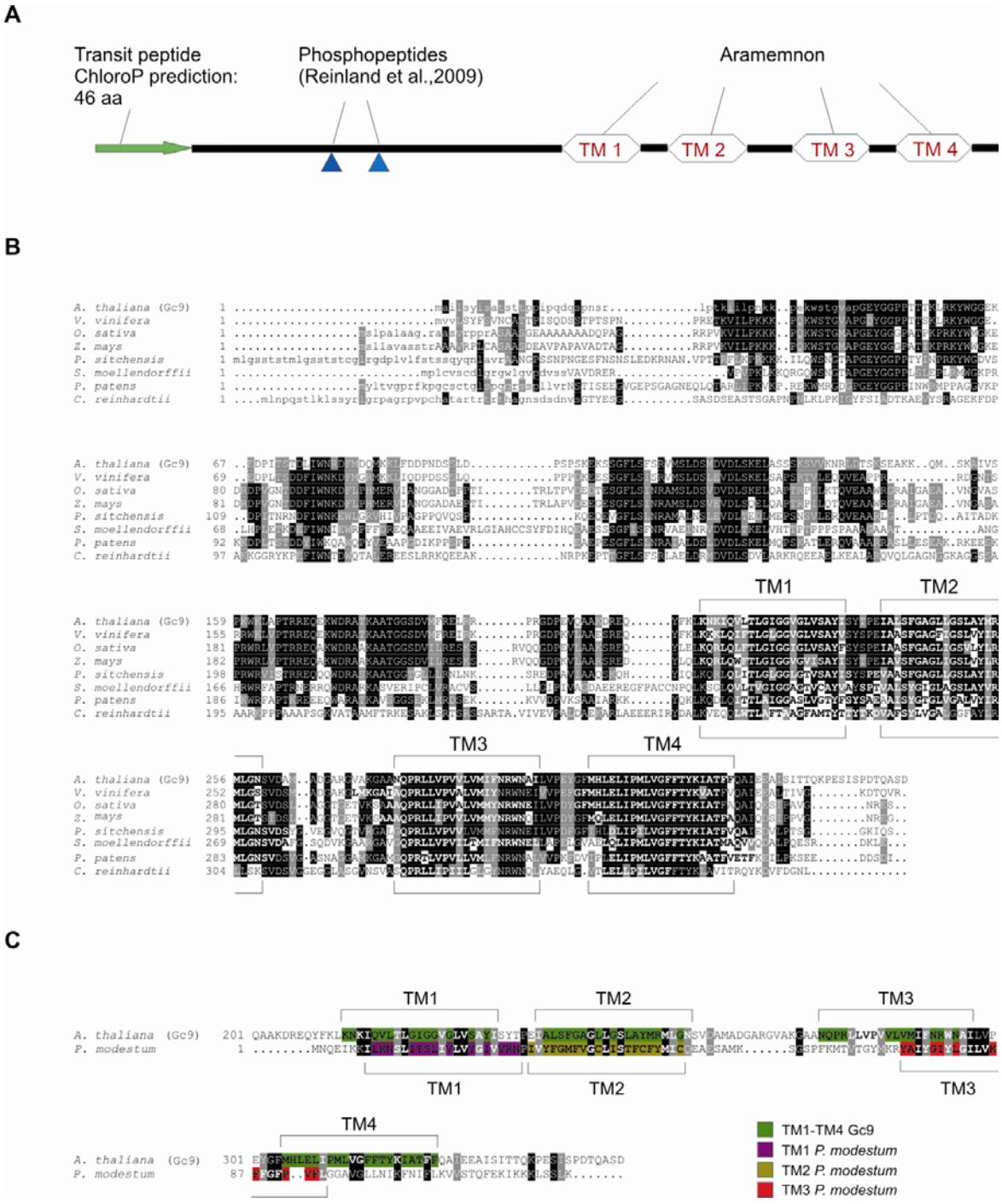

Figure 3.2 Characterization and protein sequence alignment of Gc9

A) The predicted chloroplast transit peptide (46aa), four transmembrane domains and two phosphopeptides are shown in the schematic diagram of Gc9. **B)** The protein sequence of Gc9 from *A. thaliana* was compared with its homologs from other plant and algal species. Sequence similarity/identity in at least 50 % of the sequences is colored in grey/black, respectively. Predicted chloroplast targeting sequences by ChloroP are shown in lower case letters. The transmembrane domains were predicted by the Aramemnon database for *V. vinifera (Vitis vinifera)*, *O. sativa (Oryza sativa)*, *Z. mays* (*Zea mays*) and by the MINNOU program for *P. sitchensis* (*Picea sitchensis*), *S. moellendorffii* (*Selaginella moellendorffii*), *P. patens* (*Physcomitrella patens*) and *C. reinhardtii* (*Chlamydomonas reinhardtii*). The predicted transmembrane domains are highlighted in bold letters. **C)** Sequence alignment of the Gc9 transmembrane domain with the UncI sequence of *Propionigenium modestum* (*P. modestum).* The prediction of the Gc9 transmembrane domain was adopted from the Aramemnon database, whereas the UncI transmembrane domains were predicted by SCAMPI. Transmembrane domains are shown in bold letters and are colored as indicated in the figure legends.

3.2. Gc9 knock-out plants grow slower than wild type plants

To identify the function of Gc9, two *A. thaliana (Columbia-0* ecotype) T-DNA insertion mutant lines were obtained from public available mutant line collections. T-DNA insertion sites were precisely determined by amplifying the flanking sequences using insertion- and gene-specific primers and subsequently sequencing of the respective PCR products. In *gc9-1*, the T-DNA (*ROK2* construct) is inserted in the first of nine exons, 344 bp downstream of the start codon, whereas in *gc9-2* the T-DNA is located in the 5'UTR, 72 bp upstream of the start codon (Figure 3.3 A). Leaf surface measurements performed every four days indicated that the growth rate of *gc9-1* plants is slower than the growth rate of wild type plants, whereas the growth rate of *gc9-2* is close to that of the wild type under short day conditions (Figure 3.3 B and C).

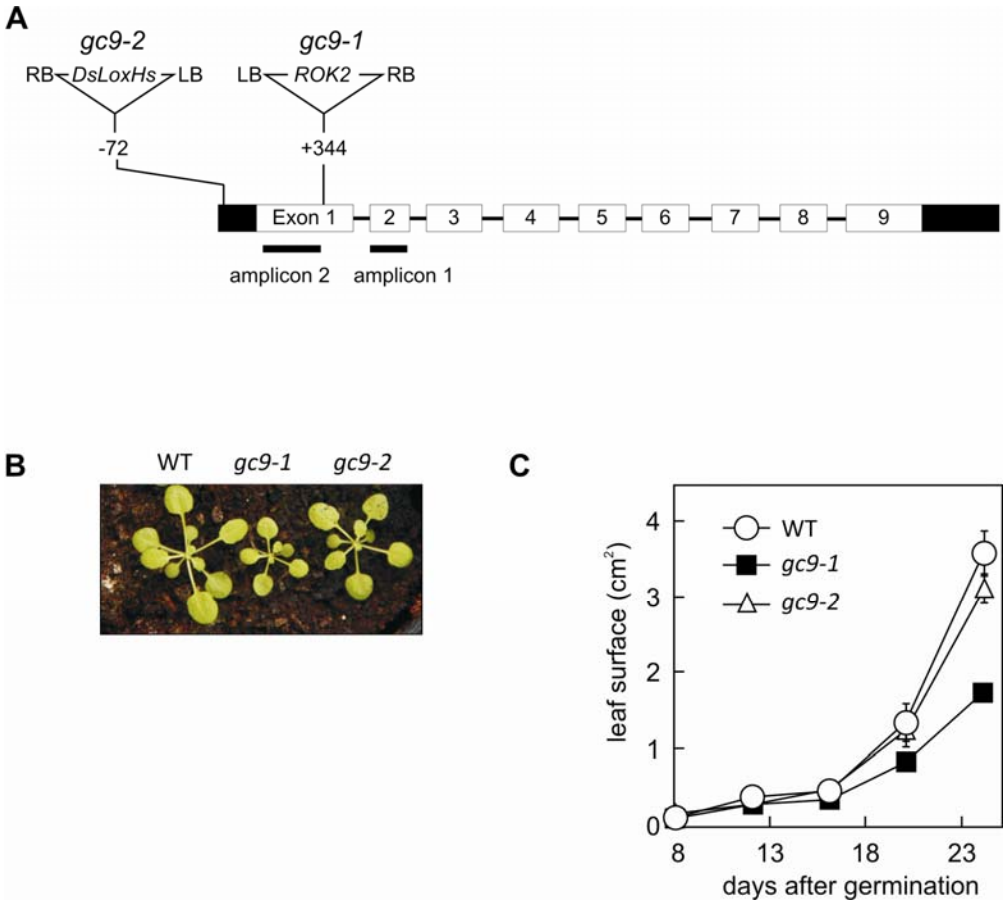

Figure 3.3 T-DNA insertion mutant lines and growth phenotype of *gc9-1* and *gc9-2*

A) Positions of T-DNA insertions in the *Gc9* gene. Untranslated regions are shown by black boxes, whereas exons are indicated by white boxes and intron sequences by black lines. Two transcript sites which were used for Real time PCR analysis are indicated by amplicon 1 and amplicon 2. **B)** Growth phenotype of four week-old wild type, *gc9-1* and *gc9-2* plants grown in the climate chamber under short day conditions (8h light/16h dark). **C)** Growth curves of wild type (Col-0) and the two mutant lines (*gc9-1*, *gc9-2*) were calculated by leaf surface measurements using the ImageJ program. Values are averages ± standard deviations of 20 plants. Standard deviations are indicated by error bars.

Real-time PCR analysis for two transcript sites on synthesised cDNA from wild type, *gc9-1* and *gc9-2* leaves revealed that *Gc9* expression was strongly reduced in *gc9-1* but *Gc9* transcripts were still detectable in *gc9-2* (Figure 3.4 A). Semi-quantitative PCR (RT-PCR) analyses were

carried out using *Gc9*- and ubiquitin-specific primers to detect transcripts in wild type and mutant plants. RT-PCR results confirmed that *Gc9* transcripts were still detectable in *gc9-2* but not in *gc9-1* (Figure 3.4 B). In addition, western blot analyses with Gc9-specific antibodies raised against fractionated thylakoid membrane proteins were performed. The mature Gc9 (33.7 kDa) was detected in wild type thylakoid membrane samples, but less than 25 % of Gc9 amounts were present in *gc9-2*, whereas Gc9 was completely absent in *gc9-1* (Figure 3.4 C). Overall, *Gc9* interruption prevents accumulation of mRNA in *gc9-1* and leads to a Gc9 knock-out mutant line with a slower growth rate. In contrast, *Gc9* mRNA accumulation is only slightly reduced in *gc9-2* and leads to a Gc9 knock-down. The presence of less than 25 % Gc9 amounts compared to wild type amounts is still sufficient for normal growth rates.

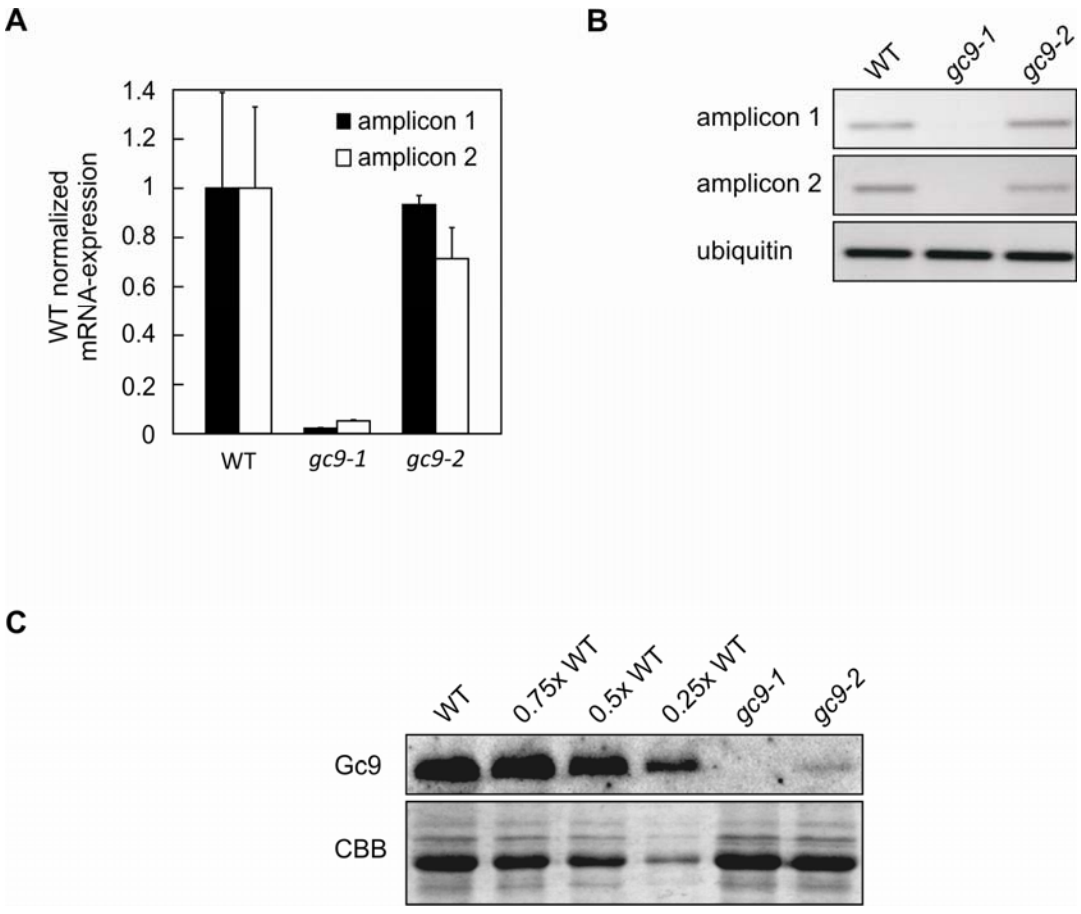

Figure 3.4 *Gc9* transcription and protein abundance in the two mutant lines

A) *Gc9* transcript levels were detected by Real-time PCR analysis for two transcript sites on exon 1 and exon 2 for the indicated genotypes. **B)** RT-PCR was performed to analyse *Gc9* gene expression. Ubiquitin expression in each genotype was taken as reference for normalization. **C)** Immunodetection of Gc9 in thylakoid membrane samples of wild type and mutant lines. Each lane was loaded with 10 µg of thylakoid proteins for the mutant plants and 10, 7.5, 5.0 and 2.5 µg of proteins for the wild type samples and then probed with an antibody raised against Gc9. Coomassie staining (CBB) of the gel was performed as a loading control.

3.3 *Gc9::EGFP* overexpressors show the same growth phenotype as the wild type

To confirm that the slower growth rate of *gc9-1* was caused by the Gc9 disruption, an overexpression construct of Gc9 (*oeGc9::EGFP*) was transformed into *gc9-1*. The overexpressor construct leads to the expression of a *Gc9-eGFP* fusion (Enhanced Green Fluorescent Protein). Two independent BASTA-resistant progenies were selected after transformation and successful complementation was confirmed by growth measurements (Figure 3.5 A). Integration of the overexpressor construct into the *gc9-1* genome was tested by PCR (for primer information see primers list). In addition, *Gc9* overexpression and Gc9::EGFP accumulation were tested by RNA blot and protein immunoblot analyses, respectively (Figure 3.5 B and C). The RNA blot analysis using a *Gc9*-specific probe revealed that the *Gc9-GFP* transcript is overexpressed (*Gc9::EGFP*) in two independent lines. Also immunoblot analyses using the Gc9 antibody confirmed the presence of the Gc9-EGFP fusion in the complemented plants. Overall, it was assumed that the lack of Gc9 is responsible for the *gc9-1* growth phenotype.

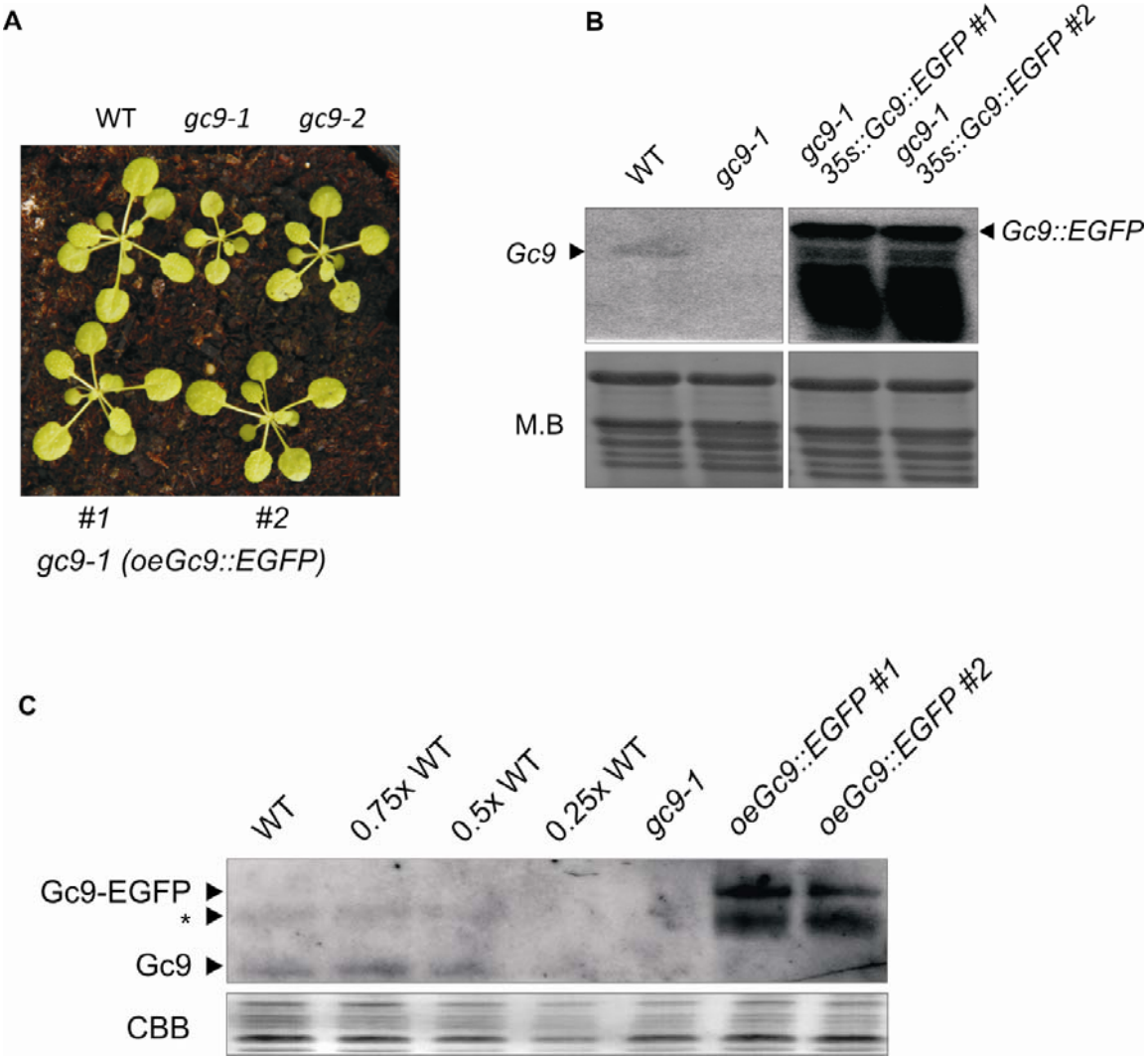

Figure 3.5 Complementation analyses by introducing a *Gc9::EGFP* overexpressor construct into *gc9-1*

A) Growth phenotype of wild type, *gc9-1* and *gc9-2* mutants and two independent complemented lines grown in the climate chamber under short day conditions for 4 weeks. The coding sequence of Gc9 was cloned into the destination vector (pB7FWG2.0) under the transcriptional control of *Cauliflower Mosaic* Virus 35S promoter. This construct (35S::Gc9::EGFP) was used to complement *gc9-1* plants. **B)** Northern analysis using a ^{32}P-labeled DNA probe specific for the *Gc9* transcript which was hybridized to fractionated RNA (5µg) from wild type, *gc9-1* and two independent complemented plants. Methylene blue staining (M.B.) of blotted RNA was carried out to assess equal loading. **C)** Gc9 immunodetection in thylakoid membrane samples isolated from wild type, *gc9-1* and overexpressors plants. Coomassie-staining of blotted proteins on PVDF membranes was performed to assess equal loading. Signals marked by an asterisk are unspecific signals which could neither be attributed to Gc9 nor to the fusion protein Gc9-EGFP.

3.4 Subcellular and suborganellar localization of Gc9

According to five prediction algorithms for subcellular localization (ChloroP, iPSORT, Predator, Protein Prowler, Bacello) Gc9 is targeted to the chloroplast. In addition, Terashima and coworkers could detect the Gc9 homolog of Chlamydomonas in the chloroplast by a mass spectrometry approach (Terashima et al., 2011). To confirm the chloroplast localization, the Gc9::EGFP fusion protein was detected in isolated protoplasts from stably transformed *gc9-1* plants carrying the overexpression construct (*oe::Gc9::EGFP*). EGFP signals overlapped with chlorophyll autofluorescence signals confirming the chloroplast localization of Gc9 (Figure 3.6 A). To determine the suborganellar localization of Gc9, chloroplasts from wild type plants were isolated and fractionated into a soluble and an insoluble fraction. Fraction purity was tested by western blot analyses using antibodies against PsaD (as a control for thylakoid proteins) or RbcL (as a control for stromal proteins). Western blots with the Gc9-specific antibody revealed that Gc9 is located in the insoluble chloroplast fraction which contains thylakoid and envelope membranes (Figure 3.6 B). Subsequently, membranes were separated into a thylakoid and an envelope fraction and subjected to immunoblot analysis. The purity of isolated fractions was tested by antibodies raised against PsaD and Tic40 as indicators for thylakoid and envelope membrane proteins, respectively. Gc9 immunodetection showed that Gc9 is only found in the thylakoid membrane fraction (Figure 3.6 C). Isolated chloroplast membranes from wild type plants were treated with different chaotropic salts and alkaline solutions. Subsequently, soluble and insoluble proteins were separated by centrifugation and subjected to western blot analysis using Gc9, Lhcb1 and PsaD antibodies. Immunodetection assays indicated that Gc9 behaved like the Lhcb1 control for an integral membrane protein since it was present in the insoluble pellet fractions after all salt treatments (Figure 3.6 D). Taken together, these results show that Gc9 is an integral membrane protein which is located in the thylakoid membranes of the chloroplast.

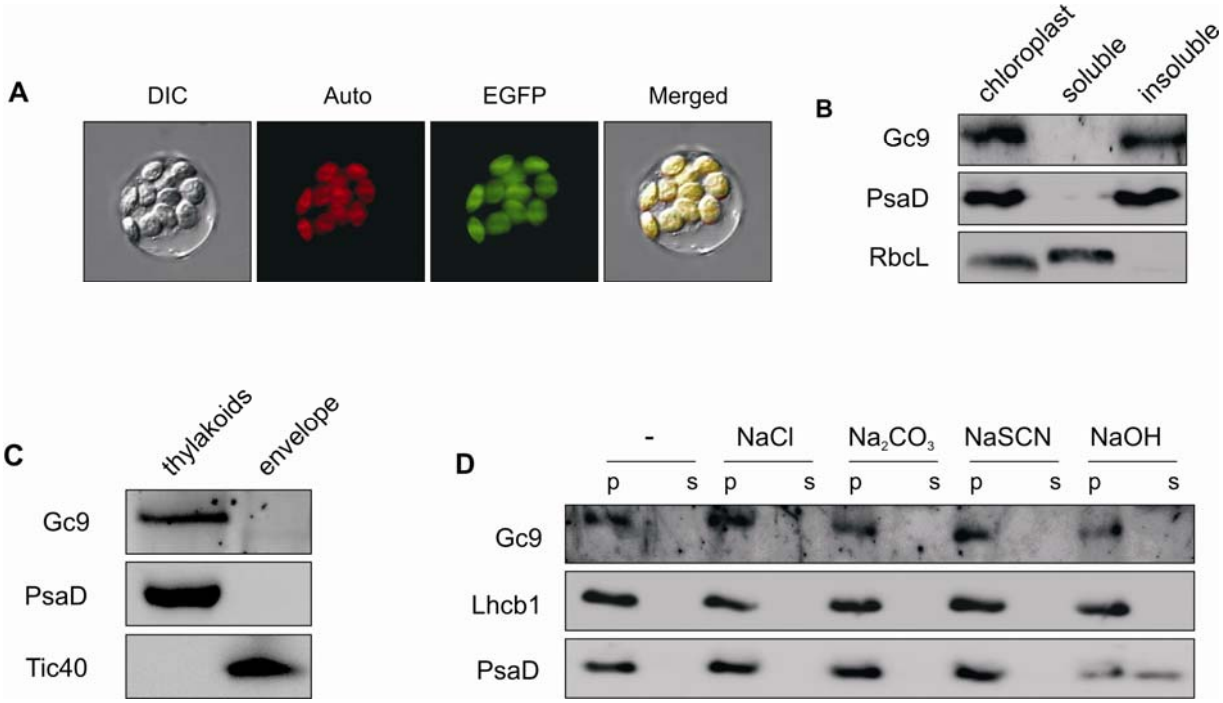

Figure 3.6 Subcellular and suborganellar localization of Gc9

A) Subcellular localization of Gc9. EGFP and chloroplast autofluorescence signals were detected in protoplasts isolated from plants carrying the EGFP-Gc9 construct. DIC: image of a single protoplast in bright field, Auto: chlorophyll autofluorescence signal, EGFP: EGFP signal, Merged: Merged image of the protoplast picture in bright field, chloroplast autofluorescence and GFP signals. **B)** Suborganellar localization of Gc9. Intact chloroplasts and soluble and insoluble chloroplast fractions were subjected to immunodetection analyses using antibodies raised against Gc9, PsaD (as a marker for an insoluble protein) and RbcL (as a marker for a soluble protein). **C)** Thylakoid and envelope membranes were isolated and subjected to western blot analysis using specific antibodies for Gc9, PsaD (as a marker for a thylakoid membrane protein) and Tic40 (as a marker for an envelope membrane protein). **D)** Thylakoid membrane association of Gc9. After incubation with different salt solutions (NaCl, Na_2CO_3, NaSCN and NaOH) solubilized (S) and insoluble proteins (P) were separated by electrophoresis and subjected to immunodetection analysis with antibodies raised against Gc9, Lhcb1 (as a control for an integral membrane protein) and PsaD (as a control for a peripherally bound membrane protein).

3.5 Photosynthesis is altered in *gc9-1*

To analyse the effect of the mutation on photosynthesis, leaf pigment analysis and Chlorophyll *a* fluorescence yield measurements were carried out. *Gc9-1* leaves are characterized by a pale

green color and chlorotic spots on the leaves after six weeks of growth in the short-day climate chamber (Figure 3.7). Leaf pigments were extracted from wild type, *gc9-1* and *oeGc9::EGFP#1* plants grown under 80-100 µmol m^{-2} s^{-1} light intensities and analyzed by reverse-HPLC (Table 3.2). Total chlorophyll and carotenoid concentrations were decreased in *gc9-1* (Chla+b: 2065 ± 268 pmol/mg, Car: 174 ± 24 pmol/mg) with respect to the wild type (Chla+b: 3086 ± 244 pmol/mg; Car: 268 ± 27 pmol/mg) and to the overexpressor line *oeGc9::EGFP#1* (Chla+b: 3647 ± 325 pmol/mg; Car: 317 ± 30 pmol/mg). The concentration of viloaxanthin (Vx) was also reduced in *gc9-1* (30 ± 4 pmol/mg) compared to the wild type (57 ± 7 pmol/mg) and the overexpressor line (70 ± 9 pmol/mg). Interestingly, protonated forms of Vx, Anteraxanthin (Ax) and Zeaxanthin (Zx) accumulated in *gc9-1* (11 ± 3 and 4 ± 2 pmol/mg), whereas levels in wild type and *oeGc9::EGFP#1* samples were under or close to the detection level. The conversion of Vx to Zx via Ax is catalyzed by the enzyme violaxanthin de-epoxidase which is activated at increasing luminal proton concentrations. Overall, accumulation of Zx and Ax indicates that the xanthophyll cycle is activated in *gc9-1*.

Figure 3.7 Leaves of 6 weeks-old wild type and *gc9-1* plants grown in the climate chamber under short day conditions

Table 3.2 Leaf pigment analyses

Leaf pigment composition of 6 week-old wild type, *gc9-1* and overexpressor (*oeGc9::EGFP#1)* plants grown in climate chamber under short day condition was detected by reverse-HPLC. Average amount of pigments ± standard deviations are reported by pmol per mg fresh weight obtained from five physiological replicates. Nx: Neoxanthin, Vx: Violaxanthin, Ax: Antheraxanthin, Lut: Lutein, Zx: Zeaxanthin, Chl a: Chlorophyll a, Chl b: Chlorophyll b, Car: Carotenoids, VAZ: Violaxanthin+Antheraxanthin+Zeaxanthin, Chla+b: total Chlorophyll, Chl a/b: Chlorophyll a to Chlorophyll b ratio. Except Chl a/b all values are given in pmol/mg.

Pigment	**Wild type**	***gc9-1***	***oeGc9::EGFP***
Nx	95 ± 6	67 ± 9	109 ± 12
Vx	57 ± 7	30 ± 4	70 ± 9
Ax	0	11 ± 3	1 ± 0
Lut	275 ± 23	191 ± 24	338 ± 33
Zx	0	4 ± 2	0
Chl b	708 ± 49	483 ± 62	830 ± 68
Chl a	2378 ± 196	1582 ± 207	2817 ± 257
Car	268 ± 27	174 ± 24	317 ± 30
VAZ	58 ± 7	45 ± 3	72 ± 9
Chla+b	3086 ± 244	2065 ± 268	3647 ± 325
Chl a/b	3.36 ± 0.06	3.27 ± 0.03	3.39 ± 0.04

During photosynthesis, absorbed light energy by PSII is converted into biochemical energy. Alternatively, absorbed light energy can be lost by chlorophyll *a* fluorescence or by heat dissipation. Those three processes are in competition, thus photochemistry and heat dissipation can be estimated by chlorophyll *a* fluorescence measurements. Chlorophyll *a* fluorescence parameters of single leaves were analyzed *in vivo* in slow induction assays by using the Dual-PAM (Pulse Amplitude Modulation) technique (Table 3.3). The maximal quantum yield (F_v/F_m)

of *gc9-1* leaves (0.79 ± 0.01) was slightly lowered compared to that of wild type leaves (0.81 ± 0.01) indicating that PSII is still functional in *gc9-1*. However, the effective quantum yield of PSII (Φ_{II}) under moderate light intensities (100 µE m^{-2} s^{-1}) was reduced in *gc9-1* (0.41 ± 0.02) with respect to the wild type (0.51 ± 0.02). Φ_{II} reduction implied that lower steady-state electron transport rates take place through PSII in *gc9-1*. Notably, non-photochemical quenching (NPQ) was increased in *gc9-1* (1.1 ± 0.06) with respect to the wild type (0.59 ± 0.08), indicating that a larger fraction of absorbed light energy is lost by heat dissipation in *gc9-1* under moderate light intensities. Dark relaxation analyses (100 µE m^{-2} s^{-1}) were performed under increasing light intensities to calculate the two different non-photochemical quenching parameters qE (energy-dependent or ΔpH-dependent quenching of Chl fluorescence) and qI (photoinhibitory quenching) (Table 3.3). No drastic difference for PSII photoinhibition (qI) could be observed between *gc9-1* (0.17 ± 0.02) and wild type (0.21 ± 0.03), but ΔpH-dependent quenching of Chl fluorescence (qE) was already increased in *gc9-1* (1.00 ± 0.06) with respect to the wild type (0.42 ± 0.07) under moderate light intensities. Photoinhibitory quenching increased almost linearly with increasing light intensities in *gc9-1* and wild type leaves, while qI values for *gc9-1* were slightly lowered at all measured light intensities compared to those for the wild type (Figure 3.8). qE values (ΔpH-dependent quenching) were elevated in *gc9-1* compared to the wild type under moderate light intensities and saturated at lower light intensities (220 µmol m^{-2} s^{-1}) in *gc9-1* with respect to the wild type (340-540 µmol m^{-2} s^{-1}). Additionally, maximal electron transport rates through PSII were lowered and NPQ values were higher in *gc9-1* compared to the wild type under increasing light intensities (13 and 530 µE m^{-2} s^{-1}) (Figure 3.8). The results indicate that *gc9-1* plants are able to cope with higher excitation pressure under moderate light intensities by ΔpH-dependent quenchingin order to protect PSII. Therefore, the high NPQ phenotype in *gc9-1* is mainly caused by ΔpH-dependent quenching. The increased proton concentration in the lumen activates the xanthophyll cycle which leads to the accumulation of oxidized forms of Vx (Zx and Ax) which could be shown by leaf pigment analyses (Table3.2).

Table 3.3 Photosynthetic parameters of wild type and *gc9-1* leaves were measured with the Dual-PAM system under moderate light intensities (100 µE m^{-2} s^{-1})

The components of non-photochemical quenching (qE and qI) were determined after a 10-min-lasting dark relaxation phase. Averages ± standard deviations were calculated from 6 physiological replicates. F_v/F_m: maximal quantum yield of PSII; Φ_{II}: effective quantum yield of PSII in actinic light (100 µE m^{-2} s^{-1}); 1-qP: excitation pressure; NPQ: non-photochemical Chlorophyll fluorescence quenching; qN: non-photochemical quenching of variable Chl fluorescence; qE: energy-dependent quenching of Chl fluorescence; qI: photoinhibitory quenching.

Parameter	F_v/F_m	Φ_{II}	1-qP	NPQ	qN	qE	qI
WT	0.81 ± 0.01	0.51 ± 0.02	0.28 ± 0.03	0.59 ± 0.08	0.6 ± 0.02	0.42 ± 0.07	0.21 ± 0.03
gc9-1	0.79 ± 0.01	0.41 ± 0.02	0.36 ± 0.02	1.10 ± 0.06	0.75 ± 0.02	1.00 ± 0.06	0.17 ± 0.02

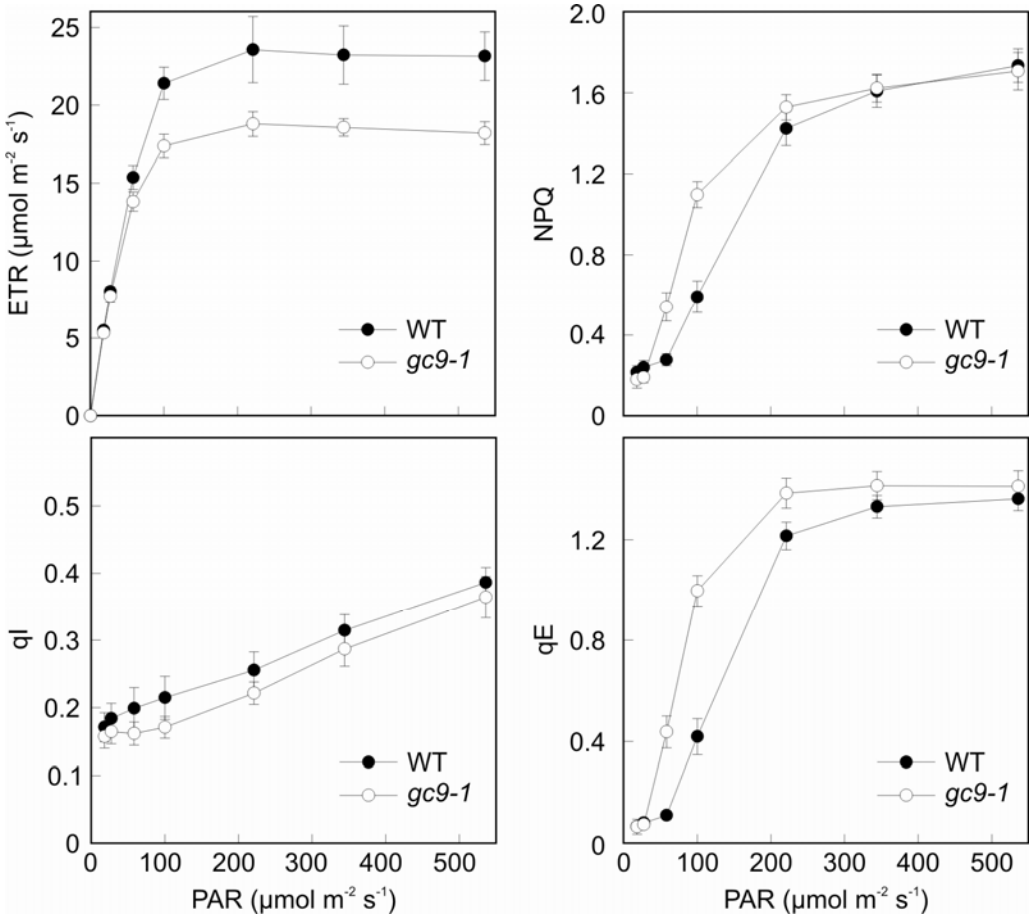

Figure 3.8 Chlorophyll *a* fluorescence induction kinetics of wild type and *gc9-1* plants
Leaves were dark-adapted for 20 min and then exposed to increasing light intensities (13, 22, 53, 95, 216, 339 and 531 µmol $m^{-2}s^{-1}$). Electron transport rates through PSII and non-photochemical quenching (NPQ) were measured after each light phase by a saturating pulse. Energy dependent quenching (qE) and photoinhibitory quenching (qI) for each light intensity were calculated after a 10-min-lasting dark relaxation phase. Average values and standard deviations (error bars) were obtained from six measurements.

To verify if the introduction of the Gc9-EGFP overexpressor construct into *gc9-1* restores wild type like photosynthesis, imaging-PAM analyses were carried out (Figure 3.9). Y (NPQ) values in two independent overexpressor lines, as well as the knock-down *gc9-2,* were similar to wild type plants. Thus, the Gc9::EGFP fusion protein was functional in the complemented lines and led to the restoration of the wild type phenotype.

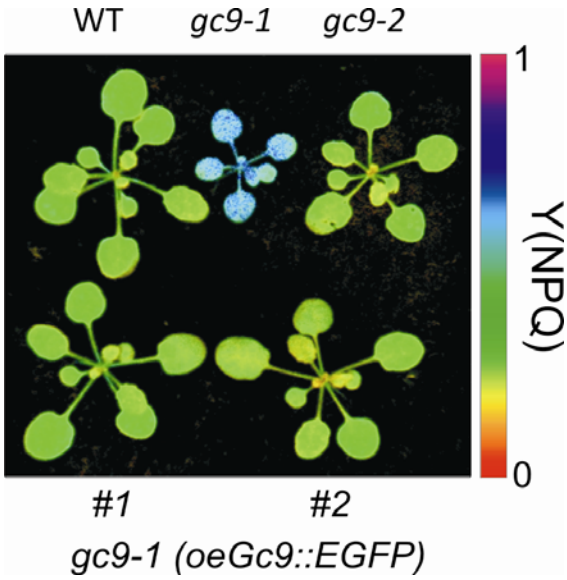

Figure 3.9 Imaging-PAM analyses of wild type, mutant (*gc9-1* and *gc9-2*) and two complemented plants
The plants were dark-adapted for 20 min and then exposed to actinic light (10 min, 100 µmol m^{-2} s^{-1}) to calculate Y (NPQ) values which are shown on the right site of the panel in false colors on a scale from 0 to 1.

3.6 Photosynthetic complexes are altered in *gc9-1*

The abundance of photosynthetic complexes was determined by western blot analyses using antibodies against marker subunits of PSII (D1, D2, CP43 and PsbO), PSI (PsaB, PsaD and PsaL), Cyt b_6f (cytf), light harvesting proteins (Lhcb2 and Lhca1) and of the ATP synthase complex (AtpA/B, AtpC, AtpE, AtpF, AtpG, AtpH and AtpI) (Figure 3.10 A). Photosynthetic complexes were all affected in *gc9-1*; PSII, PSI, Cyt b_6f and LHC were reduced to 60-80 % of the wild type levels. The most severe effect on complex abundance could be identified for the chloroplastic ATP synthase; CF_1 and CF_O subunits in thylakoid membrane preparations were reduced to about 70-80 % wild type levels, whereas ATP synthase abundance in *gc9-2* was similar to wild type plants (Figure 3.10 B). Therefore, the low amounts of Gc9 (less than 25 %) are enough for normal accumulation of the ATP synthase complex in *gc9-2* plants. Taken together, these results indicate that proton-gradient-generating complexes (PSII and Cyt b_6f) are not as strongly affected as the proton gradient-dissipating ATP synthase complex in *gc9-1*. As a consequence, protons accumulate in the thylakoid lumen and trigger energy-dependent quenching mechanisms such as the xanthophyll cycle. Additionally, acidification of the lumen and higher excitation pressure already under moderate light intensities induce long-term adaption processes such as the down regulation of photosynthetic complex synthesis as it has been shown for other mutants affected in the chloroplastic ATP synthase complex (Zoschke et al., 2012).

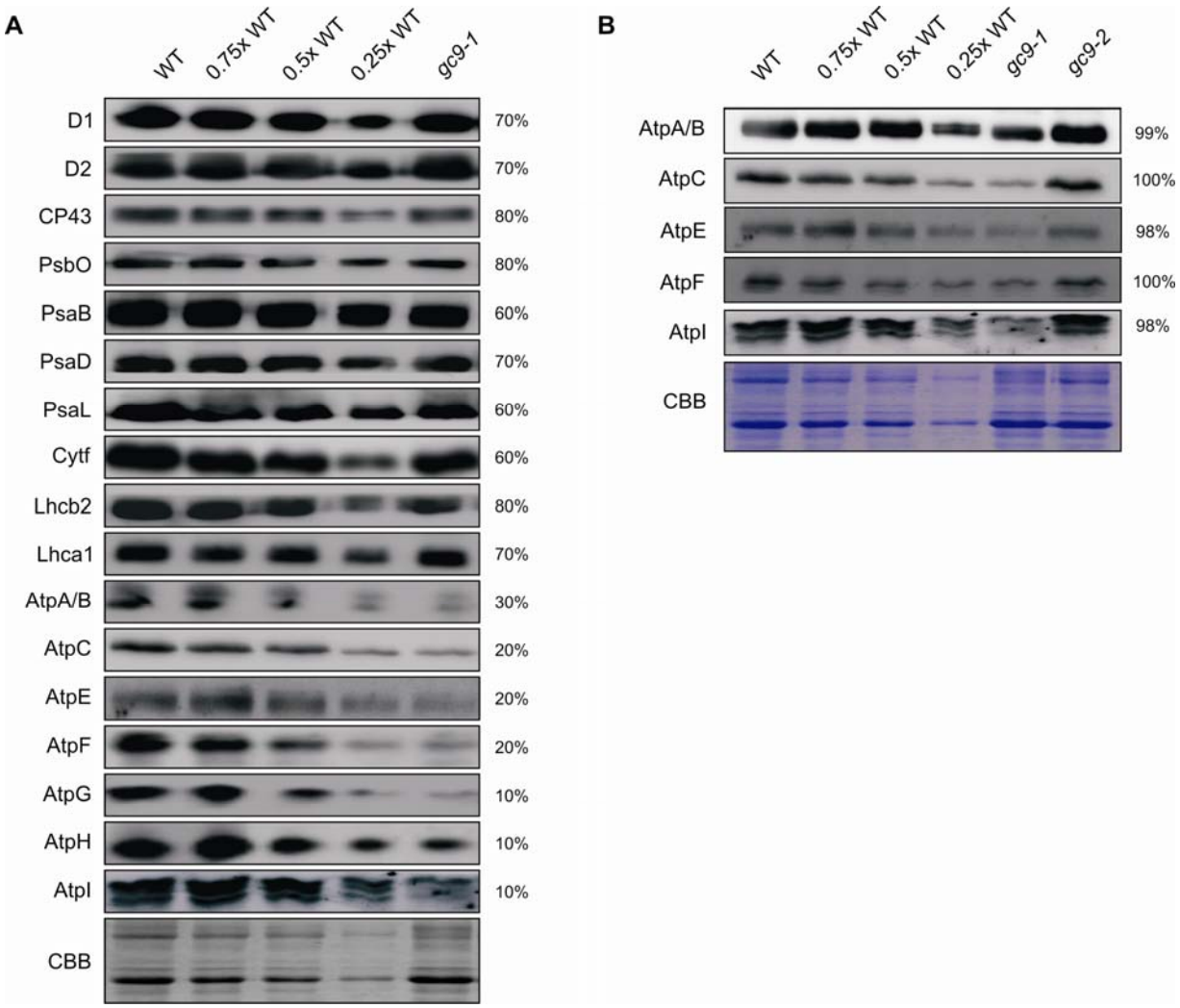

Figure 3.10 Photosynthetic complex abundance in wild type, *gc9-1* and *gc9-2*

A) Wild type and *gc9-1* thylakoid membrane samples (10µg total protein) and decreasing amounts of wild type samples (0.75, 0.5 and 0.25) were fractionated on SDS-PAGEs and blotted on PVDF membranes. Subunits of PSII (D1, D2, CP43, PsbO), PSI (PsaB, PsaD, PsaL), Cyt b_6f (Cytf), LHCs (Lhcb2, Lhca1) and the ATP synthase (AtpA/B, AtpC, AtpE, AtpF, AtpG, AtpH and AtpI) were immunodetected with the respective antibodies. Relative protein amounts (shown on the right site of the panel) were determined by comparing signals from immunodetected proteins in *gc9-1* samples to immunodetected signals from the wild type gradient. **B)** The ATP synthase abundance in *gc9-2* was determined by western blot analyses with antibodies raised against essential subunits of CF_1 and CF_O and compared to *gc9-1* and wild type samples. Relative protein amounts were determined by comparing signals from immunodetected proteins in *gc9-2* samples to immnodetected signals from the wild type gradient and shown on the right site of the panel.

3.7 Gc9 is not a subunit of the ATP synthase complex

The Gc9 to AtpC1 stoichiometry and the Gc9 abundance in different mutant lines were analyzed to clarify whether Gc9 is a subunit of the ATP synthase complex. AtpC1 and Gc9 were heterologously expressed and purified by using an N-terminal fused His-tag. Subsequently, immunodetected signals from known amounts of purified AtpC1 and Gc9 proteins were compared to those from wild type thylakoid samples (Figure 3.11 A). The comparison revealed that the AtpC1 (1.72 ± 0.21 mmol/mol Chl) to Gc9 (0.066 ± 0.001 mmol/mol Chl) ratio is about 25. Thus, the substoichiometric presence of Gc9 with respect to the ATP synthase suggests that Gc9 is not a subunit of the ATP synthase complex. In addition, Gc9 abundance in different photosynthetic mutant lines was determined by western blot analysis (Figure 3.11 B). Entire PSII, PSI, Cyt b_6f or cpATPase complexes are completely absent in *hcf136* (Plücken et al., 2002), *psad1/2* (Ihnatowicz et al., 2004), *petc* (Maiwald et al., 2003) or *atpd* (Maiwald et al., 2003), respectively. Complex abundance was verified by immundetection of marker proteins (PsbO for PSII, PsaF for PSI, Rieske for Cyt b_6f and AtpA/B for ATP synthase deficient mutants). As expected, PsbO, PsaF, Rieske and AtpA/B proteins were not detectable in *hcf136*, *psad1/2*, *petc* and *atpd*, respectively. Instead, Gc9 immunodection showed that Gc9 was present in all photosynthetic mutants, which suggests that Gc9 accumulation is independent of the assembly of all tested photosynthetic complexes. From these results it was concluded that ATP synthase assembly and Gc9 accumulation can occur independently. Overall, Gc9 is not a subunit of the ATP synthase complex, since Gc9 is present in substoichiometric amounts with respect to the ATP synthase and accumulates in the absence of the ATP synthase

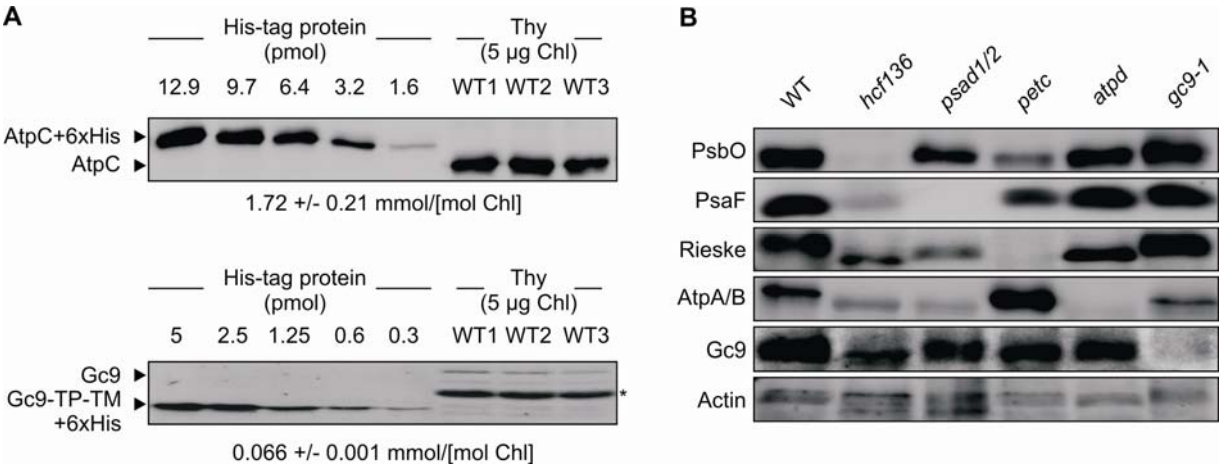

Figure 3.11 Gc9 quantification analyses and abundance in different photosynthetic mutant lines

A) AtpC1 (AtpC1-TP+6His) and Gc9 (Gc9-TP-TM+6xHis) were heterologously expressed in *E. coli* and purified. Known amounts of purified proteins and three wild type thylakoid samples corresponding to 5 µg chlorophyll were loaded on SDS-PAGE to determine the Gc9 to AtpC1 stoichiometry. Thylakoid membrane proteins were fractionated and blotted on PVDF membranes and membranes were probed with AtpC1 and Gc9 antibodies. The asterisk marks an unspecific signal which can not be attributed to Gc9. **B)** Proteins (total leaf extract) of wild type**,** photosynthetic mutant lines devoid of PSII (*hcf136*), PSI (*psad1/2*), Cyt b_6f (*petc*) or of ATP synthase (*atpd*) and *gc9-1* were loaded on Tris-Tricine gels and subsequently subjected to immunodetection analyses with antibodies raised against PsbO, PsaF, Rieske, AtpA/B and Gc9. Actin served as a loading control.

3.8 Gc9 does not form a stable complex with the ATP synthase

To study a potential complex formation of Gc9 with the ATP synthase, solubilized thylakoid complexes from wild type and *gc9-1* plants were separated on sucrose gradients. Gradients were divided into 19 fractions and subjected to western blot analyses using antibodies against AtpA/B, AtpH and Gc9 (Figure 3.12). As expected, the immunodetection assays showed that AtpA/B and AtpH subunits were reduced in *gc9-1* compared to wild type signals, whereas Gc9 was not detectable. In sucrose fractions of the wild type, AtpA/B and AtpH were mainly found in fraction 9 to 13, whereas Gc9 was present in fraction 3 to 6. The different migration pattern of Gc9 in sucrose gradients with respect to the ATP synthase indicated that Gc9 does not form a stable complex with the ATP synthase under the given experimental conditions.

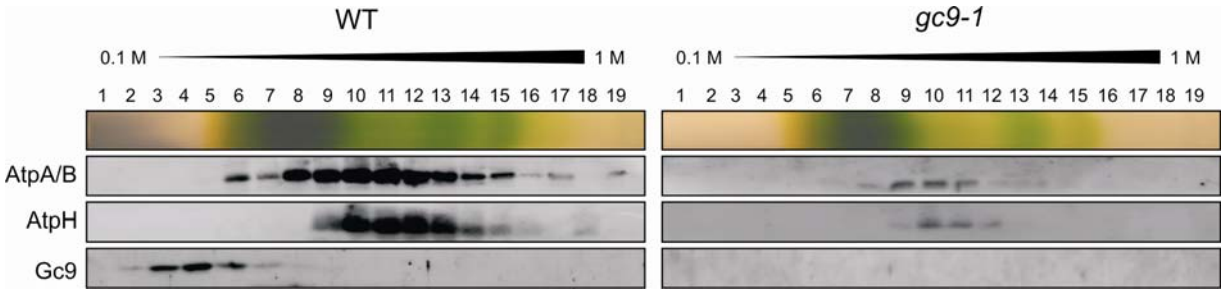

Figure 3.12 Comigration analysis of Gc9 with the ATP synthase complex

Thylakoid membranes from wild type and *gc9-1* leaves were isolated and solubilized by β-DM (1 %). Solubilized membrane complexes were fractionated on sucrose gradients (0.1 to 1 %), which were divided into 19 fractions. Proteins in the fractions were separated on SDS-PAGE and subjected to immunodetection analyses using antibodies against AtpA/B, AtpH and Gc9.

3.9 The transcript abundances of chloroplast-encoded ATP synthase subunits are slightly altered in *gc9-1*

To check if reduced ATP synthase subunit amounts in *gc9-1* are caused by altered transcription, their transcript abundance was tested by Northern blot analyses (Figure 3.13). ATP synthase subunits are encoded in the chloroplast as well as in the nuclear genome. The chloroplast-encoded subunits are organized in two different operons: the large *atpI/H/F/A* operon (encoding for AtpI, AtpH, AtpF and AtpA) and the small *atpB/E* operon (encoding for AtpB and AtpE). The large operon contains several promoters that lead to polycistronic precursors which are then processed to at least 18 different transcripts as shown for the *atpI/H/F/A* operon in maize (Pfalz et al., 2009). The small operon contains two promoters upstream of the *atpB/E* coding region and a promoter within the *atpB* coding region which lead to two dicistronic *atpB/E* and one monocistronic *atpE* transcript, respectively (Ghulam et al., 2012). RNA gel blot analyses with *atpB*- and *atpE*-specific probes revealed that *atpB* transcript amounts in *gc9-1* were similar to the amounts detected in the wild type. An *atpE*-containing transcript with a size slightly smaller than 1200 nt was present in lower amounts in *gc9-1* compared to the wild type, whereas the amount of a 400-nt-long fragment was slightly increased. Northern blot analyses using *atpA* and *atpI* probes revealed that distribution patterns or amounts of these transcripts were not altered in *gc9-1*.

Analyses with *atpH*- and *atpF*-specific probes revealed that three *atpH*-containing fragments were upregulated in *gc9-1* but the amount of an *atpF*-containing fragment was diminished in *gc9-1* with respect to the wild type. According to the RNA blot analyses, no processing defect or downregulation in ATP synthase subunit transcription could be observed which explain the drastic reduction of ATP synthase amounts in *gc9-1*.

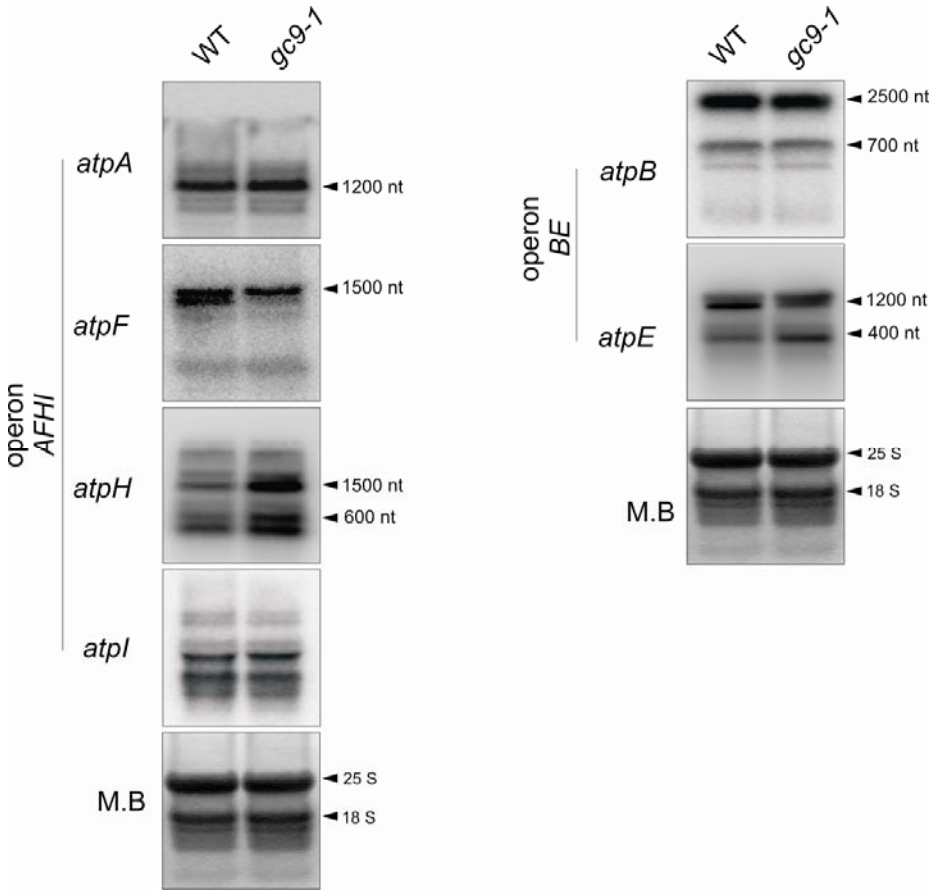

Figure 3.13 RNA gel blot analyses

Isolated total RNA from wild type and *gc9-1* leaf tissue was fractionated on denaturing RNA gels and blotted on nitrocellulose membranes. ^{32}P-labeled probes specific for plastid-encoded ATP synthase subunits were used for hybridization. 25 S and 18 S rRNA was detected by methylen blue (M.B.) staining as a control for equal loading.

3.10 *atpH*-transcript-polysome loading and chloroplast protein synthesis are affected in *gc9-1*

To study if the ATP synthase reduction in *gc9-1* is caused by an affected translation initiation or elongation, polysome analyses were carried out. The association of ATP synthase-specific transcripts to polysomes was analyzed by fractionation of polysome-enriched samples on sucrose gradients and subsequent Northern blot assays (Figure 3.14 A). Ribosome association to transcripts can be estimated by the distribution of ribosomal RNA in sucrose gradients (visualized by ethidium bromide staining of isolated and electrophoretically separated RNA from 10 different sucrose fractions). According to those results, distribution of cytoplasmic 25 S, 18 S and chloroplastic 16 S rRNAs in *gc9-1* samples were similar to the distribution of wild type samples which points to an intact, cellular translation machinery in *gc9-1*. Northern blots with an *atpB*-specific probe (as a marker transcript for the *atpB/E* operon) and an *atpH*-specific probe (as a marker transcript for the *atpI/H/F/A* operon) indicated that ribosome loading on *atpB* transcripts was not altered in *gc9-1*; the ratio of polysome-loaded *atpB* transcripts to free *atpB* transcripts in *gc9-1* (55 % / 45 % = 1.2) was similar to the ratio of the wild type (54 % / 46 % = 1.2). Total amounts of *atpH* transcripts were increased in *gc9-1* and more ribosomes were associated with *atpH* transcripts in fraction 10. However, the ratio of ribosome-associated *atpH* transcripts to unbound *atpH* transcripts in *gc9-1* (67 % / 33 % = 2) was close to that of the wild type (61 % / 39 % = 1.6, lower band). As a conclusion, Gc9 disruption does not lead to an impairment of ribosome loading in *gc9-1* as it has been shown for mutants altered in translation or translation initiation (Schult et al., 2007).

In addition to polysome analyses, *in vivo* pulse labelling experiments were carried out to examine whether the reduced ATP synthase amounts in *gc9-1* are caused by a reduced protein synthesis rates (Figure 3.14 B). Cytosolic translation was blocked by cycloheximide treatment and then radiolabelled, newly synthesized chloroplast proteins were collected after 5 and 30 minutes incubation with [35S] Met. *De novo* synthesized proteins were fractionated on denaturing gels. PsaA/B, AtpA/B, CP47, CP43 and D1/D2 subunits were annotated according to their electrophoretic mobility and to previous studies (Armbruster et al., 2010). Comparing *de novo* synthesized proteins in *gc9-1* and wild type suggests that chloroplast protein synthesis is moderately reduced in *gc9-1*.

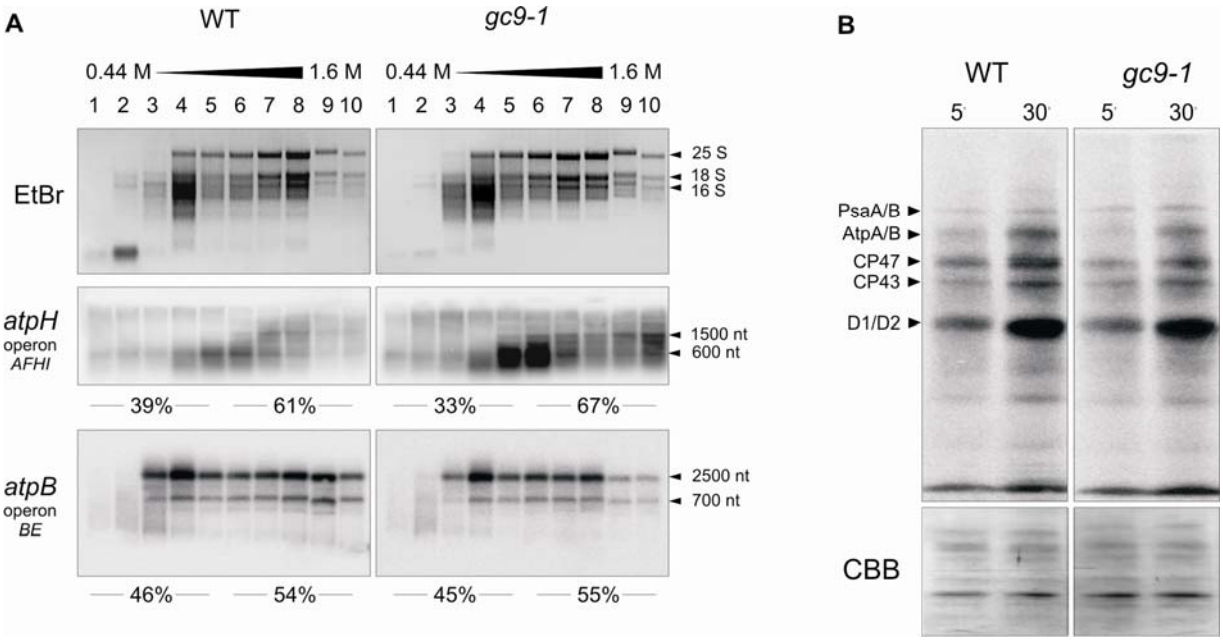

Figure 3.14 Effect of Gc9 disruption on the translation of ATP synthase subunits

A) Association of ATP synthase subunit transcripts to polysomes. Polysome-enriched samples from wild type and *gc9-1* leaves were fractionated on sucrose gradients (0.44 to 1.6 M) by ultracentrifugation. Gradients were divided into 10 fractions and subjected to RNA gel blot analyses. RNA gel blots were stained with ethidium bromide (EtBr) to visualize 25 S, 18 S and 16 S rRNAs. Nitrocellulose membranes with blotted RNA were hybridized with radio-labeled probes specific for *atpH* and *atpB* transcripts. *atpH*- (corresponding to the 600 nt band) and *atpB*-signals (corresponding to the 2500 nt band) were quantified and the ratios of signals arising from fractions 1-5 and 6-10 to the overall signal (fraction 1-10) are shown at the bottom of each RNA blot experiment (in %). **B)** Chloroplastic protein synthesis. Cytosolic translation was blocked by cycloheximide treatment in wild type and *gc9-1* leaves. Newly synthesized thylakoid proteins were isolated from leaves after 5 min (5') and 30 min (30') incubation with [35S] Met under 100 µmol m^{-2} s^{-1} light intensities. Proteins were fractionated by SDS-PAGE and then blotted on PVDF membrane. Signals of *de novo* synthesized proteins were detected by autoradiography.

3.11 AtpH monomer is enriched in the *gc9-1* mutant

To investigate a potential role of Gc9 in the assembly of the ATP synthase, BN/SDS-PAGE analyses were performed. Thylakoid membranes were solubilized with β-DM and photosynthetic complexes were fractionated by Blue Native PAGEs (Figure 3.15 A). Eight major bands, representing PSI-NDH, PSII/PSI supercomplex, monomeric PSI/dimeric PSII, dimeric cyt b_6f/monomeric PSII, multimeric LHCII, monomeric PSII minus CP43, trimeric LHCII and monomeric LHCII were detected in BN/PAGEs (Figure 3.15 A). Blue Native stripes were either stained with Coomassie or used for the second dimension to analyse the complex composition. Coomassie-staining of the BN stripes revealed that a band representing the ATP synthase complex CF_1 (2) was reduced in *gc9-1* compared to the wild type (Figure 3.15 A). The second dimension of BN/PAGE was blotted for either immunodetection or coomassie staining. The coomassie stained membranes (Figure 3.15 B) showed the reduction of AtpA/B and AtpC subunits in *gc9-1* compared to the wild type, which confirmed the results from sucrose gradient and western blot analyses. As shown by immunodetection assays (Figure 3.15 C), three intermediate complexes for the ATP synthase assembly were detected in wild type and *gc9-1*. ATP synthase complex (1) and (2) contain all tested subunits but CF_O (III) complex includes only AtpH and AtpE subunits. Also a strong reduction for all ATP synthase intermediates and monomers/dimers was identified in *gc9-1* for all ATP synthase subunits except for the AtpH monomer which accumulated in *gc9-1*. As shown by immunodetection assays from three independent experiments, the amount of unassembled AtpH in *gc9-1* was eight times higher with respect to the wild type (8 ± 3).

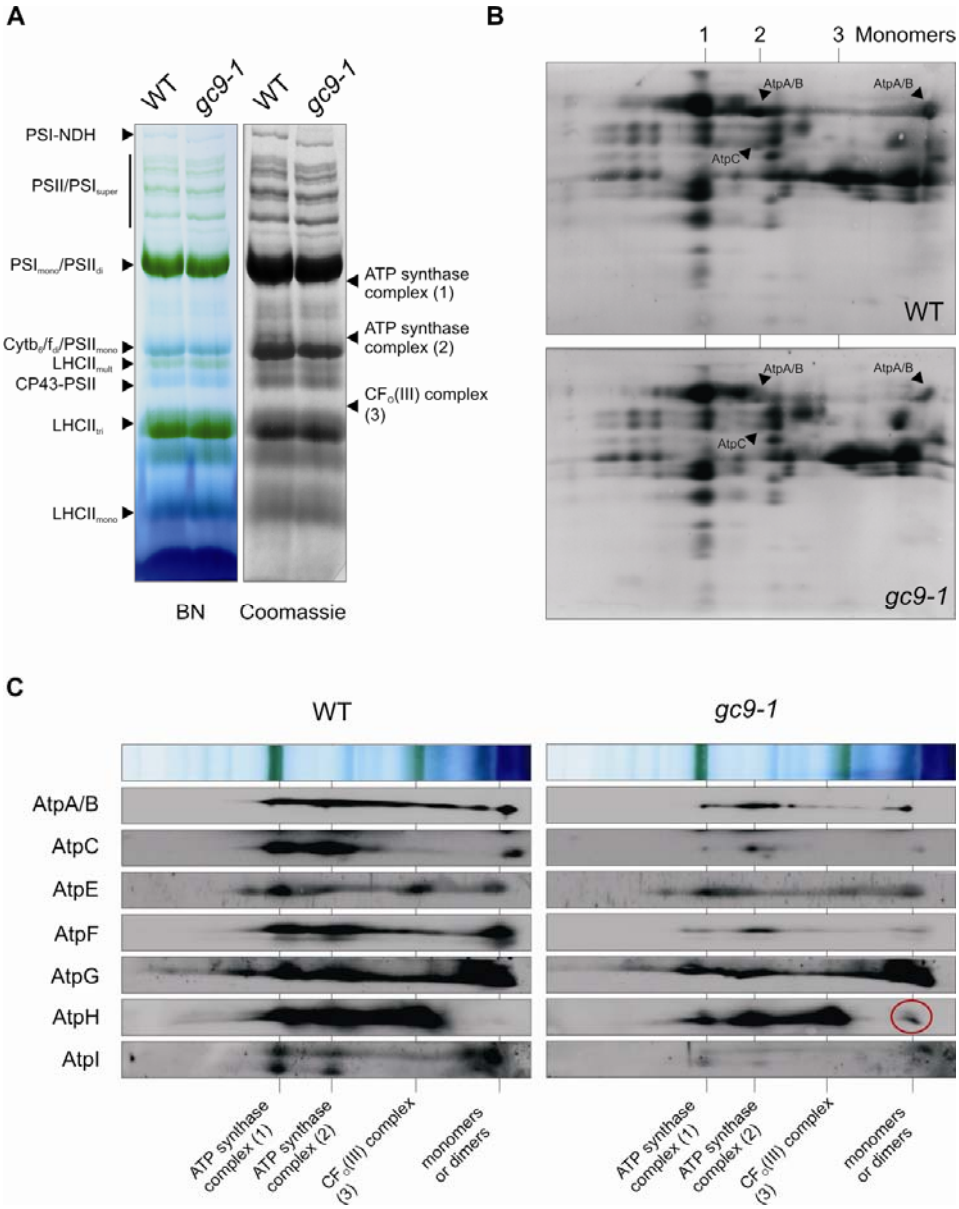

Figure 3.15 Blue Native analyses of wild type and *gc9-1* thylakoid membranes

A) Thylakoid membranes were isolated and then solubilized with β-DM (1 %). Protein amounts corresponding to 80 µg chlorophyll were fractionated on a BN gels (4-12 % gradient). Blue Native stripes were stained with Coomassie (R250) to visualize complexes containing no chlorophyll-binding proteins. **B)** Lanes of the first dimension BN/PAGE gel (160 µg Chlorophyll) were loaded on Tris-Tricine gels (10 %, 4 M urea) to separate protein complexes. Separated proteins were blotted on a PVDF membrane and stained with Coomassie (G250). **C)** Western blot analyses of thylakoid proteins separated by second dimension gel electrophoresis using antibodies against ATP synthase subunits. The accumulation of unassembled AtpH in *gc9-1* is indicated by a red circle.

3.12 Gc9 interacts with the AtpH subunit

According to co-migration analyses on sucrcose gradients, Gc9 does not form a stable complex with the ATP synthase. Transient interactions of Gc9 with the ATP synthase were examined by split-ubiquitin experiments. The mature Gc9 protein (without the predicted transit peptide) was fused to the C-terminal domain of ubiquitin (Cub) and potential interaction partners were cloned and fused with the N-terminal domain of ubiquitin (NubG) carrying a mutation which prevents auto-reconstitution of the ubiquitin protein. Yeast strains were cotransformed with different combinations of the Gc9-Cub fusion construct and NubG-interactor fusion constructs, plated on permissive medium and then the same colonies were grown on selective medium without leucine, threonine and histidine (Figure 3.16). Cell growth on selective medium indicates interaction between Gc9 and the tested fusion construct leading to ubiquitin reconstitution. The combination of Gc9-Cub and ^{NubG}Alg5 was used as a negative control, whereas the combination of Gc9-Cub and ^{NubI}Alg5 was employed as a positive control. According to the results, no interactions of Gc9-Cub with marker subunits of PSII (PsbA and PsbC), PSI (PsaA and PsaB) and other proteins like ferredoxin-NADP^{+}oxidoreductase (FNR), ferredoxin (Fd) and cpSecY were observable. However, interaction assays with ATP synthase subunits revealed that Gc9 interacts with AtpH and in a certain degree with AtpF. No interaction of Gc9 could be observed with the AtpI or AtpA subunit.

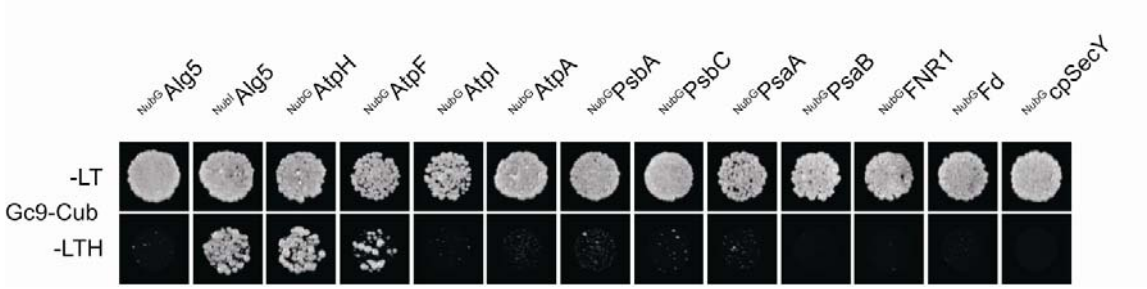

Figure 3.16 Split-ubiquitin assays to test for transient interactions of Gc9 with photosynthetic complexes

Yeast strains were cotransformed with Gc9-Cub and constructs coding for NubG-fusions of potentially interacting proteins (^{NubG}AtpH, ^{NubG}AtpF, ^{NubG}AtpI, ^{NubG}AtpA, ^{NubG}PsbA, ^{NubG}PsbC, ^{NubG}PsaA, ^{NubG}PsaB, ^{NubG}FNR1, ^{NubG}Fd and ^{NubG}cpSecY). Combinations of Gc9-Cub with ^{NubG}Alg5 and ^{NubI}Alg5 were employed as a negative and positive control, respectively. Cotransformed yeast cells were grown on permissive medium without leucine and threonine (-LT) and then on selective medium without leucine, threonine and histidine (-LTH).

4 Discussion

4.1 Photosynthetic electron transport rates are only moderately affected in *gc9-1*

It was described by Rott and his co-workers (2011) that a strong repression of ATP synthase accumulation in tobacco *(Nicotiana tabacum)* leads to a lowered linear electron flux, as well as reduced assimilation and ATP synthase activity. Moreover, a slower growth rate was observed in those mutants. However, ability of photoautotrophic growth was maintained. In contrast, tobacco leaves with a 25 % reduction of ATP synthase content relative to the wild type did not show a significant reduction in ATP synthase activity. Similarly, electron transport, assimilation capacities and all other photosynthetic parameters were not altered. This may indicate that photosynthetic electron transport is only affected by ATP synthase abundances less than 25 %.

According to our data, the lack of Gc9 causes a 70 to 90 % reduction of ATP synthase content (Figure 3.10) leading to a reduced proton translocation efficiency, which in turn results in proton accumulation in the lumen. The lowered pH in the thylakoid lumen acts as a signal to induce the activation of the violaxanthin de-epoxidase enzyme, which accumulates in its protonated form. Elevated ΔpH-dependent quenching and accumulation of protonated violaxanthin in *gc9-1* were confirmed by chlorophyll *a* fluorescence measurements and leaf pigment analyses (Figure 3.8 and Table 3.2).

In contrast, down-regulation of Gc9 expression shows a more robust growth phenotype compared to that of knock-out *gc9-1* plants (Figure 3.3). Also, quantification of ATP synthase subunit abundance by Western blot (Figure 3.10 B) did not display a significant difference. Finally, measurement of non-photochemical quenching by using imaging PAM analyses for *gc9-2* mutants clarified that those values are close to wild type values (Figure 3.9).

The increased non-photochemical quenching of chlorophyll *a* fluorescence and an accumulation of protonated forms of xanthophylls under low light were also observed in the *A. thaliana* mutant line *atpd-1* which lacks the AtpD subunit (Maiwald et al., 2003). The absence of AtpD results in a destabilization of the chloroplastic ATP synthase complex and leads to a slower dissipation of the transthylakoid proton gradient. In addition, the absence of AtpC destabilizes the entire ATP

synthase complex in which a high proton gradient and an elevated ΔpH-dependent quenching (qE) is responsible for most of the non-photochemical quenching (Dal Bosco et al., 2004). Those results confirm that lowered ATP synthase abundance in *gc9-1* is the reason for an elevated thylakoid lumen proton concentration, higher non-photochemical quenching and an activated xantophyll cycle.

4.2 Conserved secondary structure in Gc9

Gc9 is conserved in all organisms from the green lineage (Figure 3.2 B), with its transmembrane domain at the C-terminus being more conserved than the N-terminal part. The conserved N-terminal domain is found only in eukaryotic species and contains two phosphorylation sites, (Reiland et al. 2009). Those sites may play a role in regulation of protein function and thus emphasize further functional or regulatory features for Gc9. A BLAST analysis of the Gc9 sequence against the CDD database revealed a homology to the Atp1/UncI-like domain (Marchler-Bauer et al., 2011). Atp1/UncI is encoded in the F_1F_O ATP synthase operon of bacteria and cyanobacteria (Gay and Walker, 1981). Although the putative transmembrane domains predicted for Gc9 show only moderate sequence similarities with Atp1 proteins from different cyanobacteria (similarity/identity 33.6/18.6 %) (Figure 4.1), their positions align well and constitute a conserved, secondary structure for Gc9 in the eukaryotic green lineage species as well as for Atp1 in various cyanobacteria.

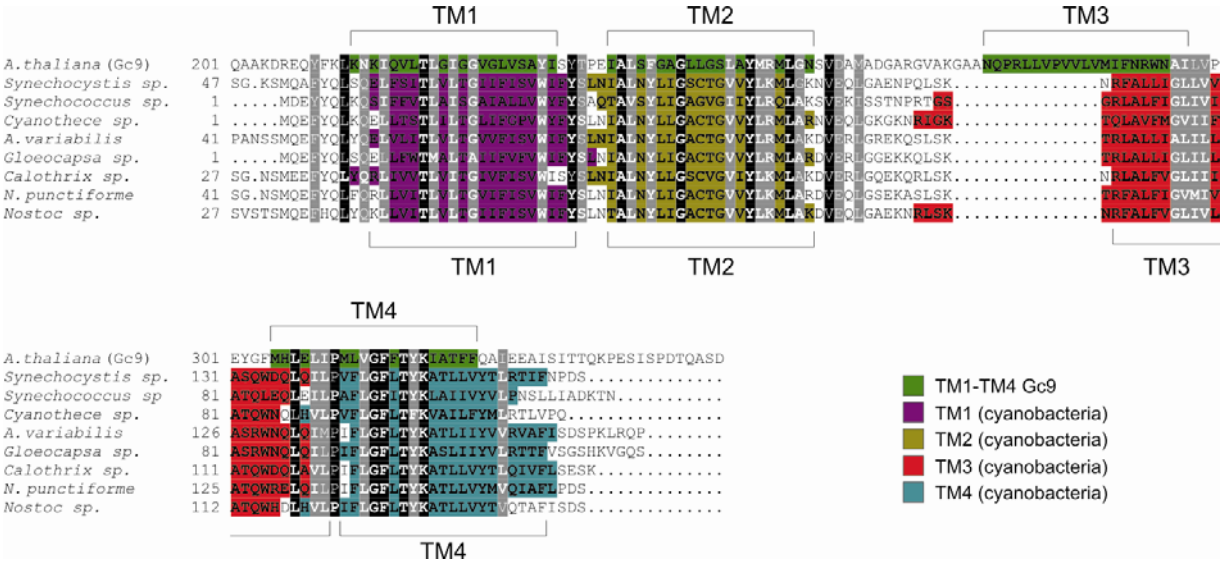

Figure 4.1 Sequence alignment of the Gc9 transmembrane domain with Atp1 from various cyanobacteria

The putative transmembrane domain of Gc9 (201-350 aa) was aligned to Atp1 sequences of *Synechocystis sp.* (*Synechocystis spec.*), *Synechococcus sp.* (*Synechococcus spec.*), *Cyanothece sp.* (*Cyanothece spec.*), *A. variabilis* (*Anabaena variabilis*), *Gloeocapsa sp.* (*Gloeocapsa spec.*), *Calothrix sp.* (*Calothrix spec.*), *N. punctiforme* (*Nostoc punctiforme*) and *Nostoc sp.* (*Nostoc spec.*). The transmembrane domains of Gc9 protein were predicted using the Aramemnon database. SCAMPI was used for prediction of Atp1 transmembrane domains. Residues belonging to putative transmembrane domains are highlighted in bold. Identical and similar amino acids are shaded in black and grey, respectively. Non-conserved amino acids within the putative transmembrane domains are coloured according to the figure legend.

4.3 Upregulation of *atpH* transcripts can be a compensatory mechanism in response to an altered F_O assembly

Gc9 disruption does not lead to severe effects on transcription of ATP synthase subunits (Figure 3.13). Therefore, altered transcription is not the reason for the reduction of ATP synthase subunits in *gc9-1* mutants.

The AtpH ring sructure is directly involved in luminal proton efflux. Therefore, AtpH integration within the lipid bilayer and AtpH ring formation is a critical step for ATP synthase assembly and function (Rochaix, 2011).

Since the fact that ATPH ring formation is affected in *gc9-1* mutants, it can be deduced that unassembled AtpH monomers can lead to a feedback response on *atpH* transcription in an assembly-dependent manner. This feedback response triggers upregulation of *atpH* transcription. RNA gel blot analyses with *atpH* specific probes revealed over accumulation in steady-state levels of these transcripts in *gc9-1* mutants (Figure 3.13).

4.4 Gc9 involvement in the AtpH co-translational membrane integration

The mechanism of AtpH membrane integration was described in the literature for subunit c, the AtpH counterpart in *E. coli* (van Bloois et al., 2004). Using *in vitro* cross-linking experiments in combination with *in vivo* protease mapping techniques, it could be shown that AtpH is co-translationally targeted to the membrane by the signal recognition particle (SRP). The SRP delivers the nascent subunit c to the YidC protein, a member of the Alb3/Oxa1/YidC protein family which functions as a subunit c insertase in a Sec-independent mechanism. Hence, AtpH integration into the membrane is a co-translational integration process.

The results described in this work are in line with observations made by van Bloois et al (2004). The rRNA distribution in *gc9-1* mutants was similar to wild-type plants, so that a general translational effect could be excluded in *gc9-1* chloroplasts. Besides higher amounts of *atpH* transcript, polysome-loading of *atpH* was more pronounced in *gc9-1* mutants (fraction 10, Figure 3.14 A). Taken together these results may provide an evidence for an incomplete membrane integration in *A. thaliana* chloroplasts and are suggestive of a role for Gc9 as co-translational regulator in this insertional process. The conserved N-terminal domain of Gc9 in eukaryotic species may assist in AtpH cotranslational insertion, although AtpH monomer detection in thylakoid membranes of *gc9-1* suggest that other factors beside Gc9 may be involved in the insertional process.

4.5 Gc9 acts as an AtpH ring assembler in chloroplasts

Chloroplast fractionation and subsequent western blot analyses show that Gc9 is a component of the thylakoid membrane (Figure 3.6). Also salt wash experiments imply that Gc9 is an integral membrane protein (Figure 3.6 D) with four putative transmembrane domains (Figure 3.2). Gc9

blast searches against the protein domain database CDD revealed that Gc9 harbors an Atp1/UncI like-domain. Therefore, it was hypothesized that the Gc9 function is the same as the UncI function.

UncI is a hydrophobic protein that contains 130 residues in *E. coli* and its homologs in *Saccharomyces cerevisiae* are YHL007c-a, VMA21 and YHL007c-a. The function of UncI in bacteria (*Propionigenium modestum*) was identified by Suzuki et al. (2007). They reported that the UncI protein plays a chaperone-like role to assist in the *c*-ring assembly of the ATP synthase complex.

The accumulation of unassembled AtpH subunits as a monomer or dimer was detected in *gc9-1* mutants (Figure 3.15 C) and interaction of Gc9 with the AtpH subunit was confirmed by split ubiquitin analyses (Figure 3.16). Those results are clear indications that Gc9 is involved in the efficient assembly of AtpH into the chloroplastic ATP synthase.

Since the abundance of ATP synthase subunits in *gc9-2* knock-down mutants is not as drastically altered as in *gc9-1*, it seems that the presence of 10 % Gc9 is sufficient for the AtpH ring formation (Figure 3.10 B). CF_O is the structural component of the ATP synthase which triggers luminal proton efflux, but it also plays an essential role in ATP synthesis. Hence, the correct assembly of the CF_O domain has a high impact on photosynthesis and needs to be tightly regulated (Weber and Senior, 2000).

Therefore, a disruption in the early steps of the assembly causes an overall reduction of functional ATP synthases leading to several physiological consequences and to long-term adaptational processes (Rott et al., 2011; Maiwald et al., 2003; Dal Bosco et al., 2004) : 1) Acidification of the lumen inhibits the electron transfer between photosystem II and photosystem I (Kramer et al., 2003). Consequently, photochemical activity in the PSII is reduced (Figure 3.8 and Table 3.3) due to enhancement of heat dissipation of energy in the light harvesting antenna of PSII (Jahns et al., 2012).

2) It was hypothesized that plastid gene expression is dependent on the redox state of the electron transport chain (Allen, 1993). The alteration in photosynthetic complex expression as a

secondary effect of Gc9 disruption was detected by immunoblot analyses in *gc9-1* mutants (Figure 3.10 A).

3) Also lowered, overall ATP synthase activity causes lower ATP supply for chloroplast protein synthesis in *gc9-1* that leads to moderate and general reduction of chloroplast protein synthesis, confirmed by *in vivo* pulse labelling analyses (Figure 3.14 B).

4.6 Current model of the F_OF_1 ATP synthase assembly

It could be shown that assembly of the F_1, F_O and stator portions of the ATP synthase occur in independent processes (Tzagoloff, 1969; Velours and Arselin, 2000). The assembly of F_1 takes place in the cytoplasm/stroma where the subunits AtpA, AtpB, AtpC, AtpD and AtpE form a globular structure.

The sequential F_O assembly steps are unknown (Pícková et al., 2005) in which oligomerization of subunit AtpH into the ring can be the initiating step in this process (Lai-Zhang et al., 1999; Duvezin-Caubet et al., 2006). Some factors were identified in *Saccharomyces cerevisiae*, which are involved in transcription or translation of subunit AtpH. The C-terminal half of the Atp25p (cAtp25p) and Aep1p are *atpH* mRNA-specific stability factors (Zeng et al., 2008; Ziaja et al., 1993) and AEP2/ATP13 are involved in expression of subunit *atpH* (Finnegan et al., 1995).

The insertion of subunit AtpH into the inner membrane of *E. coli* is induced by the YidC pathway (Scotti et al., 2000). The N-terminal peptide of Atp25p (32kDa) of *Saccharomyces cerevisiae* functions in oligomerization of AtpH into a proper size ring structure (Zeng et al., 2008) and UncI of *Propionigenium modestum* acts in subunit AtpH ring assembly (Suzuki et al., 2007; Ozaki et al., 2008).

Also our results suggest that Gc9 is a nucleus-encoded protein for ATP synthase complex assembly and function in the AtpH ring formation. The assembled ATP synthase (10-30 %) in *gc9-1* mutants implies that either self-assembly (Arechaga et al., 2002) or other proteins assist in the AtpH ring formation in chloroplasts (Zeng et al., 2008).

The stator formation is required for the initial interaction of F_1 with the ring by stabilization of the AtpH ring/F_1 complex in yeast cells (Tzagoloff, 1970). The assembly of the stator is initiated

with the insertion of subunit AtpG into the inner membrane of mitochondria, followed by interaction between hydrophilic region of subunit AtpI and OSCP, and then terminated with AtpI interaction (Straffon et al., 1998). It was proposed that the hydrophilic subunits of the stator are added to the preassembled F_1 and then this complex interacts with the membrane-embedded part of the stator (subunit AtpI) and the AtpH ring.

Several factors were identified which interacts with subunit AtpF and the AtpH ring in *Saccharomyces cerevisiae*. ATP10 binds to newly translated AtpH subunits and is required for the interaction of the AtpH ring with subunit AtpF, but is not involved in ring assembly (Tzagoloff et al., 2004). Also Atp23p and Oxa1p are involved in the ring/AtpF complex formations (Osman et al., 2007; Jia et al., 2007).

The ATP synthase assembly process in chloroplasts is less understood than in *E. coli* and yeast cells. It could be shown that the YidC homolog ALB4 interacts physically with AtpB and AtpG in the Arabidopsis chloroplast and plays a role in assembly and/or stabilization of the CF_1CF_0–ATP synthase (Benz et al., 2009). The data presented in the thesis show clearly that Gc9 participates in the AtpH ring formation in chloroplasts, but the involvement of Gc9 in other steps of the ATP synthase assembly is still an open question. Nevertheless, Gc9 is the first described ATP synthase assembly factor in chloroplasts and future work will provide more insights into the early ATP synthase assembly steps.

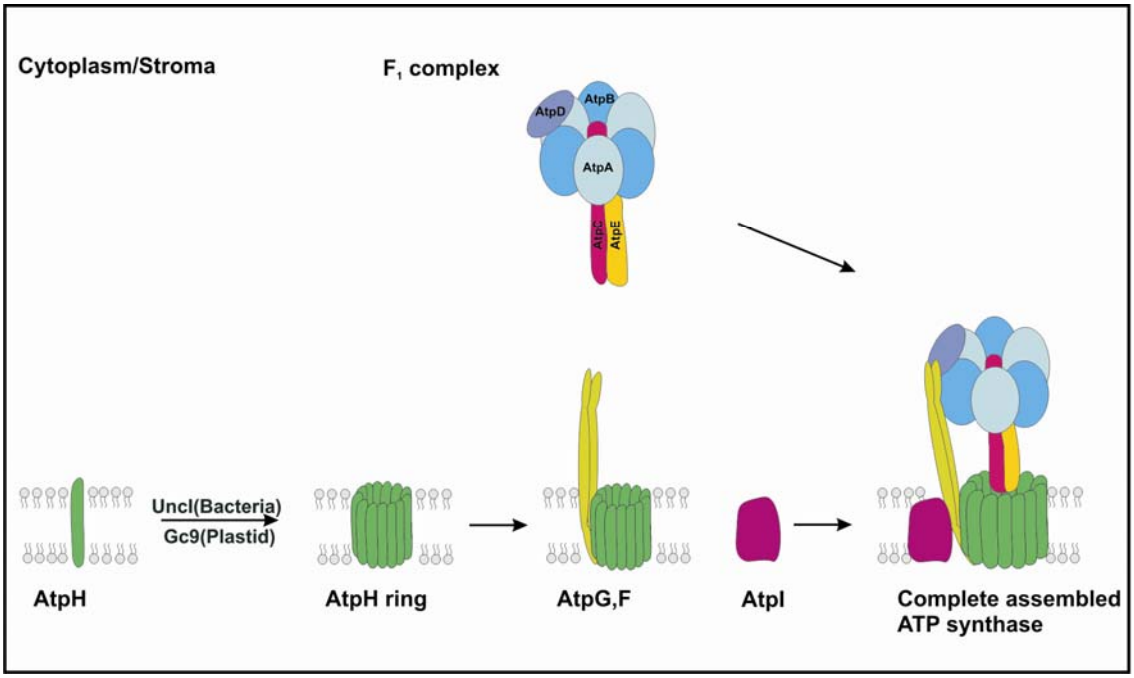

Figure 4.2 Current model of the F_OF_1 ATP synthase assembly

F_1 portion assembly occurs in the cytoplasm/stroma, whereas F_O assembly takes place in the membrane. F_O assembly is initiated by AtpH ring formation in which UncI or Gc9 are involved in. F_O assembly is terminated with AtpI integration and generates the complete ATP synthase after assembly with the F_1 portion.

5 References

Abdallah, F., Salamini, F. and Leister, D. (2000) A prediction of the size and evolutionary origin of the proteome of chloroplasts of Arabidopsis. *Trends Plant Sci*, **5**, 141-142.

Abramoff, M.D., Magelhaes, P.J. and Ram, S.J. (2004) Image Processing with ImageJ. Biophotonics International, volume **11**, 36-42.

Ackerman, S.H. (2002) Atp11p and Atp12p are chaperones for F (1) - ATPase biogenesis in mitochondria. *Biochim Biophys Acta*, **1555**, 101–105.

Ackerman, S.H. and Tzagoloff, A. (1990) ATP10, a yeast nuclear gene required for the assembly of the mitochondrial F1-Fo complex. *J Biol Chem*, **265**, 9952–9959.

Albertsson, P. (2001) A quantitative model of the domain structure of the photosynthetic membrane. *Trends Plant Sci,* **6**, 349–358.

Allen, J.F. (1993) Control of gene expression by redox potential and the requirements for chloroplast and mitochondrial genomes. *J Theor Biol*, **165**, 609-631.

Allen, J., Bennett, J., Steinback, K. and Arntzen, C. (1981) Chloroplast protein phosphorylation couples plastoquinone redox state to distribution of excitation energy between photosystems. *Nature*, **291**, 25–29.

Alonso, J.M., Stepanova, A.N., Leisse, T.J., Kim, C.J., Chen, H., Shinn, P., Stevenson, D.K., Zimmerman, J., Barajas, P., Cheuk, R., Gadrinab, C., Heller, C., Jeske, A., Koesema, E., Meyers, C.C., Parker, H., Prednis, L., Ansari, Y., Choy, N., Deen, H., Geralt, M., Hazari, N., Hom, E., Karnes, M., Mulholland, C., Ndubaku, R., Schmidt, I., Guzman, P., Aguilar-Henonin, L., Schmid, M., Weigel, D., Carter, D.E., Marchand, T., Risseeuw, E., Brogden, D., Zeko, A., Crosby, W.L., Berry, C.C. and Ecker, J.R. (2003) Genome-wide insertional mutagenesis of *Arabidopsis thaliana*. *Science*, **301**, 653-657.

Altamura, N., Capitanio, N., Bonnefoy, N., Papa, S. and Dujardin, G. (1996) The *Saccharomyces cerevisiae* OXA1 gene is required for the correct assembly of cytochrome c oxidase and oligomycin sensitive ATP synthase. *FEBS Lett*, **382**, 111–115.

Arechaga, I., Butler, P.J. and Walker, J.E. (2002) Self-assembly of ATP synthase subunit c rings. *FEBS Lett*, **515**, 189–193.

Armbruster, U., Zühlke, J., Rengstl, B., Kreller, R., Makarenko, E., Rühle, T., Schünemann, D., Jahns, P., Weisshaar, B., Nickelsen, J. and Leister, D. (2010) The Arabidopsis thylakoid protein PAM68 is required for efficient D1 biogenesis and photosystem II assembly. *Plant Cell*, **22**, 3439–3460.

Balsera, M., Goetze, T.A., Kovács-Bogdán, E., Schürmann, P., Wagner, R., Buchanan, B.B., Soll, J. and Bölter, B. (2009) Characterization of Tic110, a channel-forming protein at the inner envelope membrane of chloroplasts, unveils a response to Ca^{2+} and a stromal regulatory disulfide bridge. *J Biol Chem*, **284**, 2603–2616.

Barkan, A. (1988) Proteins encoded by a complex chloroplast transcription unit are each translated from both monocistronic and polycistronic mRNAs. *EMBO J*, **7**, 2637–2644.

Barkan, A. (2011) Expression of plastid genes: organelle-specific elaborations on a prokaryotic scaffold. *Plant Physiol*, **155**, 1520–1532.

Bar-Zvi, D. and Shavit, N. (1982) Modulation of the chloroplast ATPase by tight ADP binding. Effect of uncouplers and ATP. *J Bioenerg Biomembr*, **14**, 467–478.

Bauer, M., Behrens, M., Esser, K., Michaelis, G. and Pratje, E. (1994) PET1402, a nuclear gene required for proteolytic processing of cytochrome oxidase subunit 2 in yeast. *Mol Gen Genet*, **245**, 272–278.

Becker, T., Hritz, J., Vogel, M., Caliebe, A., Bukau, B., Soll, J. and Schleiff, E. (2004) Toc12, a novel subunit of the intermembrane space preprotein translocon of chloroplasts. *Mol Biol Cell*, **15**, 5130–5144.

Beckers, G., Berzborn, R.J. and Strotmann, H. (1992) Zero-length crosslinking between subunit δ and I of the H+-translocating ATPase of chloroplasts. *Biochim Biophys Acta*, **1101**, 97–104.

Bellafiore, S., Ferris, P., Naver, H., Göhre, V. and Rochaix, J.D. (2002) Loss of Albino3 leads to the specific depletion of the light-harvesting system. *Plant Cell*, **14**, 2303–2314.

Benz, M., Bals, T., Gügel, I., Piotrowski, M., Kuhn, A., Schünemann, D., Soll, J. and Ankele, E. (2009) Alb4 of Arabidopsis Promotes Assembly and Stabilization of a Non Chlorophyll-Binding Photosynthetic Complex, the CF_1CF_0–ATP Synthase. *Mol Plant*, **2**, 1410–1424.

Bergantino, E., Segalla, A., Brunetta, A., Teardo, E., Rigoni, F., Giacometti, G.M. and Szabò I. (2003) Light- and pH-dependent structural changes in the PsbS subunit of photosystem II. *Proc Natl Acad Sci U S A*, **100**, 15265–15270.

Boekema, E.J., Fromme, P. and Gräber, P. (1988) On the Structure of the ATP-Synthase from Chloroplasts. *Ber Bunsenges Phys Chem*, **92**, 1031-1036.

Bonnefoy, N., Chalvet, F., Hamel, P., Slonimski, P.P. and Dujardin, G. (1994) OXA1, a *Saccaromyces cerevisiae* nuclear gene whose sequence is conserved from prokaryotes to eukarytes controls cytochrome oxidase biogenesis. *J Mol Biol*, **239**, 201–210.

Boyer, P.D. (1993) The binding change mechanism for ATP synthase: Some probabilities and possibilities. *Biochim Biophys Acta*, **1140**, 215–250.

Briantais, J.M., Vernotte, C., Picaud, M. and Krause, G. (1979) A quantitative study of the slow decline of chlorophyll a fluorescence in isolated chloroplasts. *Biochim Biophys Acta*, **548**, 128–138.

Bukau, B., Weissman, J. and Horwich, A. (2006) Molecular chaperones and protein quality control. *Cell*, **125**, 443–451.

Cline, K. and Dabney-Smith, C. (2008) Plastid protein import and sorting: different paths to the same compartments. *Curr Opin Plant Biol*, **11**, 585–592.

Clough, S.J. and Bent, A.F. (1998) Floral dip: a simplified method for Agrobacterium-mediated transformation of *Arabidopsis thaliana*. *Plant J*, **16**, 735-743.

Contamine, V. and Picard, M. (2000) Maintenance and integrity of the mitochondrial genome: a plethora of nuclear genes in the budding yeast. *Microbiol Mol Biol Rev*, **64**, 281–315.

Cramer, W.A., Zhang, H., Yan, J., Kurisu, G. and Smith, J.L. (2006) Transmembrane traffic in the cytochrome b_6f complex. *Annu Rev Biochem*, **75**, 769-790.

Dal Bosco, C., Lezhneva, L., Biehl, A., Leister, D., Strotmann, H., Wanner, G. and Meurer, J. (2004) Inactivation of the chloroplast ATP synthase gamma subunit results in high non-photochemical fluorescence quenching and altered nuclear gene expression in *Arabidopsis thaliana*. *J Biol Chem*, **279**, 1060-1069.

Dekker, J.P. and Boekema, E.J. (2005) Supramolecular organization of thylakoid membrane proteins in green plants. *Biochim Biophys Acta*, **1706**, 12–39.

Demmig, B., Winter, K., Krüger, A. and Czygan, F.C. (1987) Photoinhibition and zeaxanthin formation in intact leaves. A possible role of the xanthophyll cycle in the dissipation of excess light. *Plant Physiol*, **84**, 218–224.

Dent, R.M., Haglund, C.M., Chin, B.L., Kobayashi, M.C. and Niyogi, K.K. (2005) Functional genomics of eukaryotic photosynthesis using insertional mutagenesis of *Chlamydomonas reinhardtii*. *Plant Physiol*, **137**, 545-556.

Dühring, U., Ossenbühl, F. and Wilde, A. (2007) Late assembly steps and dynamics of the cyanobacterial photosystem I. *J Biol Chem*, **282**, 10915– 10921.

Duvezin-Caubet, S., Rak, M., Lefebvre-Legendre, L., Tetaud, E., Bonnefoy, N. and di Rago, J.P. (2006) A "petite obligate" mutant of *Saccharomyces cerevisiae*: functional mtDNA is lethal in cells lacking the delta subunit of mitochondrial F_1-ATPase. *J Biol Chem*, **281**, 16305–16313.

Eberhard, S., Finazzi, G. and Wollman, F.A. (2008) The dynamics of photosynthesis. *Annu Rev Genet*, **42**, 463-515.

Emanuelsson, O., Nielsen, H. and von Heijne, G. (1999) ChloroP, a neural network-based method for predicting chloroplast transit peptides and their cleavage sites. *Protein Sci*, **8**, 978-984.

Esteban, R., Olano, J.M., Castresana, J., Fernández-Marín, B., Hernández, A., Becerril, J.M. and García-Plazaola, J.I. (2009) Distribution and evolutionary trends of photoprotective isoprenoids (xanthophylls and tocopherols) within the plant kingdom. *Physiol Plant*, **135**, 379–389.

Evron, Y. and McCarty, R.E. (2000) Simultaneous measurement of deltapH and electron transport in chloroplast thylakoids by 9-aminoacridine fluorescence. *Plant Physiol*, **124**, 407-414.

Evron, Y., Johnson, E.A. and McCarty, R.E. (2000) Regulation of proton flow and ATP synthesis in chloroplasts. *J Bioenerg Biomembr*, **32**, 501-506.

Färber, A., Young, A.J., Ruban, A.V., Horton, P. and Jahns, P. (1997) Dynamics of xanthophyll-cycle activity in different antenna subcomplexes in the photosynthetic membranes of higher plants (The relationship between zeaxanthin conversion and nonphotochemical fluorescence quenching). *Plant Physiol*, **115**, 1609-1618.

Finnegan, P.M., Ellis, T.P., Nagley, P. and Lukins, H.B. (1995) The mature AEP2 gene product of *Saccharomyces cerevisiae*, required for the expression of subunit 9 of ATP synthase, is a 58 kDa mitochondrial protein. *FEBS Lett*, **368**, 505–508.

Folch, J. and Lees, M. (1951) Proteolipides, a new type of tissue lipoproteins; their isolation from brain. *J Biol Chem*, **191**, 807-817.

Fromme, P., Boekema, E.J. and Gräber, P. (1987) Isolation and characterization of a supramolecular complex of subunit III of the ATP synthase from chloroplasts. *Z Naturforsch*, **42c,** 1239-1245**.**

Fromme, P., Gräber, P. and Salnikow, J. (1987) Isolation and identification of a fourth subunit in the membrane part of the chloroplast ATP Synthase. *FEBS Lett*, **218**, 27-30.

Garcia-Plazaola, J.I., Matsubara, S. and Osmond, C.B. (2007) The lutein epoxide cycle in higher plants: its relationships to other xanthophyll cycles and possible functions. *Funct Plant Biol*, **34**, 759–773.

Gay, N.J. and Walker, J.E. (1981) The atp operon: nucleotide sequence of the promoter and the genes for the membrane proteins, and the delta subunit of *Escherichia coli* ATP-synthase. *Nucleic Acids Res*, **9**, 3919-3926.

Gay, N.J. and Walker, J.E. (1981) The atp operon: nucleotide sequence of the region encoding the alpha-subunit of *Escherichia coli* ATP-synthase. *Nucleic Acids Res*, **9**, 2187-2194.

Ghulam, M.M., Zghidi-Abouzid, O., Lambert, E., Lerbs-Mache, S. and Merendino, L. (2012) Transcriptional organization of the large and the small ATP synthase operons, *atpI/H/F/A* and *atpB/E*, in *Arabidopsis thaliana* chloroplasts. *Plant Mol Biol*, **79**, 259-272.

Gokirmak, T., Paul, A.L. and Ferl, R.J. (2010) Plant phosphopeptide-binding proteins as signaling mediators. *Curr Opin Plant Biol*, **13**, 527–532.

Grossman, A.R., Karpowicz, S.J., Heinnickel, M., Dewez, D., Hamel, B., Dent, R., Niyogi, K.K., Johnson, X., Alric, J., Wollman, F.A., Li, H. and Merchant, S.S. (2010) Phylogenomic analysis of the Chlamydomonas genome unmasks proteins potentially involved in photosynthetic function and regulation. *Photosynth Res*, **106**, 3-17.

Groth, G. and Junge, W. (1993) Proton slip of the chloroplast ATPase: Its nucleotide dependence, energetic threshold and relation to an alternating site mechanisms of catalysis. *Biochemistry*, **32**, 8103–8111.

Groth, G. and Pohl, E. (2001) The structure of the chloroplast F_1-ATPase at 3.2 Å resolution. *J Biol Chem*, **276**, 1345–1352.

Groth, G. and Strotmann, H. (1999) New results about structure, function and regulation of the chloroplast ATP synthase (CF_0CF_1). *Physiol Plant*, **106**, 142–148.

Havaux, M., Dall'Osto, L. and Bassi, R. (2007) Zeaxanthin has enhanced antioxidant capacity with respect to all other xanthophylls in Arabidopsis leaves and functions independent of binding to PSII antennae. *Plant Physiol*, **145**, 1506–1520.

Helfenbein, K.G., Ellis, T.P., Dieckmann, C.L. and Tzagoloff, A. (2003) ATP22, a nuclear gene required for expression of the F_O sector of mitochondrial ATPase in *Saccharomyces cerevisiae*. *J Biol Chem*, **278**, 19751–19756.

Hisabori, T., Kato, Y., Motohashi, K., Kroth-Pancic, P., Strotmann, H. and Amano, T. (1997) The regulatory functions of the gamma and epsilon subunits from chloroplast CF_1 are transferred to the core complex, alpha3beta3, from thermophilic bacterial F_1. *Eur J Biochem*, **247**, 1158–1165.

Hisabori, T., Ueoka-Nakanishi, H., Konno, H. and Koyama, F. (2003) Molecular evolution of the modulator of chloroplast ATP synthase: origin of the conformational change dependent regulation. *FEBS Lett*, **545**, 71–75.

Holzwarth, A.R., Miloslavina, Y., Nilkens, M. and Jahns, P. (2009) Identification of two quenching sites active in the regulation of photosynthetic light-harvesting studied by time-resolved fluorescence. *Chem Phys Lett*, **483**, 262–267.

Horton, P., Wentworth, M. and Ruban, A. (2005) Control of the light harvesting function of chloroplast membranes: the LHCII-aggregation model for non-photochemical quenching. *FEBS Lett*, **579**, 4201–4206.

Ihnatowicz, A., Pesaresi, P., Varotto, C., Richly, E., Schneider, A., Jahns, P., Salamini, F. and Leister, D. (2004) Mutants of photosystem I subunit D of *Arabidopsis thaliana*: effects on photosynthesis, photosystem I stability and expression of nuclear genes for chloroplast functions. *Plant J*, **37**, 839-852.

Jackson-Constan, D., Akita, M. and Keegstra, K. (2001) Molecular chaperones involved in chloroplast protein import. *Biochim Biophys Acta*, **1541**, 102–113.

Jahns, P. and Holzwarth, A.R. (2012) The role of the xanthophyll cycle and of lutein in photoprotection of photosystem II. *Biochim Biophys Acta*, **1817**, 182-193.

Jahns, P., Latowski, D. and Strzalka, K. (2009) Mechanism and regulation of the violaxanthin cycle: the role of antenna proteins and membrane lipids. *Biochim Biophys Acta*, **1787**, 3–14.

Jansson, S., Stefansson, H., Nystrom, U., Gustafsson, P. and Albertsson, P.A. (1997) Antenna protein composition of PS I and PS II in thylakoid sub-domains. *Biochim Biophys Acta*, **1320**, 297-309.

Jia, L., Dienhart, M.K. and Stuart, R.A. (2007) Oxa1 directly interacts with Atp9 and mediates its assembly into the mitochondrial F_1F_o-ATP synthase complex. *Mol Biol Cell*, **18**, 1897–1908.

Johnson, M.P., Davison, P.A., Ruban, A.V. and Horton, P. (2008) The xanthophyll cycle pool size controls the kinetics of non-photochemical quenching in *Arabidopsis thaliana*. *FEBS Lett*, **582**, 262–266.

Kalituho, L., Rech, J. and Jahns, P. (2007) The role of specific xanthophylls in light utilization, *Planta*, **225**, 423–439.

Kanazawa, A. and Kramer, D.M. (2002) In vivo modulation of non-photochemical exciton quenching (NPQ) by regulation of the chloroplast ATP synthase. *Proc Natl Acad Sci U S A,* **99**, 12789–12794.

Karimi, M., Inze, D. and Depicker, A. (2002) GATEWAY vectors for Agrobacterium-mediated plant transformation. *Trends Plant Sci*, **7**, 193-195.

Karnauchov, I., Herrmann, R.G. and Klosgen, R.B. (1997) Transmembrane topology of the Rieske Fe/S protein of the cytochrome b_6/f complex from spinach chloroplasts. *FEBS Lett*, **408**, 206-210.

Karpowicz, S.J., Prochnik, S.E., Grossman, A.R. and Merchant, S.S. (2011) The GreenCut2 resource, a phylogenomically derived inventory of proteins specific to the plant lineage. *J Biol Chem*, **286**, 21427–21439.

Keegstra, K. and Cline, K. (1999) Protein import and routing systems of chloroplasts. *Plant Cell*, **11**, 557–570.

Kothen, G., Schwarz, O. and Strotmann, H. (1995) The kinetics of photophosphorylation at clamped ΔpH indicate a random order of substrate binding. *Biochim Biophys Acta*, **1229**, 208–214.

Kramer, D.M., Cruz, J.A. and Kanazawa, A. (2003) Balancing the central roles of the thylakoid proton gradient. *Trends Plant Sci*, **8**, 27-32.

Kramer, D.M., Johnson, G., Kiirats, O. and Edwards, G.E. (2004) New fluorescence parameters for the determination of q (a) redox state and excitation energy fluxes. *Photosynth Res*, **79**, 209-218.

Krause, G.H. (1988) Photoinhibition of photosynthesis. An evaluation of damaging and protective mechanisms. *Physiol Plant*, **74**, 566–574.

Krause, G.H., Vernotte, C. and Briantais, J.M. (1982) Photoinduced quenching of chlorophyll fluorescence in intact chloroplasts and algae. Resolution into two components. *Biochim Biophys Acta*, **679**, 116–124.

Kuhn, A., Stuart, R., Henry, R. and Dalbey, R.E. (2003) The Alb3/Oxa1/YidC protein family: membrane localized chaperones facilitating membrane protein insertion? *Trends Cell Biol*, **13**, 510–516.

Lai-Zhang, J., Xiao, Y. and Mueller, D.M. (1999) Epistatic interactions of deletion mutants in the genes encoding the F_1-ATPase in yeast *Saccharomyces cerevisiae*. *EMBO J*, **18**, 58–64.

Lambrev, P.H., Nilkens, M., Miloslavina, Y., Jahns, P. and Holzwarth, A.R. (2010) Kinetic and spectral resolution of multiple nonphotochemical quenching components in Arabidopsis leaves. *Plant Physiol*, **152**, 1611–1624.

Lefebvre-Legendre, L., Vaillier, J., Benabdelhak, H., Velours, J., Slonimski, P.P. and di Rago, J.P. (2001) Identification of a nuclear gene (FMC1) required for the assembly/stability of yeast mitochondrial F(1)- ATPase in heat stress conditions. *J Biol Chem*, **276**, 6789 – 6796.

Leister, D. (2003) Chloroplast research in the genomic age. *Trends Genet*, **19**, 47–56.

Li, H.M. and Chiu, C.C. (2010) Protein transport into chloroplasts. *Annu Rev Plant Biol*, **61**, 157–180.

Li, X.P., Gilmore, A.M., Caffarri, S., Bassi, R., Golan, T., Kramer, D. and Niyogi, K.K. (2004) Regulation of photosynthetic light harvesting involves intrathylakoid lumen pH sensing by the PsbS protein. *J Biol Chem*, **279**, 22866–22874.

Li, X.P., Muler-Moule, P., Gilmore, A.M. and Niyogi, K.K. (2002) PsbS-dependent enhancement of feedback de-excitation protects photosystem II from photoinhibition. *Proc Natl Acad Sci U S A*, **99**, 15222–15227.

Li, Z., Wakao, S., Fischer, B.B. and Niyogi, K.K. (2009) Sensing and responding to excess light. *Annu Rev Plant Biol*, **60**, 239–260.

Ludlam, A., Brunzelle, J., Pribyl, T., Xu, X., Gatti, D.L. and Ackerman, S.H. (2009) Chaperones of F_1-ATPase. *J Biol Chem*, **284**, 17138-17146.

Maier, U.G., Bozarth, A., Funk, H.T., Zauner, S., Rensing, S.A., Schmitz-Linneweber, C., Börner, T. and Tillich, M. (2008) Complex chloroplast RNA metabolism: just debugging the genetic programme? *BMC Biol*, **6**, 36-45.

Maiwald, D., Dietzmann, A., Jahns, P., Pesaresi, P., Joliot, P., Joliot, A., Levin, J.Z., Salamini, F. and Leister, D. (2003) Knock-out of the genes coding for the Rieske protein and the ATP- synthase delta-subunit of Arabidopsis. Effects on photosynthesis, thylakoid protein composition, and nuclear chloroplast gene expression. *Plant Physiol*, **133**,191-202.

Marchler-Bauer, A., Anderson, J.B., DeWeese-Scott, C., Fedorova, N.D., Geer, L.Y., He, S., Hurwitz, D.I., Jackson, J.D., Jacobs, A.R., Lanczycki, C.J., Liebert, C.A., Liu, C., Madej, T., Marchler, G.H., Mazumder, R., Nikolskaya, A.N., Panchenko, A.R., Rao, B.S., Shoemaker, B.A., Simonyan, V., Song, J.S., Thiessen, P.A., Vasudevan, S., Wang, Y., Yamashita, R.A., Yin, J.J. and Bryant, S.H. (2003) CDD: a curated Entrez database of conserved domain alignments. *Nucleic Acids Res*, **31**, 383–387.

Marchler-Bauer, A., Lu, S., Anderson, J.B., Chitsaz, F., Derbyshire, M.K., DeWeese-Scott, C., Fong, J.H., Geer L.Y., Geer, R.C., Gonzales, N.R., Gwadz, M., Hurwitz, D.I., Jackson,

J.D., Ke, Z., Lanczycki, C.J., Lu, F., Marchler, G.H., Mullokandov, M., Omelchenko, M.V., Robertson, C.L., Song, J.S., Thanki, N., Yamashita, R.A., Zhang, D., Zhang, N., Zheng, C. and Bryant, S.H. (2011) CDD: a Conserved Domain Database for the functional annotation of proteins. *Nucleic Acids Res,* **39**, 225-229.

Mathis, P., Butler, W.L. and Satoh, K. (1979) Carotenoid triplet-state and chlorophyll fluorescence quenching in chloroplasts and sub-chloroplast particles. *Photochem Photobiol*, **30**, 603–614.

Menke, W. (1962) Structure and chemistry of plastids. *Annu Rev Plant Physiol Plant Mol Biol*, **13**, 27–44.

Merchant, S.S., Prochnik, S.E., Vallon, O., Harris, E.H., Karpowicz, S.J., Witman, G.B., Terry, A., Salamov, A., Fritz-Laylin, L.K., Mare´chal-Drouard, L., Marshall, W.F., Qu, L.H., Nelson, D.R., Sanderfoot, A.A., Spalding, M.H., Kapitonov, V.V., Ren, Q., Ferris, P., Lindquist, E., Shapiro, H., Lucas, S.M., Grimwood, J., Schmutz, J., Cardol, P., Cerutti, H., Chanfreau, G., Chen, C.L., Cognat, V., Croft, M.T., Dent, R., Dutcher, S., Ferna´ndez, E., Fukuzawa, H., Gonza´lez-Ballester, D., Gonza´lez-Halphen, D., Hallmann, A., Hanikenne, M., Hippler, M., Inwood, W., Jabbari, K., Kalanon, M., Kuras, R., Lefebvre, P.A., Lemaire, S.D., Lobanov, A.V., Lohr, M., Manuell, A., Meier, I., Mets, L., Mittag, M., Mittelmeier, T., Moroney, J.V., Moseley, J., Napoli, C., Nedelcu, A.M., Niyogi, K., Novoselov, S.V., Paulsen, I.T., Pazour, G., Purton, S., Ral, J.P., Riaño-Pachón, D.M., Riekhof, W., Rymarquis, L., Schroda, M., Stern, D., Umen, J., Willows, R., Wilson, N., Zimmer, S.L., Allmer, J., Balk, J., Bisova, K., Chen, C.J., Elias, M., Gendler, K., Hauser, C., Lamb, M.R., Ledford, H., Long, J.C., Minagawa, J., Page, M.D., Pan, J., Pootakham, W., Roje, S., Rose, A., Stahlberg, E., Terauchi, A.M., Yang, P., Ball, S., Bowler, C., Dieckmann, C.L., Gladyshev, V.N., Green, P., Jorgensen, R., Mayfield, S., Mueller-Roeber, B., Rajamani, S., Sayre, R.T., Brokstein, P., Dubchak, I., Goodstein, D., Hornick, L., Huang, Y.W., Jhaveri, J., Luo, Y., Martínez, D., Ngau, W.C., Otillar, B., Poliakov, A., Porter, A., Szajkowski, L., Werner, G., Zhou, K., Grigoriev, I.V., Rokhsar, D.S. and Grossman, A.R. (2007) The Chlamydomonas genome reveals the evolution of key animal and plant functions. *Science*, **318**, 245–250.

Mills, J.D., Austin, P.A. and Turton, J.S. (1995) Thioredoxin and control of F_0F_1: function and distribution. *Biochem Soc Trans*, **23**, 775-780.

Moroney, J.V., Lopresti, L., McCarty, R.E. and Hammes, G.G. (1983) The M_r value of chloroplast coupling factor 1. *FEBS Lett*, **158**, 58-62.

Naver, H., Boudreau, E. and Rochaix, J.D. (2001) Functional studies of Ycf3: its role in assembly of photosystem I and interactions with some of its subunits. *Plant Cell*, **13**, 2731–2745.

Nelson, D.L. and Cox, M.M. (2005) Lehninger Principles of Biochemistry, 4th Edn, Worth Publishers, N.Y.

Nelson, N. and Ben-Shem, A. (2004) The complex architecture of oxygenic photosynthesis. *Nat Rev Mol Cell Biol*, **5**, 971-982.

Nilkens, M., Kress, E., Lambrev, P., Miloslavina, Y., Müller, M., Holzwarth, A.R. and Jahns, P. (2010) Identification of a slowly inducible zeaxanthin-dependent component of non-photochemical quenching of chlorophyll fluorescence generated under steady state conditions in Arabidopsis. *Biochim Biophys Acta*, **1797**, 466–475.

Osman, C., Wilmes, C., Tatsuta, T. and Langer, T. (2007) Prohibitins interact genetically with Atp23, a novel processing peptidase and chaperone for the F_1F_O-ATP synthase. *Mol Biol Cell*, **18**, 627–635.

Ozaki, Y., Suzuki, T., Kuruma, Y., Ueda, T. and Yoshida, M. (2008) UncI protein can mediate ring assembly of c-subunits of F_OF_1-ATP synthase in vitro. *Biochem Biophys Res Commun*, **367**, 663–666.

Ozawa, S., Nield, J., Terao, A., Stauber, E.J., Hippler, M., Koike, H., Rochaix, J.D. and Takahashi, Y. (2009) Biochemical and structural studies of the large Ycf4- photosystem I assembly complex of the green alga *Chlamydomonas reinhardtii*. *Plant Cell*, **21**, 2424–2442.

Patrie, W.J. and McCarty, R.E. (1984) Specific binding of coupling factor 1 lacking the delta and epsilon subunits to thylakoids. *J Biol Chem*, **259**, 11121-11128.

Pfalz, J., Bayraktar, O.A., Prikryl, J. and Barkan, A. (2009) Site-specific binding of a PPR protein defines and stabilizes 5' and 3' mRNA termini in chloroplasts. *EMBO J*, **28**, 2042-2052.

Pícková, A., Potocký, M. and Houstek, J. (2005) Assembly factors of F_1F_O-ATP synthase across genomes. *Proteins*, **59**, 393–402.

Pick, U. and Racker, E. (1979) purification and reconstitution of the N,N'-dicyclohexylcarbodiimide- sensitive ATP ase complex from spinach chloroplasts. *J Biol Chem*, **254**, 2793-2799.

Plücken, H., Müller, B., Grohmann, D., Westhoff, P. and Eichacker, L.A. (2002) The HCF136 protein is essential for assembly of the photosystem II reaction center in *Arabidopsis thaliana*. *FEBS Lett*, **532**, 85-90.

Pogoryelov, D., Yu, J., Meier, T., Vonck, J., Dimroth, P. and Muller, D.J. (2005) The c15 ring of the Spirulina platensis F-ATP synthase: F_1/F_O symmetry mismatch is not obligatory. *EMBO Rep*, **6**, 1040-1044.

Porra, R.J., Thompson, W.A. and Kriedermann, P.E. (1989) Determination of accurate extinction coefficient and simultaneous equations for assaying chlorophylls *a* and *b* extracted with four different solvents: Verification of the concentration of chlorophyll standards by atomic absorption spectroscopy. *Biochim Biophys Acta*, **975**, 384–394.

Qbadou, S., Becker, T., Mirus, O., Tews, I., Soll, J. and Schleiff, E. (2006) The molecular chaperone Hsp90 delivers precursor proteins to the chloroplast import receptor Toc64. *EMBO J*, **25**, 1836–1847.

Reiland, S., Messerli, G., Baerenfaller, K., Gerrits, B., Endler, A., Grossmann, J., Gruissem, W. and Baqinsky, S. (2009) Large-scale Arabidopsis phosphoproteome profiling reveals novel chloroplast kinase substrates and phosphorylation networks. *Plant Physiol*, **150**, 889–903.

Richter, M.L., Hein, R. and Huchzermeyer, B. (2000) Important subunit interactions in the chloroplast ATP synthase. *Biochim Biophys Acta*, **1458**, 326-342.

Richter, M.L., Patrie, W.J. and McCarty, R.E. (1984) Preparation of the epsilon subunit and epsilon subunit-deficient chloroplast coupling factor 1 in reconstitutively active forms. *J Biol Chem*, **259**, 7371–7373.

Rochaix, J.D. (2011) Assembly of the photosynthetic apparatus. *Plant Physiol*, **155**, 1493-1500.

Rohácek, K. (2010) Method for resolution and quantification of components of the non-photochemical quenching (q (N)). *Photosynth Res*, **105**, 101–113.

Rott, M., Martins, N.F., Thiele, W., Lein, W., Bock, R., Kramer, D.M. and Schöttler, M.A. (2011) ATP synthase repression in tobacco restricts photosynthetic electron transport, CO_2 assimilation, and plant growth by overacidification of the thylakoid lumen. *Plant Cell*, **23**, 304–321.

Sambrook, J. and Russell, D.W. (2001) Molecular Cloning: A laboratory manual, Ed 3. Cold Spring Harbor Laboratory Press.

Schägger, H. (2006) Tricine-SDS-PAGE. *Nat Protoc*, **1**, 16-22.

Schägger, H., Cramer, W.A. and von Jagow, G. (1994) Analysis of molecular masses and oligomeric states of protein complexes by blue native electrophoresis and isolation of membrane protein complexes by two-dimensional native electrophoresis. *Anal Biochem*, **217**, 220-230.

Schult, K., Meierhoff, K., Paradies, S., Toller, T., Wolff, P. and Westhoff, P. (2007) The nuclear-encoded factor HCF173 is involved in the initiation of translation of the psbA mRNA in *Arabidopsis thaliana*. *Plant Cell*, **19**, 1329–1346.

Schwacke, R., Schneider, A., Van Der Graaff, E., Fischer, K., Catoni, E., Desimone, M., Frommer, W.B., Flügge, U.I. and Kunze, R. (2003) ARAMEMNON, a Novel Database for Arabidopsis Integral Membrane Proteins. *Plant Physiol*, **131**, 16–26.

Scotti, P.A., Urbanus, M.L., Brunner, J., de Gier, J.W., von Heijne G., van der Does, C., Driessen, A.J., Oudega, B. and Luirink, J. (2000) YidC, the *Escherichia coli* homologue of mitochondrial Oxa1p, is a component of the Sec translocase. *EMBO J*, **19**, 542–549.

Seelert, H. and Dencher N.A. (2011) ATP synthase superassemblies in animals and plants: Two or more are better. *Biochim Biophys Acta*, **1807**, 1185-1197.

Seelert, H., Poetsch, A., Dencher, N.A., Engel, A., Stahlberg, H. and Müller, D.J. (2000) Structural biology. Proton-powered turbine of a plant motor. *Nature*, **405**, 418–419.

Sharma, M.R., Wilson, D.N., Datta, P.P., Barat, C., Schluenzen, F., Fucini, P. and Agrawal, R.K. (2007) Cryo-EM study of the spinach chloroplast ribosome reveals the structural and functional roles of plastid-specific ribosomal proteins. *Proc Natl Acad Sci U S A*, **104**, 19315–19320.

Siefermann-Harms, D. (1985) Carotenoids in photosynthesis. I. Location in photosynthetic membranes and light-harvesting function. *Biochim Biophys Acta*, **811**, 325–335.

Soll, J. and Schleiff, E. (2004) Protein import into chloroplasts. *Nat Rev Mol Cell Biol*, **5**, 198–208.

Soteropoulos, P., Suess, K.H. and McCarty, R.E. (1992) Modifications of the gamma subunit of chloroplast coupling factor 1 alter interactions with the inhibitory epsilon subunit. *J Biol Chem*, **267**, 10348–10354.

Staehelin, L.A. (2003) Chloroplast structure: from chlorophyll granules to supra-molecular architecture of thylakoid membranes. *Photosynth Res*, **76**, 185–196.

Straffon, A.F., Prescott, M., Nagley, P. and Devenish, R.J. (1998) The assembly of yeast mitochondrial ATP synthase: subunit depletion in vivo suggests ordered assembly of the stalk subunits b, OSCP and d. *Biochim Biophys Acta*, **1371**, 157–162.

Strotmann, H., Shavit, N. and Leu, S. (2004) Assembly and function of the chloroplast ATP synthase. *Advances in Photosynthesis and Respiration*, **7**, 477-500.

Süß, K. H. and Schmidt, O. (1982) Evidence for an α_3, β_3, γ, δ, I, II, ε, III_5 subunit stoichiometry of the chloroplast ATP synthetase complex (CF_1-CF_O). *FEBS Lett*, **144**, 213-218.

Sunamura, E., Konno, H., Imashimizu, M., Mochimaru, M. and Hisabori, T. (2012) A conformational change of the γ subunit indirectly regulates the activity of cyanobacterial F_1-ATPase. *J Biol Chem*, **287**, 38695–38704.

Sundberg, E., Slagter, J.G., Fridborg, I., Cleary, S.P., Robinson, C. and Coupland, G. (1997) ALBINO3, an Arabidopsis nuclear gene essential for chloroplast differentiation, encodes a chloroplast protein that shows homology to proteins present in bacterial membranes and yeast mitochondria. *Plant Cell*, **9**, 717–730.

Suzuki, T., Ozaki, Y., Sone, N., Feniouk, B.A. and Yoshida, M. (2007) The product of UncI gene in F_1F_O-ATP synthase operon plays a chaperone-like role to assist c-ring assembly. *Proc Natl Acad Sci U S A*, **104**, 20776–20781.

Terashima, M., Specht, M. and Hippler, M. (2011) The chloroplast proteome: a survey from the *Chlamydomonas reinhardtii* perspective with a focus on distinctive features. *Curr Genet*, **57**, 151-168.

Tikhonov, A.N. (2012) Energetic and regulatory role of proton potential in chloroplasts. *Biochemistry (Mosc)*, **77**, 956-974.

Tzagoloff, A. (1969) Assembly of the mitochondrial membrane system. II. Synthesis of the mitochondrial adenosine triphosphatase. F_1. *J Biol Chem*, **244**, 5027–5033.

Tzagoloff, A. (1970) Assembly of the mitochondrial membrane system. 3. Function and synthesis of the oligomycin sensitivity-conferring protein of yeast mitochondria. *J Biol Chem*, **245**, 1545–1551.

Tzagoloff, A., Barrientos, A., Neupert, W. and Herrmann, J.M. (2004) Atp10p assists assembly of Atp6p into the F_O unit of the yeast mitochondrial ATPase. *J Biol Chem*, **279**, 19775–19780.

Urbanus, M.L., Fröderberg, L., Drew, D., Björk, P., de Gier, J.W., Brunner, J., Oudega, B. and Luirink, J. (2002) Targeting, insertion, and localization of *Escherichia coli* YidC. *J Biol Chem*, **277**, 12718–12723.

Vallon, O., Bulte, L., Dainese, P., Olive, J., Bassi, R. and Wollman, F.A. (1991) Lateral redistribution of cytochrome b_6/f complexes along thylakoid membranes upon state transitions. *Proc Natl Acad Sci U S A*, **88**, 8262–8266.

Van Bloois, E., Jan Haan, G., De Gier, J.W., Oudega, B. and Luirink, J. (2004) F(1)F(O) ATP synthase subunit c is targeted by the SRP to YidC in the *E. coli* inner membrane. *FEBS Lett*, **576**, 97–100.

Van Walraven, H.S., Strotmann, H., Schwarz, O. and Rumberg, B. (1996) The H+/ATP coupling ratio of the ATP synthase from thiol-modulated chloroplasts and two cyanobacterial strains is four. *FEBS Lett*, **379**, 309-313.

Vasilyeva, E.A., Minkov, I.B., Fitin, A.F. and Vinogradov, A.D. (1982) Kinetic mechanism of mitochondrial adenosine triphosphatase. ADP-specific inhibition as revealed by the steady- state kinetics. *Biochem J*, **202**, 9–14.

Velours, J. and Arselin, G. (2000) The *Saccharomyces cerevisiae* ATP synthase. *J Bioenerg Biomembr*, **32**, 383–390.

Vollmar, M., Schlieper, D., Winn, M., Büchner, C. and Groth, G. (2009) Structure of the c14 rotor ring of the proton translocating chloroplast ATP synthase. *J Biol Chem*, **284**, 18228-18235.

Von Ballmoos, C., Wiedenmann, A. and Dimroth, P. (2009) Essentials for ATP synthesis by F_1F_O ATP synthases. *Annu Rev Biochem*, **78**, 649–672.

Walker, J.E., Fearnley, I.M., Gay, N.J., Gibson, B.W., Northrop, F.D., Powell, S.J., Runswick, M.J., Saraste, M. and Tybulewicz, V.L. (1985) Primary structure and subunit stoichiometry of F_1-ATPase from bovine mitochondria. *J Mol Biol*, **184**, 677-701.

Wang, H. and Oster, G. (1998) Energy transduction in the F_1 motor of ATP synthase. *Nature*, **396**, 279–282.

Watt, I.N., Montgomery, M.G., Runswick, M.J., Leslie, A.G. and Walker, J.E. (2010) Bioenergetic cost of making an adenosine triphosphate molecule in animal mitochondria. *Proc Natl Acad Sci U S A*, **107**, 16823-16827.

Weber, J. and Senior, A.E. (2000) Features of F(1)-ATPase catalytic and noncatalytic sites revealed by fluorescence lifetimes and acrylamide quenching of specifically inserted tryptophan residues. *Biochemistry*, **39**, 5287-5294.

Woody, S.T., Austin-Phillips, S., Amasino, R.M. and Krysan, P.J. (2007) The WiscDsLox T-DNA collection: an arabidopsis community resource generated by using an improved high-throughput T-DNA sequencing pipeline. *J Plant Res*, **120**, 157-165**.**

Yagi, H., Kajiwara, N., Tanaka, H., Tsukihara, T., Kato-Yamada, Y., Yoshida, M. and Akutsu, H. (2007) Structures of the thermophilic F1-ATPase ε subunit suggesting ATP-regulated arm motion of its C-terminal domain in F_1. *Proc Natl Acad Sci U S A*, **104**, 11233–11238.

Yasuda, R., Noji, H., Kinosita, K. Jr. and Yoshida, M. (1998) F_1-ATPase is a highly efficient molecular motor that rotates with discrete 120 degree steps. *Cell*, **93**, 1117-1124.

Yi, L. and Dalbey, R.E. (2005) Oxa1/Alb3/YidC system for insertion of membrane proteins in mitochondria, chloroplasts and bacteria. *Mol Membr Biol*, **22**, 101–111.

Zeng, X., Barros, M.H., Shulman, T. and Tzagoloff, A. (2008) ATP25, a new nuclear gene of *Saccharomyces cerevisiae* required for expression and assembly of the Atp9p subunit of mitochondrial ATPase. *Mol Biol Cell*, **19**, 1366–1377.

Zhang, X.P. and Glaser, E. (2002) Interaction of plant mitochondrial and chloroplast signal peptides with the Hsp70 molecular chaperone. *Trends Plant Sci*, **7**, 14–21.

Ziaja, K., Michaelis, G. and Lisowsky, T. (1993) Nuclear control of the messenger RNA expression for mitochondrial ATPase subunit 9 in a new yeast mutant. *J Mol Biol*, **229**, 909–916.

Zoschke, R., Kroeger, T., Belcher, S., Schöttler, M.A., Barkan, A. and Schmitz-Linneweber, C. (2012) The Pentatricopeptide Repeat-SMR Protein ATP4 promotes translation of the chloroplast *atpB/E* mRNA. *Plant J*, **72**, 547-558.

Acknowledgements

Firstly, I would like to thank Prof. Dr. Dario Leister for giving me the opportunity to perform my Ph.D. research in his research group.

Additionally, I am grateful to Dr. Thilo Rühle, for their supervision and willing to help during my Ph.D. research.

I would like to thank Prof. Dr. Jörg Nickelsen for taking over the second position in the exam commission.

I would like to thank Dr. Cordelia Bolle for helping about my practical and lecture courses, Dr. Jörg Meurer for giving antibodies against ATP synthase subunits, Prof. Paolo Pesaresi and Prof. Roberto Barbato for providing antibody against Gc9, Prof. Peter Jahns for pigment analyses and Prof. Danja Schüneman for Spilit ubiquitin assay.

I would like to thank Dr. Alexander Hertle, Dr. Michael Scahrfenberg, Stefania Viola, Evgenia Vamvaka, Chiara Gandini, Salar Torabi and other colleagues in this nice group for helping and discussing in my project.

I would like to thank Dr. Thilo Rühle, Stefania Viola and Evgenia Vamvaka for reading and correcting my dissertation.

I would like to thank the ministry of Science, Research and Technology in IRAN, for funding this scholarship in Germany.

I would like to dedicate this work to my parents who always gave me the real safety.

To my lovely kid Zahra.

To Mahdiyeh, my better half who shares with me the whole life.

Curriculum vitae

PERSONAL DATA

Date of birth: 01.03.1980

Place of Birth: Tabriz, IRAN

Nationality: Iranian

EDUCATION

October 2009 - now

Ludwig-Maximilians-Universität München

Department Biology I, Botany

Ph.D., Supervisor Prof. Dr. Dario Leister & Dr. Thilo Rühle

October 2004 – December 2006

University of Tabriz, IRAN

Department of Life Science

Master, Supervisor Dr. Ali movafeghi & Dr. Djavanshir Djozan

October 2000 - February 2004

University of Tabriz, IRAN

Department of Life Science

Bachelor of General Biology

RESEARCH EXPERIENCES

October 2009 - now

Ludwig-Maximilians-Universität München

Department Biology I, Botany

Ph.D. Dissertation- Gc9 is involved in the efficient ring assembly of the chloroplast F_OF_1 ATP synthase in Arabidopsis.

October 2004 – December 2006

University of Tabriz, IRAN

Department of Life Science

Master Thesis- Identification of volatile organic compounds in leaves, roots and gum of Astragalus species using solid phase microextraction followed by GC-MS analysis

LANGUAGES

Farsi, mother tongue

English, fluent

German, basic

Eidesstattliche Erklärung

Hiermit versichere ich an Eides statt, dass ich die vorliegende Arbeit selbständig und nur unter Verwendung der angegebenen Hilfsmittel und Quellen angefertigt habe. Der Autor hat zuvor nicht versucht, anderweitig eine Dissertation einzureichen oder sich einer Doktorprüfung zu unterziehen. Die Dissertation wurde keiner weiteren Prüfungskommission weder in Teilen noch als Ganzes vorgelegt.

München, 10. September 2013

.....

Jafar Angouri Razeghi